Title
The regulation of bone remodeling by TGF-[beta]

Author
Erlebacher, Adrian,

Publication Date
1997

Peer reviewed|Thesis/dissertation

The regulation of bone remodeling by TGF-β

by

Adrian Erlebacher

DISSERTATION

Submitted in partial satisfaction of the requirements for the degree of

DOCTOR OF PHILOSOPHY

in

Cell Biology

in the

GRADUATE DIVISION

of the

UNIVERSITY OF CALIFORNIA

San Francisco

To the memory of my father,

Walter Erlebacher

11/22/33 - 8/20/91

ACKNOWLEDGMENTS

I would like to take this opportunity to thank the many people that have helped me throughout my graduate school years.

On the faculty side, I would like to thank Keith Yamamoto and Zena Werb, who together with Rik comprised my thesis committee. Keith has been extremely supportive and encouraging, and on many occasions has given me invaluable graduate school 'life advice,' for which I am very grateful. Zena has similarly encouraging, and I have felt very lucky that her door has always been open to me for all kinds of discussions, both practical and general. I would also like to thank Richard Weiner, who taught me how to make transgenic mice, and Arnie Kahn, who taught me a great deal about bone biology when I first started out in the lab.

I would also like to thank the members of the Derynck lab, for their constant advice and camaraderie. In particular, Alfred Kuo has been a devoted friend and great graduate school compatriot. Over the years, Dan Gazit, Paivi Miettinen, and Xin-Hua Feng have also made my experience in the Derynck lab that much more enjoyable. I would also like to thank the bone section of the lab, Steve Gitelman and Ellen Filvaroff, for their thoughtful input into my work and encouragement.

I would like to thank the many people outside the lab who have provided helpful discussions and insight into my work, and in particular those who have contributed directly. I am very grateful to Ilse Sauerwald and Nilda Ubana for their excellent histological support. Ilse also set up the techniques for embedding and sectioning undecalcified bone samples used throughout this project. I would also like to thank Hye-Rim Park and

Brendan Boyce for performing the osteoclast density, osteoclast apoptosis and ruffled borders analyses described in Chapter 5.

I have been very lucky to be blessed with great friends while at UCSF, and their enthusiasm, encouragement and love have perhaps most strongly colored my graduate school years. In particular, I would like to thank Sean Bohen, Michelle Rhyu, Lee Honigberg, Josh Gordon, and Dave Leonardo. I would also like to thank Angie Choi for her love and support. Lastly, this whole endeavor would not have been possible without the constant support and encouragement of my brother Jonah and my mother Martha.

Lastly, I would like to thank Rik Derynck, who has been an excellent advisor. I have benefited from his wisdom, insight and generosity. I am very grateful to Rik for encouraging me to deeply explore the many directions that my project has taken me, and for supporting me on many risky ventures. The broad range of techniques, issues, and approaches that my thesis work has entailed has greatly enriched my development as a scientist.

The regulation of bone remodeling by TGF-β

by

Adrian Erlebacher

ABSTRACT

Transforming growth factor-β (TGF-β) has many potent effects on the activities and differentiation of osteoblasts and osteoclasts, although the physiological role of this growth factor during bone development and turnover has remained unclear. I have generated transgenic mice that overexpress TGF-β2 specifically in osteoblasts. These mice showed a dramatic age-dependent loss of bone mass similar to that seen in osteoporosis and other metabolic bone diseases, with surprisingly few defects in skeletal development or growth. Mice with the highest level of transgene expression had three major histological alterations: an increase in osteocyte density, an increase in osteoblastic bone formation, and an increase in osteoclastic bone resorption. These results suggested that TGF-β2 overexpression increases the rate of bone remodeling by modulating the coordinated interactions of osteoblasts and osteoclasts.

The three observed histological alterations provided a basis for studying the skeletal physiology of TGF-β. To detect effects that required osteoblastic responsiveness to TGF-β, I used transgenic mice that overexpressed a dominant-negative type II TGF-β receptor in osteoblasts. To detect effects that required osteoclasts, I used both *c-fos* knockout mice, which completely lack osteoclasts, and alendronate, a specific inhibitor of bone resorption. Surprisingly, I found that the increase in bone formation in

transgenic mice was an indirect compensatory response to the increase in bone resorption. In contrast, the increase in osteocyte density was a direct effect of TGF-β2 on osteoblasts caused by an increase in their steady-state rate of differentiation. Osteoclastic activity greatly stimulated this latter effect, suggesting that TGF-β is important in coupling osteoblastic differentiation to sites of bone resorption in vivo. Lastly, I found that the increase in bone resorption did not correlate with increases in the number of osteoclasts or their apparent activity assessed histologically and biochemically. Rather, the increase in resorption required the direct effects of TGF-β on osteoblasts, suggesting that osteoblasts can directly control rates of bone resorption. These results shed new light onto the pathogenesis of osteoporosis in humans, and implicate TGF-β as a mediator of high-turnover bone loss.

TABLE OF CONTENTS

[1]Reproduced from Cell, 1995, 80:371-378, by copyright permission of Cell Press.
[2]Reproduced from the Journal of Cell Biology, 1996, 132:195-210, by copyright permission of The Rockefeller University Press.

LIST OF TABLES

Chapter 4

Chapter 6

LIST OF FIGURES

ADVISOR'S STATEMENT

Regarding inclusion of material with multiple authors

Chapter 1 has been previously published as "Toward a Molecular Understanding of Skeletal Development" in Cell 80: 371-378 (1995), with myself, Ellen H. Filvaroff, and Steven E. Gitelman as co-authors. Adrian Erlebacher was the primary author of the entire review except for the section "The Role of Collagens," which was written by Stephen Gitelman, and the section "Mesenchymal Differentiation," which was co-authored by Adrian Erlebacher and Ellen Filvaroff. My role was as senior author. Adrian's contribution represents scholarship comparable in scope to a standard thesis chapter.

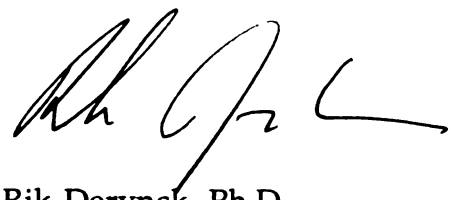

Rik Derynck, Ph.D.

Thesis Advisor

UNIVERSITY OF CALIFORNIA, SAN FRANCISCO

BERKELEY • DAVIS • IRVINE • LOS ANGELES • RIVERSIDE • SAN DIEGO • SAN FRANCISCO SANTA BARBARA • SANTA CRUZ

ADRIAN ERLEBACHER
DEPARTMENT OF GROWTH AND DEVELOPMENT
C603, 521 PARNASSUS AVENUE, BOX 0640
SAN FRANCISCO, CALIFORNIA 94143-0640

TEL: 415-476-6081
FAX: 415-476-1499
e-mail: adrian@cgl.ucsf.edu

Cell Press
1050 Massachusetts Avenue
Cambridge, MA 02138

September 22, 1997

Dear Cell Press,

I would like permission from Cell Press to reprint, for my Ph.D. thesis, the article "Toward a Molecular Understanding of Skeletal Development" by myself, Ellen H. Filvaroff, Stephen E. Gitelman, and Rik Derynck (Cell 80:371-378 [1995]). The dissertation will be placed on microfilm by University Microfilms who request permission to supply single copies on demand. Please respond by fax to (415) 476-1499.

Thank you very much.

Sincerely,

Adrian Erlebacher

Permission granted subject to citation of the original manuscript, and notation that copyright is held by Cell Press. (Our permission is contingent on permission of the author.)

Jessica A. Donaky

SEP 24 1997

The Rockefeller
University Press
1114 First Avenue, 4th Floor
New York, New York 10021
(212) 327-7938
Fax (212) 327-8587

September 24, 1997

Dear Dr. Erlebacher:

We shall be glad to grant you permission for the reproduction of the material referred to in your letter of 22 September 1997.*

Our only requirements are that you also obtain permission from the author(s) and give suitable acknowledgment to the source in the following manner: Reproduced from **The Journal of Cell Biology, year, vol., pp.** by copyright permission of The Rockefeller University Press.

Sincerely yours,

THE JOURNAL OF
CELL BIOLOGY

Iris Vallecilla
Copyright Permission

Dr. Adrian Erlebacher
University of California-San Francisco
Dept. of Growth and Development
C603
521 Parnassus Avenue
Box#0640
San Francisco, CA 94143-0640

P.S. Article to be used in Ph.D. thesis.

*JCB-132,195-210,1996 -article.

Chapter 1:

Toward a molecular understanding of skeletal morphogenesis

Much of our initial knowledge about cartilage and bone has come from descriptive anatomy, endocrinology, and cellular studies of bone turnover. Recent work has led to the identification of local factors that regulate skeletal morphogenesis. Molecular and biochemical studies of bone and cartilage cells in vitro, gene inactivation in mice, and the identification of genes responsible for mouse and human skeletal abnormalities have documented the importance of specific growth and differentiation factors, extracellular matrix proteins, signaling mediators and transcription factors in bone and cartilage development. The successful convergence of mouse and human genetics in skeletal biology is illustrated in this issue of Cell with two papers which show that mutations in collagen type XI cause chondrodysplasia both in cho/cho mice as well as in patients with Stickler syndrome (Li et al., 1995, Vikkula et al., 1995).

In general, recent results emphasize the need to view skeletal development at various integrated levels of organization and illustrate how single gene products affect development at these different levels. Pattern information determines not only the body plan of the early skeleton but also the shape of each individual skeletal element. In addition, the sequence of events during bone growth and development must be temporally and spatially controlled to insure correct proportions of bony elements. Positional information must also regulate the establishment of bone internal structure throughout growth, while local homeostatic mechanisms must maintain bone integrity throughout adult life. Lastly, a complex extracellular matrix must generate skeletal tissues with specific biomechanical properties.

Ultimately, the morphogenesis of the skeleton derives from the regulated differentiation, function, and interactions of its component cell

types. Three major cell types contribute to the skeleton: chondrocytes which form cartilage, osteoblasts which deposit bone matrix, and osteoclasts which resorb bone. Chondrocytes and osteoblasts are of mesenchymal origin, whereas osteoclasts derive from the hematopoietic system. Once embedded in bone matrix, osteoblasts mature into terminally differentiated osteocytes. The activity and differentiation of osteoblasts and osteoclasts is closely coordinated during development as bone is formed, and during growth and adult life, as bone undergoes continuous remodeling. More specifically, the formation of internal bone structures and bone remodeling result from coupling bone resorption by activated osteoclasts with subsequent deposition of new matrix by osteoblasts (Fig. 1). Bone remodeling also links bone turnover to the endocrine homeostasis of calcium and phosphorus, since the mineralized bone matrix serves as the major repository for these ions in the body.

Descriptive embryology and anatomy distinguishes two types of bone development: intramembranous and endochondral. Intramembranous ossification occurs when mesenchymal precursor cells differentiate directly into bone-forming osteoblasts, a process employed in generating the flat bones of the skull as well as in adding new bone to the outer surfaces of long bones. In contrast, endochondral bone formation entails the conversion of an initial cartilage template into bone and is responsible for generating most bones of the skeleton. Cartilage templates originally form during embryogenesis when mesenchymal cells condense and then differentiate into chondrocytes. These cells subsequently undergo a program of hypertrophy, calcification and cell death. Concomitant neovascularization occurs and osteoclasts and osteoblasts are recruited to gradually replace the cartilage

Figure 1. Bone remodeling. Activated multinucleated osteoclasts derived from bone marrow monocytes resorb a discrete area of mineralized bone matrix. Subsequently, capillary endothelial cells provide a microvasculature and cuboidal osteoblasts and fibroblastic osteoprogenitor cells, which can locally differentiate into osteoblasts, migrate and proliferate into the resorption lacuna. The osteoblasts deposit new bone matrix, which is initially unmineralized and called osteoid. Once embedded in osteoid, the osteoblasts mature into terminally differentiated osteocytes.

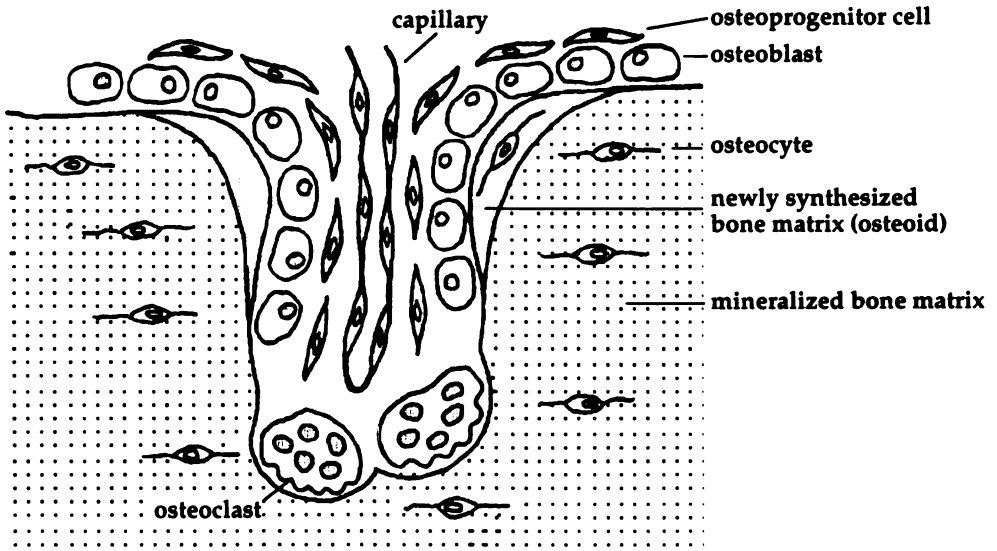
capillary
osteoprogenitor cell
osteoblast
osteocyte
newly synthesized
bone matrix (osteoid)
mineralized bone matrix
osteoclast

scaffold with bone matrix and to excavate the bone marrow cavity. Longitudinal bone growth takes place through a similar pattern of endochondral ossification in the growth plates located at the epiphyses (ends) of long bones. In these epiphyseal plates, the calcified, hypertrophic cartilage provides a scaffold for the formation of new trabecular bone. Ultimately, all remaining cartilage is replaced by bone except at the articular surfaces of the joints (Fig. 2).

Skeletal patterning.

Classical embryology has shown that three distinct embryonic lineages contribute to the early skeleton. The neural crest gives rise to the branchial arch derivatives of the craniofacial skeleton, whereas the sclerotome generates most of the axial skeleton and lateral plate mesoderm forms the appendicular skeleton. Transplantation studies have indicated that information regarding the number and anatomic "identity" of derived skeletal elements already resides in these lineages by the time of their appearance long before overt skeletogenesis.

The family of transcription factors encoded by homeobox genes play a central role in this aspect of skeletal pattern formation (reviewed in Morgan and Tabin, 1993; Krumlauf, 1994). Specific homeobox genes are expressed in distinct patterns at the time when the embryonic lineages initially form. Furthermore, targeted inactivation or ectopic expression of these genes in the mouse results in the deletion or addition of skeletal elements, or the transformation of skeletal elements into shapes resembling other elements. For example, the hoxa-2 gene is expressed in fourth rhombomere neuroepithelium before the migration of neural crest cells and their

Figure 2. Endochondral ossification center of a long bone. Longitudinal bone growth occurs at the epiphyseal growth plate in which the chondrocytes proliferate and mature, and the calcified matrix of the hypertrophic cartilage provides a scaffold for new trabecular bone formation. In the epiphysis above the growth plate, the cartilage of the secondary ossification center has already been replaced with bone and bone marrow.

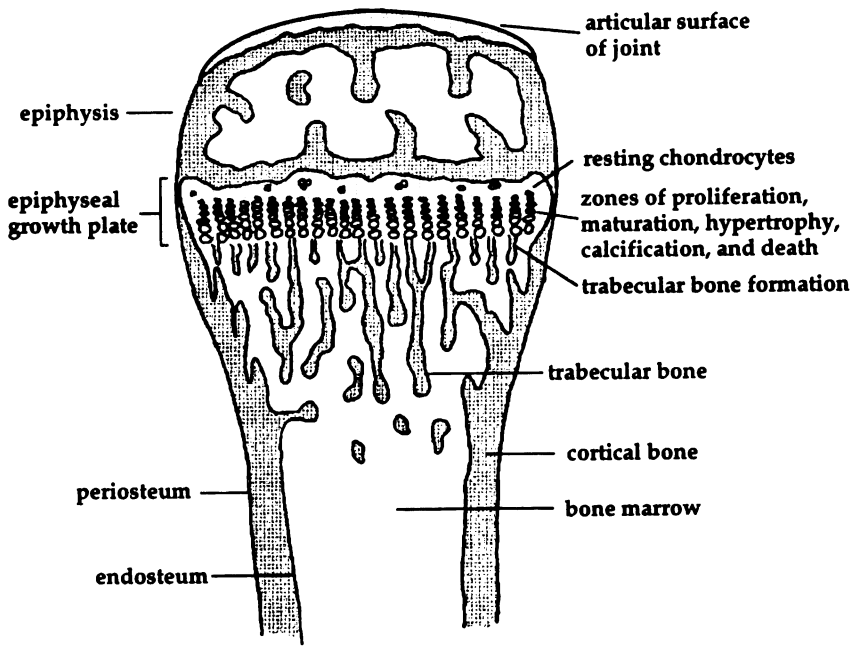
articular surface
of joint
epiphysis
resting chondrocytes
epiphyseal
growth plate
zones of proliferation,
maturation, hypertrophy,
calcification, and death
trabecular bone formation
trabecular bone
cortical bone
periosteum
bone marrow
endosteum

subsequent differentiation into the skeletal elements of the second branchial arch. Its localized expression combined with the results from transplantation experiments suggests that this gene is required for the determination of second branchial arch identity. Accordingly, inactivation of the hoxa-2 gene results in the deletion of the craniofacial elements derived from the second branchial arch and their replacement by elements resembling those derived from the first branchial arch (Gendron-Maguire et al., 1993; Rijli et al., 1993). Thus, in the absence of the hoxa-2 gene product, the skeletogenic neural crest of the second arch defaults to a first arch identity. The same principles can be demonstrated for the axial and appendicular skeleton using the hoxd-13 homeobox gene as an example. Hoxd-13 is expressed in the presomitic mesoderm of the posterior region of the embryo before sclerotome formation and appearance of the mesodermal skeletal lineages, as well as in the posterior distal region of the limb bud mesenchyme. Inactivation of the hoxd-13 gene results in a transformation of the fourth sacral vertebrae into a bone resembling the third, and an assortment of deletions and additions of distal limb skeletal elements (Dolle et al., 1993).

The well studied system of limb development has revealed the additional importance of inductive interactions in regulating skeletal patterning. Signals essential for limb patterning emanate from the zone of polarizing activity (ZPA) which is located in the posterior limb mesoderm underlying the apical ectodermal ridge (AER) of a developing limb bud. Transplantation of the ZPA underneath the AER on the anterior margin of another limb bud results in a mirror-image duplication of skeletal elements, a phenomenon that also occurs when retinoic acid is applied at the same anterior site. The secreted factor sonic hedgehog (shh) has been identified as a

key inductive signal that mediates the activity of the ZPA (Riddle et al., 1993). Shh induces fibroblast growth factor-4 (FGF-4) in the AER, which in turn also regulates shh expression and serves as an ectodermal competence factor for shh responsiveness in the underlying mesoderm (Laufer et al., 1994). These inductive interactions may regulate limb skeletal patterning by establishing the expression patterns of homeobox genes in the limb bud mesenchyme. For example, shh induces the local expression of hoxd-13, which as mentioned above is required for normal limb patterning. Shh also induces the local expression of bone morphogenetic protein-2 (BMP-2), a TGF-β related factor with cartilage-inducing activity. Similar inductive interactions are likely to play an important role in skeletal patterning in other areas of the developing embryo.

Local control of bone shape.

The individual shapes of skeletal elements are largely determined during embryogenesis when their respective cartilage templates form from localized mesenchymal condensations. The importance of paracrine factors in regulating the process of mesenchymal condensation has been emphasized by the recent characterizations of the mouse mutations *short ear* (*se*) and *brachypodism* (*bp*) (reviewed in Kingsley, 1994). In these mutant mice, various skeletal elements throughout the body have altered shapes and sizes. For example, the *se* phenotype includes an altered shape of the sternum and the external ear cartilage, whereas the *bp* mutation leads to a reduction in size of appendicular long bones. These adult abnormalities can be attributed to defects in size and shape already apparent in the mesenchymal condensations of the affected skeletal elements. The *se* and *bp* mutations result from

inactivation of the genes for BMP-5 and GDF-5, two members of the TGF-β superfamily, respectively (Kingsley et al., 1992, Storm et al., 1994). The developmental expression pattern of these two factors is consistent with their potential role in the local control of patterns of mesenchymal condensations. For example, BMP-5 is expressed in condensing mesenchyme which gives rise to external ear cartilage, whereas GDF-5 is expressed in mesenchyme surrounding limb condensations. Furthermore, the ability of BMP-5 and other BMPs to induce cartilage and bone formation when injected into non-skeletal sites in vivo further supports a role for these factors in the local induction of cartilage. These factors may also be involved in fracture repair, as suggested by the increased expression of BMP-4 at fracture sites (Nakase et al., 1994) and the impairs fracture healing in *se* mice.

The current data on the regulation of skeletogenesis suggest a two-step model for the specification of the pattern and shape of the embryonic skeleton. First, the patterned expression of homeobox genes confers information to cells of the early mesenchymal lineages that specifies the overall pattern of the skeleton and the archetypal shape and identity of the individual elements. Second, the shape of a skeletal element is further defined through the local regulation of mesenchymal condensation by secreted autocrine/paracrine factors. Evolution of the skeleton may result from modifications of early cell-intrinsic patterning information and local control of mesenchymal condensation by these differentiation factors.

Bone shape during growth.

Bone growth is regulated by various systemic factors. Skeletal growth ultimately ceases when the growth plate is entirely replaced with bone, a

process that requires estrogen in both males and females (Federman, 1994, Smith et al., 1994). The rate of skeletal growth until epiphyseal closure is regulated by growth hormone which is released by the pituitary gland and acts predominantly through the local and systemic expression of IGF-1. Mice which lack IGF-1 as a result of gene inactivation (Baker et al., 1993) and humans with reduced growth hormone levels resulting in hypopituitary dwarfism, have a reduced size of the skeleton but with only small alterations of the proportions between or within bones.

During growth, the shapes of individual bones and the relative proportions of the skeleton are maintained likely as a result of a complex process with multiple local mediators, as suggested by the wide spectrum of clinical abnormalities related to disproportionate bone growth. In the skull, the intramembranous bones grow by peripheral addition of new bone at osteogenic fronts, which generate the suture lines. Osteoblastic differentiation within the sutures and consequent bone deposition are intimately coordinated with the growth of the skull and the timing of suture closure. Deregulated coordination results in premature suture closure leading to various skull abnormalities collectively known as craniosynostoses. In bones which develop based on cartilage templates, endochondral ossification must be coordinated with the simultaneous growth of the epiphyses, longitudinal growth at the epiphyseal growth plate and the radial growth of the periosteum. Achondroplasia, the most common cause of human dwarfism, results from incomplete coordination of these processes and is characterized by short, wide bones and overgrowth of the periosteum relative to the epiphyses.

Recently, cell signaling by FGFs has been implicated in coordinating proportional bone growth. At least nine members of the FGF family interact with varying specificities and affinities to four transmembrane tyrosine kinase FGF-receptors, FGF-R1 through FGF-R4 (reviewed in Givol and Yayon, 1992). FGF-receptor signaling regulates various cellular processes, most notably the proliferation and differentiation of cells of mesenchymal and neurectodermal origin. Recently, several dominantly inherited human skeletal disorders have been correlated with mutations in FGF-receptors. Mutations in the transmembrane region of FGF-R3 in patients with achondroplasia suggests that impaired ligand-induced receptor dimerization and signaling may be the cause of this disease (Rousseau et al., 1994, Shiang et al., 1994). The expression of FGF-R3 in resting chondrocytes and not in the periosteum (Peters et al., 1993) may explain why achondroplasia results in abnormalities in only those bones which develop based on cartilage templates and not in the intramembranous bones of the skull. The craniosynostosis seen in Crouzon syndrome has been correlated with mutations in the extracellular domain of FGF-R2, which may affect ligand binding (Reardon et al., 1994). Finally, patients with Pfeiffer syndrome and Jackson-Weiss syndrome, which have craniosynostoses as well as limb defects, have similar mutations in FGF-R1 and FGF-R2 respectively (Jabs et al., 1994, Muenke et al., 1994). It is unclear how different point mutations in FGF-R2 give rise to different skeletal defects in Crouzon syndrome and Jackson-Weiss syndrome. The identification of these mutations in these inherited skeletal disorders implies a local role of FGF-mediated signaling in skeletal development and suggests transgenic approaches to the characterization of the role of these factors in skeletal development.

The restricted expression patterns of the FGF-Rs and their ligands and in vitro data on the effects of FGFs suggest that specific FGFs might regulate intrinsic growth rates of distinct zones of the epiphysis, and that FGF-mediated autocrine and paracrine interactions within and between these zones control their relative growth. An internal network of local homeostatic interactions via FGFs might then be integrated with effects of systemic factors to control overall skeletal growth and proportions. Further evidence for such an integration of signals and communication between different zones of the epiphyseal plate comes from studies on parathyroid hormone-related protein (PTHrP). While PTHrP is expressed in various locations throughout the epiphysis, its receptor expression in growth plate cartilage is localized mainly to the transitional zone between proliferating and hypertrophic chondrocytes, suggesting that cells in this zone coordinate the rate of chondrocyte maturation. In mice with an inactivated PTHrP gene, the reduced proliferation and premature differentiation of chondrocytes in the epiphyseal plate leads to a greatly increased rate of endochondral ossification, resulting in a skeleton that is almost completely ossified by the time of birth (Amizuka et al., 1994, Karaplis et al., 1994).

Possibly related to growth factor signaling in skeletal growth control is the recent finding that diastrophic dysplasia can be ascribed to a defect in the gene for a putative sulfate transporter (Hastbacka, et al., 1994). In this disease, the undersulfation of proteoglycans may be responsible for the mechanical defects in cartilage and bone matrix which result in a severely malformed skeleton, progressive joint disease and dwarfism. The deformities in diastrophic dysplasia and the FGF-related diseases described above share some similarities. For example, in diastrophic dysplasia, the deformities in

the short bones are similar to those seen in achondroplasia, the broad great toes are similar to Jackson-Weiss and Pfeiffer syndromes, and the broad thumbs are reminiscent of Pfeiffer syndrome. A mechanistic basis for the relationship between these two types of diseases is also suggested by the requirement of heparan sulfates for the high-affinity interactions of FGF with its receptor (Yayon et al., 1991, Givol and Yayon, 1992. Whether the defect in sulfation in diastrophic dysplasia decreases the availability of heparan sulfates and impairs FGF signaling during skeletal development remains to be tested.

The importance of transcription factors in the regulation of bone growth is illustrated by the mutation in the msx2 homeobox gene in patients with Boston type craniosynostosis (Jabs et al., 1993). Consistent with its involvement in suture function and closure, msx2 mRNA is localized at the sutures and various other sites during craniofacial development of the mouse. Inactivation of the closely related msx1 further suggests that this class of homeobox genes plays a role in normal growth of intramembranous bones at osteogenic fronts (Satokata and Maas, 1994). The cleft palate in these mice is due to failure of the palatal shelves to grow towards each other and fuse, and is consistent with the expression of msx1 in the osteogenic fronts of the palatal shelves. Remarkably, the expression of both msx1 and msx2 has been shown, at least in developing teeth, to be controlled by BMP-4, a TGF-β related factor with cartilage and bone-inducing activity (Vainio et al., 1993). Lastly, mutations in SOX9, which encodes a putative transcription factor related to SRY, have been shown to cause sex-reversal with associated campomelic dysplasia, a congenital skeletal malformation syndrome with the prominent

feature of bowed long bones (Foster et al., 1994). How this gene product is involved in bone development is unknown.

Bone structure, modeling and remodeling.

The coordinated activities of osteoclasts and osteoblasts in bone resorption and deposition form the internal structure of a bone. In long bones, a tube of dense cortical bone encases the bone marrow space and is capped by the two epiphyseal growth plates. The bone marrow cavity contains a large number of bone spicules (trabeculae) arranged with increasing density towards the epiphyseal plates (Fig. 2). The importance of bone resorption in bone modeling is illustrated by the structural defects in osteopetrosis, a disease associated with impaired osteoclastic function. While the external shapes are normal, osteopetrotic bones are characterized by a homogeneous dense trabeculation in the bone marrow space and a less compact consistency of the cortical bone. In several mouse models, the inactivation of specific genes results in impaired osteoclastic differentiation and consequent osteopetrosis. In osteopetrotic op/op mice, osteoclast differentiation is blocked at an early stage as a result of defective production of CSF-1 (Wiktor-Jedrzejczak et al., 1990, Yoshida et al., 1990). The inability of bone marrow transplantation to cure this form of osteopetrosis suggests that CSF-1 is normally provided by cells external to the hematopoietic system. In contrast, several other types of osteopetrosis in mice can be rescued by bone marrow transplantation. For example, mi/mi mice develop osteopetrosis as a result of a mutation in a putative transcription factor that contains a basic helix-loop-helix (bHLH) domain and a leucine zipper domain (Hodgkinson et

al., 1993). In addition, inactivation of the c-src gene results in a rescuable osteopetrosis in which the multinucleated osteoclasts are present but lack bone resorption activity (Lowe et al., 1993, Soriano et al., 1991). Finally, inactivation of the c-fos gene also results in osteopetrosis, but in this case the phenotype is due to a complete absence of differentiated osteoclasts (Grigoriadis et al., 1994). The expression of c-fos in differentiating osteoclasts and the rescue of the phenotype following transplantation of normal bone marrow suggests that this transcription factor is required for early osteoclast differentiation. Taken together, these mouse mutations not only emphasize the importance of osteoclastic activity in both the resorption of trabecular bone and the establishment of the definitive cortex, but also implicate several factors in osteoclast differentiation and activity.

Mechanical tension can also alter local bone architecture by influencing bone remodeling. The requirement for mechanical tension in the formation of bony tubercles at sites of tendon insertions is elegantly demonstrated in mice in which the genes for both myf-5 and myoD are inactivated (Rudnicki et al., 1993). These mice lack bony tubercles presumably as a result of impaired muscle development and therefore reduced mechanical tension at tendon insertion sites. How tension is sensed by resident bone cells, and how such signals contribute to the cellular and molecular control of bone remodeling are major unresolved issues in skeletal biology.

Bone remodeling itself is a poorly understood process. While much is known about the kinetics of bone turnover at the cellular level, little is understood about the local regulation of bone remodeling at the molecular level (reviewed in Canalis et al., 1991). Presumably, specific factors regulate each step of a remodeling cycle, the coordination of remodeling with the local

differentiation of osteoclasts and osteoblasts from their respective precursor cell populations, and the integration of bone remodeling with the endocrine control of bone turnover. Understanding these various levels of control is important because deregulated bone remodeling lies at the basis of many metabolic bone diseases. For example, osteoporosis is characterized by reduced bone mass and is thought to result from an imbalance between bone formation and resorption. While the association of this disease with endocrinological imbalances such as reduced estrogen and increased corticosteroids has long been apparent, how these systemic factors influence the local regulation of bone remodeling is still not known. A recent example of this dichotomy comes from the association of reduced bone density with common alleles of the gene encoding the vitamin D receptor (Morrison et al., 1994). Vitamin D stimulates osteoclast and osteoblast differentiation in vitro and regulates bone mineralization and homeostasis in vivo, but how changes in receptor expression lead to the cellular changes resulting in osteoporosis remains unclear. A potentially fruitful new approach to the problem is to establish appropriate transgenic mouse models to study the many paracrine growth and differentiation factors that based upon cell culture studies have been implicated in bone remodeling (see below). The initial success of this approach can be seen with the demonstration that transgenic mice overexpressing interleukin-4 develop osteoporosis due to impaired osteoblastic function (Lewis et al., 1993).

The role of collagens.

Collagens represent the major proteins in bone and cartilage matrices and play an important role in determining the size, shape and strength of

these tissues (reviewed in van der Rest and Garrone, 1991). Collagens form a family of at least 25 members, several of which are expressed at defined times and places during endochondral bone formation: collagen type II is the principal protein of cartilage, collagen type X the major protein found in hypertrophic cartilage, and collagen type I is the most abundant protein in bone. All collagens contain globular domains at the amino and carboxy termini and a triple-helical domain in between. Newly synthesized collagen monomers associate into trimeric microfibrils, which, once secreted, aggregate into larger structures. Based on their structure, the collagens can be subdivided into six distinct categories. Among these, the fibrillar collagens include types I, II, and XI, the fibril-associated collagens include type IX, and the network collagens include type X collagen. The recent characterization of collagen mutations in mice and man has provided insights into the function of different collagens in cartilage and bone (reviewed in Tilstra and Byers, 1994).

The best characterized fibrillar collagen is the type I collagen, which consists of two α1(I) and one α2(I) polypeptide chains. Mutations in the corresponding procollagen genes cause osteogenesis imperfecta, a heritable disorder resulting in decreased bone mass and bone fragility (reviewed in Byers and Steiner, 1992, Willing, et al., 1993). In addition, a wide range of clinical defects ranging from isolated osteoporosis to recurrent fractures and death in utero are also associated with collagen type I mutations. Several of the more than 100 molecular defects in procollagen type I genes characterized in man have been reconstituted in transgenic mice with resulting bone defects. Analysis of human and mouse mutations have shown that null alleles give rise to mild phenotypes. Such mutations may result in altered mRNA

levels or instability of the protein, perhaps through its inability to polymerize with the wild type monomers. More severe phenotypes result from dominant negative mutations that result in an aberrant protein still capable of multimerizing with wild-type collagen type I fibrils. The severity of the phenotype depends on the nature and location of the mutation, and its effects on protein structure. In general, the impact of point mutations on the phenotype decreases as the mutation shifts towards the N-terminal portion of the molecule. The relationship between genotype and phenotype has been reviewed elsewhere (Kuivaniemi et al., 1991).

Mutations in collagen type II, a homotrimer of α1(II), have been correlated with a variety of chondrodysplasias (reviewed in Vikkula, et al., 1994)). This heterogeneous group of cartilage disorders may result in dwarfism, joint deformities, and other skeletal anomalies. As with collagen type I mutations, many different molecular defects have been reported, with dominant negative mutations resulting in the most severe defects in cartilage development and structure. The available transgenic mouse models with defects in collagen type II should help clarify how such cartilage mutations affect subsequent endochondral bone formation. Recently, a patient with impaired chondrogenesis and with a documented dominant negative mutation in the α1(II) gene was found to express collagen type I in chondrocytes, suggesting a possible compensatory mechanism for aberrant collagen type II expression (Freisinger et al., 1994).

In this issue of Cell, Li et al. (1995) and Vikkula et al. (1995) provide the first insights into the role of another fibrillar collagen, collagen type XI, in bone and cartilage formation. This minor component of cartilage collagen is thought to play a role in the regulation of collagen fibril diameter and the

association of proteoglycans with the collagen fibrillar network. Li and colleagues report that a mutation in collagen type XI lies at the basis of chondrodysplasia in cho/cho mice. In these mice, the absence of a1(XI) collagen expression results in severe abnormalities in cartilage of the limbs, ribs, mandible and trachea and death at birth. At the epiphyses, the columnar arrangement of chondrocytes is disordered and chondrocytic maturation is delayed. In addition, the bones are wider but only about half the normal overall length. The collagen fibrils are abnormally thick and the proteoglycans are readily extractable, which is consistent with the purported function of collagen type XI. Vikkula et al. (1995) correlate a dominant negative mutation in the human COL11A2 gene encoding the α2(XI) chain with a form of Stickler's syndrome, which is characterized by mild spondyloepiphyseal dysplasia, osteoarthritis, and sensorineural hearing loss. They also mapped a more severe autosomal recessive human osteochondrodysplasia to the COL11A2 gene, and speculate that this disease arises from a mutation resulting in a null allele. If this indeed proves to be the case, then it will be interesting to determine why such a mutation is lethal in the cho/cho mouse, but not in man: as Vikkula et al. suggest, alternate collagen family members may be able to compensate for the null mutations in man.

Collagen type IX is a prototype of another subset of collagens, the fibril-associated collagens. This collagen localizes to the surface of collagen II fibrils and was thought to play a major role in development. However, transgenic overexpression of a dominant negative mutant of collagen IX (Nakata et al., 1993) and gene inactivation in mice (Fassler et al., 1994) results in surprisingly mild phenotypes, characterized by degenerative joint disease

resembling human osteoarthritis and mild chondrodysplasia. Thus, collagen IX may not play a major role in osteo- and chondrogenesis or in other human osteochondrodysplasias.

Finally, collagen X, a prototype of short chain collagens, is exclusively expressed in hypertrophic chondrocytes, where it forms distinct hexagonal arrays. Although its specific role in hypertrophic cartilage is not known, it may serve as a substrate for mineralization or vascular invasion. Some insight into its function has been gained through analysis of transgenic mouse models and characterization of human mutations (reviewed in Jacenko et al., 1994). Mice with a mutant type X collagen transgene exhibit compression of the hypertrophic growth plate cartilage and decreased bone formation in a pattern that resembles spondylometaphyseal dysplasia and metaphyseal chondrodysplasias in man. Subsequent analysis has confirmed that such patients indeed bear collagen X mutations, which are all localized to the carboxy-terminal, non-triple helical domain of the protein. The lack of detectable abnormalities in mice with an inactivated type X gene suggests that other collagens may compensate for its absence and emphasize again that null alleles of collagens result in a less severe phenotype than overexpression of a dominant negative mutant.

Mesenchymal differentiation.

The study of bone and cartilage cell differentiation in vitro provides an important counterpoint to the study of these cell populations in vivo. For example, experiments on cells derived from osteopetrotic mouse mutants will continue to add to the in vitro characterization of osteoclast differentiation. In vitro approaches have also made valuable contributions to our

understanding of the differentiation of chondrocytes and osteoblasts. By analogy with other cell types, chondrocyte and osteoblast differentiation involves at least two distinct processes. First, precursor cells commit to the cartilage or bone lineages. Since these lineages probably arise from the same population of undifferentiated mesenchymal cells, these studies have mainly concentrated on embryonic primary cultures and pluripotential mesenchymal cell lines. Second, consecutive maturation events lead to a fully differentiated phenotype, a process required in vivo for the constant replenishment of cartilage and bone cells from their respective committed precursor cell populations. Studies on the acquisition and modulation of the differentiated phenotype have mostly relied on cultures of committed precursor cells and tumor cell lines.

Members of the TGF-β superfamily of secreted growth and differentiation factors have received considerable attention as potent regulators of mesenchymal differentiation in vivo and in vitro. Several BMPs are thought to regulate the early commitment of mesenchymal cells to the chondrogenic and osteogenic lineages, as suggested by their ability to induce ectopic cartilage and bone formation at non-skeletal sites such as muscle (Wozney et al., 1988, Wozney, 1992). Accordingly, these factors can stimulate osteoblastic differentiation of uncommitted mesenchymal cells in vitro (Yamaguchi et al., 1991, Wozney, 1992) and can induce cells other than osteoblasts to express osteoblastic markers (Katagiri et al., 1994). TGF-β itself may regulate the further differentiation of committed precursor cells, as suggested by its ability to induce cartilage and bone formation when administered under the periosteum (Joyce et al., 1990), but not when injected into non-skeletal sites (Centrella et al., 1993). TGF-β has also been shown to

stimulate chondrocytic differentiation in vitro, but whether it modulates osteoblastic differentiation is unclear due to differential responses of various cell systems (reviewed in Centrella et al., 1993). The biological effects of different TGF-β related factors together with their expression patterns during cartilage and bone development suggest that distinct TGF-βs and BMPs act sequentially to drive successive stages of differentiation (Lyons et al., 1989). Consistent with such a model, differentiating cells may alter their responsiveness to these factors by modulating receptor levels (Centrella et al., 1993) and the associated signal transduction mechanisms (Siddhanti and Quarles, 1994).

In vitro work has also identified many other extracellular factors that can modulate mesenchymal differentiation, including steroid and peptide hormones, growth and differentiation factors, and collagens and other extracellular matrix proteins. A full understanding of the effects of these factors on mesenchymal differentiation, however, has been hampered by the limitations of in vitro cell culture. One difficulty has been the lack of specific phenotypic markers to follow successive differentiation events. Type II collagen secretion is considered a major early marker of chondrocyte differentiation, while the synthesis of alkaline phosphatase is an early marker of osteoblast differentiation. Mature osteoblasts also produce osteopontin, osteonectin, and osteocalcin, three extracellular matrix proteins deposited together with type I collagen into mineralized bone matrix (Rodan and Noda, 1991). Unfortunately, only a few differentiation markers have been identified and several of these, such as alkaline phosphatase, osteopontin and osteonectin, are not specific for osteogenic differentiation, while others, such as osteocalcin, are rarely expressed in vitro. In addition, mesenchymal cell

lines and primary cultures of differentiating chondrocytes and osteoblasts display a variable phenotype and are often a mixture of cell types at different stages of differentiation. Finally, cells are typically cultured on plastic without a substrate of extracellular matrix. Such conditions may not allow complete differentiation since interaction with extracellular matrix proteins and a three-dimensional structure may be required for full differentiation.

In vitro culture systems have also proven valuable in elucidating the cell-type specificity of signal transduction and transcriptional regulation. In this respect, mesenchymal cell lines are useful for the evaluation of osteoblast and chondrocyte-specific transcription factors. Those belonging to the bHLH family are of particular interest because of their role in the commitment and differentiation of many cell types. For example, factors of the muscle-specific MyoD family are required for the differentiation of skeletal myoblasts and can induce several cell types to express a skeletal muscle phenotype (Olson and Klein, 1994). In the case of osteoblasts, no specific bHLH genes have as yet been identified, yet indirect evidence suggests their existence. First, the expression of Id, an antagonist of bHLH protein binding to the promoter, is downregulated during osteoblast differentiation (Ogata and Noda, 1991, Kawaguchi et al., 1992), and overexpression of Id inhibits osteoblastic differentiation (Murray et al., 1992). Second, the promoter regions of several genes expressed in osteoblasts contain E-boxes which can act as DNA binding domains for bHLH proteins (Siddhanti and Quarles, 1994). Finally, induction of osteoblastic differentiation is associated with increased binding of nuclear extracts to E-boxes (Kawaguchi et al., 1992). Once specific transcription factors are identified, studies assessing the interaction between these transcriptional regulators and known secreted osteoinductive factors will be

of great interest to understand the patterning and regulation of mesenchymal differentiation in vivo.

In conclusion, recent studies of mice and humans with various skeletal abnormalities have pointed to many genes important in bone and cartilage development. In vivo and in vitro approaches have also led to an understanding of some of the molecular mechanisms that control the activity and differentiation of bone and cartilage cells. In the future, the convergence of these various approaches should provide greater insight into the morphogenesis of this complex organ system.

Chapter 2:

The tissue physiology of TGF-β

The transforming growth factor-β (TGF-β) superfamily of secreted peptide growth factors has been implicated in a vast array of cellular processes in the vertebrate animal. Besides the three TGF-β isoforms, TGF-β1, -β2, and -β3, which I will discuss here, the TGF-β superfamily includes the bone morphogenetic proteins (BMPs), the activins and inhibins, and the growth and differentiation factors (GDFs) (for a review see Kingsley, 1994). With TGF-β1 as a prototype, great progress has been made in understanding the molecular biology and biochemistry of these factors, and recently there have been rapid advances elucidating the mechanisms by which they evoke their cellular responses. Furthermore, the large literature on in vitro effects of TGF-β has provided substantial insights into potential cell-type specific activities. In more recent years, transgenic methodologies have started to reveal specific roles for the three TGF-β isoforms in development and tissue morphogenesis, and it is from this perspective that I will discuss their biology and tissue physiology. In keeping with this perspective, and because the literature on the in vitro physiology of TGF-β is so massive, I will reserve my citations of the primary literature generally to only those references that concern in vivo data.

Molecular biology and biochemistry.

The biochemical structures of the three mammalian TGF-β isoforms are very similar even though they are encoded by three separate genes with distinct patterns of expression (for a review see Derynck, 1994). TGF-β is made as a precursor peptide of 390 amino acids (TGF-β1) or 412 amino acids (TGF-β2 and -β3) that is composed of an N-terminal signal peptide, a large pro-segment called the latency-associated polypeptide (LAP), and the 112

amino acid C-terminal segment that constitutes the mature TGF-β monomer. This segment is 70-80% identical between the three TGF-β isoforms. In the golgi, mature TGF-β is cleaved from its pro-segment, however the two fragments remain associated. Processed TGF-β is secreted as a disulfide-linked dimer of the mature peptide associated non-covalently with two LAPs.

The extracellular physiology of TGF-β is quite complex (Derynck, 1994). Due to the binding of the LAPs, secreted TGF-β is inactive or "latent," since it cannot in this form bind cell-surface receptors. Furthermore, latent TGF-β associates with another protein named latent TGF-β binding protein (LTBP), which interacts through at least one disulfide bond with one of the LAPs. The generation of mature active TGF-β in vivo is thought to require the proteolytic processing of latent TGF-β to release the mature peptide, and this reaction might involve participation of the LTBP. Activation presumably occurs at the cell surface, where the mannose-6-phosphate-containing carbohydrates linked to the pro-segments of TGF-β interact with mannose-6-phosphate receptors, and appears to require the activity of type II transglutaminase. The primary proteolytic activators of TGF-β in vivo are thought to be plasmin and cathepsins, although other mechanisms, such as acid-activation by osteoclasts, are also possible.

The binding of latent and active TGF-β to various extracellular matrix components is thought to be important in regulating the storage of TGF-β and its presentation to cells (Derynck, 1994). Binding to the proteoglycans decorin and biglycan inactivate TGF-β, while binding to thrombospondin, fibronectin, and several collagens including type IV collagen may create a sequestrated reservoir of active TGF-β. LTBP itself can be considered part of the extracellular matrix, as it may serve as a structural matrix protein in bone

(Dallas et al., 1995). Lastly, the high-affinity binding of α-2-macroglobulin is thought to be important in the inactivation of active TGF-β, its scavenging from tissues and plasma, and its ultimate hepatic clearance.

TGF-β receptor signaling.

TGF-β binds to the cell surface via three classes of high-affinity transmembrane receptors (for a review see Derynck and Feng, 1997). On most cell types, the type III receptor is the proteoglycan betaglycan, whereas on vascular endothelial cells and several hematopoetic cell types, the type III receptor is the glycoprotein endoglin. Both molecules are expressed as homodimers with large extracellular domains but minimal cytoplasmic tails, and so they are not thought to be directly involved in downstream TGF-β signaling. However, type III receptors are thought to be involved in the presentation and binding of TGF-β to the signaling type I and II receptors. This is particularly important in the case of TGF-β2, which has only a very low affinity for the type II receptor in the absence of betaglycan, and may explain the relative resistance of endothelial and hematopoetic cells to this isoform (Ohta et al., 1987; Ottmann and Pelus, 1988; Merwin et al., 1991; Qian et al., 1992). The extracellular domain of betaglycan can also be released from the cell surface by plasmin, suggesting that this soluble form may bind and sequestrate TGF-β in the extracellular matrix. Mutations in endoglin have been shown to be the cause of hereditary hemorrhagic telangiectasia type I, implicating defective TGF-β signaling in the pathogenesis of this disease (McAllister et al., 1994).

The signaling receptors for TGF-β are the type I and II receptors, called TβRI and TβRII (Derynck and Feng, 1997). Both molecules are transmembrane

serine and threonine kinases. The final TGF-β signaling complex is thought to be a heterotetramer of two type I and two type II molecules. While type I and type II receptors might unstably associate with one another in the absence of ligand, ligand binding stabilizes the receptor heteromer and allows for the transphosphorylation of type I receptors by type II receptors, which are constitutively active. Further downstream signaling is thought to occur through the type I receptor, with lower levels of activation leading to the transcriptional induction of extracellular matrix components and protease inhibitors, and higher levels leading additionally to growth arrest responses (see below).

Signaling downstream from the type I receptor is thought to occur via interactions with the Smad family of proteins, although other cytoplasmic proteins have been shown to interact with TGF-β receptors (Derynck and Feng, 1997). Upon receptor activation, type I receptors are thought to phosphorylate Smad2 and Smad3, which then are released from the receptor complex to bind Smad4. This activated Smad complex then translocates to the nucleus where it acts as a transcriptional activator, possibly in conjunction with other nuclear factors. Since different Smads share overlapping specificities for different receptors of the TGF-β superfamily, and inhibitory Smads also exist, complex combinatorial control of Smad-receptor and Smad-Smad interactions are likely to play a major role in integrating the cellular responses to TGF-β and related factors.

Cellular responses to TGF-β.

TGF-β has many potent effects on cells in tissue culture (for reviews see Derynck, 1994; Roberts and Sporn, 1990). First, TGF-β regulates cell

proliferation, as will be discussed below. Second, TGF-β regulates cell differentiation in a highly cell type-specific fashion that also depends heavily on culture conditions. Third, TGF-β regulates extracellular matrix (ECM) turnover by inducing ECM components such as fibronectin, thrombospondin, tenascin, osteopontin, osteonectin and several proteoglycans and collagens, and by controlling the secretion and activation of ECM proteases and their inhibitors. Fourth, TGF-β induces integrin expression and therefore modulates cell-matrix interactions. Lastly, TGF-β is a potent chemoattractant for several cell-types, especially those involved in inflammatory responses. Overall, the physiological relevance of these effects towards normal development and tissue homeostasis has been unclear, because virtually every cell type in tissue culture expresses TGF-β isoforms and receptors, yet expression of these molecules is very restricted during development and adult life. Rather, many tissue culture phenomena may be analogous to effects induced by TGF-β during wound healing or tissue repair processes. Indeed, the induction of TGF-β activity by disrupted cell-matrix interactions and inflammatory mediators at sites of tissue damage is thought to be a key aspect of the would healing response in vivo (Border and Noble, 1994).

In general, TGF-β inhibits the proliferation of epithelial and hematopoetic cells, and stimulates the proliferation of mesenchymal cells (for reviews see Derynck and Feng, 1997; Derynck, 1994). The inhibition of epithelial cell proliferation is a direct effect of TGF-β that is thought to occur primarily through the induction of several cdk inhibitors. The induction of cdk inhibitors leads to the inactivation of corresponding G1 cdk/cyclin complexes, which in turn prevents these complexes from

hyperphosphorylating pRB. With pRB maintained in its underphosphorylated form, the cell cycle arrests in late G1. In contrast, the stimulation of mesenchymal cell proliferation is likely to be indirectly mediated through the induction or enhancement of other stimulatory growth factors or cell-matrix effects. In the case of smooth muscle cells, fibroblasts and chondrocytes, low concentrations of TGF-β induce the endogenous production of PDGF-AA, which acts in an autocrine fashion to stimulate cell growth. Interestingly, this stimulation is not seen at higher concentrations of TGF-β due to its concomitant down-regulation of PDGF receptor α subunits. These kinds of complex bimodal effects might be relevant to development and tissue morphogenesis.

Requirements for TGF-β during development.

Mice with inactivated alleles of the three TGF-β isoforms or the type II TGF-β receptor have provided substantial insights into the requirements for these factors during development. The lethal defects seen in TGF-β1 knockout mice (Shull et al., 1992; Kulkarni et al., 1993) occur either early in development or during postnatal life, with embryonic survival determined by interactions with other strain-specific loci (Bonyadi et al., 1997). Embryonic death occurs at around embryonic day 10.5, due to defective hematopoiesis and endothelial differentiation in the extraembryonic yolk sac (Dickson et al., 1995). These defects are nicely corroborated by the identical abnormalities seen in mice with targeted disruption of the type II receptor (Oshima et al., 1996). Postnatal death in TGF-β1 deficient mice occurs by about three weeks of age due to a multifocal lymphocyte-mediated inflammatory response (Diebold et al., 1995), showing that TGF-β1 is normally

required for the endogenous suppression of immune responses, as suggested by previous in vitro data (Derynck, 1994). Since the inflammatory defect in TGF-β1 knockout mice can be prevented by crossing the targeted allele onto a severe combined immunodeficiency (SCID) background (Diebold et al., 1995), analysis of other tissue pathologies caused by TGF-β1 deficiency should now be possible (e.g. see the discussion of epidermal cell proliferation below).

TGF-β3 knockout mice show perinatal lethality due to a defect in secondary palate fusion and a delay in embryonic lung morphogenesis, two processes that involve epithelial-mesenchymal interactions (Kaartinen et al., 1995; Proetzel et al., 1995). Interestingly, overexpression of TGF-β1 during lung morphogenesis in transgenic mice inhibits the differentiation of the pulmonary epithelium (Zhou et al., 1996), suggesting that the positive requirement for TGF-β3 may be restricted to earlier stages of lung development.

Lastly, targeted disruption of TGF-β2 leads to perinatal lethality with abnormalities in heart, lung, eye, inner ear and urogenital development (Sanford et al., 1997). Mice also show hypoplasia of several cranial, appendicular and axial skeletal structures, suggesting a role for TGF-β2 in early bone and cartilage development. Many of the perturbed developmental processes require epithelial-mesenchymal interactions or neural crest cell contributions. Surprisingly, the defects seen in TGF-β2 knockout mice are almost entirely non-overlapping with those seen in the TGF-β1 and TGF-β3 knockouts, showing that the three TGF-β isoforms have very distinct functions during development.

The role of TGF-β in tissue morphogenesis and homeostasis.

Whereas knockout experiments have revealed the absolute requirements for the specific TGF-β isoforms during development, several issues have clouded the assessment of TGF-β physiology during later tissue development. First, functional redundancy may prevent the identification of sites of TGF-β action other than those affected in single knockout experiments. Furthermore, the embryonic and perinatal lethality of knockout mice precludes analysis at later stages of development, and early developmental defects may alter the appearance of later defects. Finally, analysis of TGF-β1 knockout mice surviving to adulthood is complicated by the need to distinguish systemic responses from local primary effects.

Instead, transgenic models using tissue-specific promoters to drive the overexpression of either TGF-β ligands, for gain-of-function analysis, or dominant-negative TGF-β receptors, for loss-of-function analysis, promise to reveal important aspects of TGF-β physiology in mature tissues. Indeed, two general themes have already emerged from this approach, both which bear out predictions from cell culture work. First, TGF-β is both necessary and sufficient for inhibiting the proliferation of a number of epithelial cell types. Besides the transgenic studies discussed below, in vivo evidence comes from the observations that mutations in type II TGF-β receptors are associated with a number of human epithelial cancers (Markowitz and Roberts, 1996), and that defects in *DPC-4*, the human homologue of Smad4, are present in the majority of pancreatic cancers (Hahn et al., 1996). The second general theme is that TGF-β induces inflammatory processes associated with fibrosis, as first observed in vivo following injection of TGF-β1 (Roberts et al., 1986). However, these effects have not been consistently seen in TGF-β

overexpression experiments, and it is possible that they instead reflect physiological or enhanced tissue repair responses to other primary pathologies. Besides those discussed below, examples of this phenomenon potentially include the hepatic fibrosis, arteritis, myocarditis, glomerulonephritis and glomerulosclerosis seen in mice overexpressing high levels of bioactive TGF-β1 from the albumin promoter, which leads to systemic levels of TGF-β1 activity (Sanderson et al., 1995; Kopp et al., 1996), and the overproduction of extracellular matrix following injury-induced astrogial activation in transgenic mice overexpressing TGF-β1 in astrocytes (Wyss-Coray et al., 1995).

In the epidermis, TGF-β1 overexpression from the K1 keratin promoter causes neonatal lethality associated with a strong inhibition of basal keratinocyte proliferation, and a reduction in the number of hair follicles (Sellheyer et al., 1993). Reciprocally, overexpression of a truncated (dominant-negative) type II TGF-β receptor in the epidermis from the loricrin promoter causes an increase in basal and suprabasal keratinocyte proliferation, and a hyperplastic and hyperkeratotic phenotype (Wang et al., 1997). Similarly, TGF-β1 knockout mice show increased basal keratinocyte proliferation, and loss of TGF-β expression during epidermal carcinogenesis correlates with hyperproliferation and a high risk for malignant conversion (Glick et al., 1993). Lastly, TGF-β1-null keratinocytes initiated by the v-ras^{Ha} oncogene rapidly progress to squamous cell carcinoma when transplanted onto nude mice (Glick et al., 1994). Together, these results strongly suggest that a major role of TGF-β in the skin is to suppress keratinocyte proliferation. Interestingly, overexpression of TGF-β1 from the epidermal K10 promoter inhibits the increase in basal keratinocyte proliferation caused by treatment of

adult mice with the tumor promoter TPA, as would be expected, but stimulates proliferation in the uninduced state (Cui et al., 1995). Growth inhibition correlates with the TPA-induced upregulation of type II TGF-β receptors. Furthermore, these and related mice are resistant to the induction of benign skin tumors by chemical carcinogenesis, but their malignant conversion rate is greatly increased (Cui et al., 1996). One possibility that might explain these seemingly contradictory results is that TGF-β stimulation of the underlying dermis indirectly induces keratinocyte proliferation through a secondary signal. Indeed, the proliferation of TGF-β1-null keratinocytes is reduced when they are transplanted along with TGF-β1-null stromal cells (Glick et al., 1994). Thus, TGF-β produced by keratinocytes might inhibit keratinocyte proliferation as a direct autocrine effect, but TGF-β produced at either high levels by the epidermis, or within the dermis itself, induces the dermal production of a secondary factor that stimulates keratinocyte proliferation.

In the mammary gland, TGF-β1 overexpression from the whey-acidic protein (WAP) promoter prevents the formation of the secretory mammary epithelium that develops during pregnancy and that is required for lactation (Jhappan et al., 1993). Transplantation experiments showed that this is a direct autocrine effect of TGF-β1 on the epithelium itself, and is associated with an increase in the rate of epithelial cell apoptosis and a decrease in the rate of epithelial cell proliferation (Kordon et al., 1995). Significantly, these mice show no defects in mammary duct development. In contrast, overexpression of TGF-β1 from the MMTV enhancer/promoter inhibits ductal development, associated again with a decrease in the proliferation of the epithelium (Pierce et al., 1993). Furthermore, its expression markedly suppresses mammary

tumor formation caused by coexpression of a MMTV-TGF-α transgene (Pierce et al., 1995). Interestingly, MMTV-TGF-β mice show no defects in the outgrowth of the secretory mammary epithelium during pregnancy (Pierce et al., 1993). Since expression of the WAP promoter is restricted to mammary epithelial cells committed to a secretory state and is upregulated during pregnancy, the differential effects of the WAP-TGF-β1 versus MMTV-TGF-β1 transgenes may correlate with their patterns of expression, indicating a very local mode of action for secreted TGF-β (Kordon et al., 1995).

Lastly, overexpression of TGF-β1 in the pancreas from the insulin promoter suppresses acinar cell proliferation and causes an inflammatory cell infiltration and a progressive fibrosis to eventually replace all of the exocrine pancreas (Lee et al., 1995). Islet cell mass, however, is not affected. Reciprocally, expression of a dominant-negative type II TGF-β receptor from the metallothionein 1 promoter, which led in this experiment to transgene expression in acinar cells, causes an increase in the proliferation and apoptosis of acinar cells, and potentially their dedifferentiation into ductular cells (Bottinger et al., 1997). Acinar cells were progressively replaced with adipose tissue and intralobular fibrosis. The fibrosis was explained as the result of a compensatory upregulation of TGF-β1 and TGF-β3 by acinar cells, inducing extracellular matrix production by the surrounding stroma. Together, these transgenic mice suggest that TGF-β is required for the suppression of acinar cell proliferation and the maintenance of their differentiated state.

In conclusion, transgenic methodologies have begun to allow the assessment of the roles of the multifunctional growth factor TGF-β in tissue development and homeostasis. Experiments overexpressing either TGF-β

ligands or dominant-negative TGF-β receptors have provided significant insights into the functions of TGF-β in three epithelial tissues in particular: the epidermis, mammary gland and pancreas. The work presented in this dissertation applies this kind of transgenic approach towards understanding the actions of TGF-β in the skeletal system.

Chapter 3:

Increased expression of TGF-β2 in osteoblasts results in an osteoporosis-like phenotype

ABSTRACT

The development of the skeleton requires the coordinated activities of bone-forming osteoblasts and bone-resorbing osteoclasts. The activities of these two cell types are likely to be regulated by TGF-β, which is abundant in bone matrix. We have used transgenic mice to evaluate the role of TGF-β2 in bone development and turnover. Osteoblast-specific overexpression of TGF-β2 resulted in progressive bone loss associated with increases in osteoblastic matrix deposition and osteoclastic bone resorption. This phenotype closely resembles the bone abnormalities seen in human hyperparathyroidism and osteoporosis. Furthermore, a high level of TGF-β2 overexpression resulted in defective bone mineralization and severe hypoplasia of the clavicles, a hallmark of the developmental disease cleidocranial dysplasia. Our results suggest that TGF-β2 functions as a local positive regulator of bone remodeling and that alterations in TGF-β2 synthesis by bone cells, or in their responsiveness to TGF-β2, may contribute to the pathogenesis of metabolic bone disease.

INTRODUCTION

Normal skeletal morphogenesis relies upon the coordinated activities of multiple cell types. The principal cell types in bone are osteoblasts, which are of mesenchymal origin and synthesize bone matrix, and osteoclasts, which are derived from the hematopoietic system and resorb bone. During development and adult life, osteoblasts and osteoclasts continuously replace old bone with new bone through a process termed bone remodeling (reviewed in Parfitt, 1994). Bone remodeling occurs through discrete cycles of localized resorption followed by new bone synthesis in resorbed areas. The coordinated nature of these cycles implies the existence of mechanisms that couple osteoblastic bone formation to osteoclastic bone resorption in a site-specific manner and link the remodeling cycle to the local differentiation of osteoblasts and osteoclasts from their respective precursor populations. By matching resorption with formation, bone remodeling normally maintains skeletal integrity and preserves bone mass and shape.

The failure to coordinate osteoclastic bone resorption with osteoblastic bone deposition results in metabolic bone disease. In many cases, such as osteoporosis and hyperparathyroidism, this failure leads to a progressive net loss of bone mass with time. The nature of the bone remodeling defects observed in various bone diseases suggests that distinct components of the remodeling cycle, including the frequency and extent of osteoclastic bone resorption, as well as the rate of osteoblastic bone deposition, are actively regulated (Parfitt, 1983). Several systemic hormones are known to influence bone turnover, and it is likely that they act through local factors present within bone (Mundy, 1993). How these factors control bone development and

remodeling by locally regulating the activity, differentiation and interactions of resident bone cells, is largely unknown.

Several lines of evidence have suggested that the secreted polypeptide transforming growth factor-β (TGF-β) could be involved in the local regulation of skeletal development and turnover (reviewed in Centrella et al., 1994). High concentrations of all three TGF-β isoforms (TGF-β1, TGF-β2 and TGF-β3) can be extracted from mineralized bone matrix and TGF-β is synthesized by osteoblasts and osteoclasts in vivo (Seyedin et al., 1985; Robey et al., 1987; Sandberg et al., 1988; Pelton et al., 1991). TGF-β has potent effects on bone cells in vitro and in vivo. Local injection of TGF-β under the periosteum stimulates cartilage and bone formation (Noda and Camilliere, 1989; Joyce et al., 1990), and systemic injection of TGF-β2 leads to a generalized increase in osteoblastic activity (Rosen et al., 1994). In vitro, TGF-β induces extracellular matrix secretion by osteoblasts, inhibits matrix mineralization, and modulates osteoprogenitor cell proliferation and the expression of osteoblastic differentiation markers (reviewed in Bonewald and Dallas, 1994; Centrella et al., 1994). Results, however, have varied substantially depending upon the cell system. The effects of TGF-β on osteoclast differentiation and bone resorption are also complex and may be indirectly modulated through non-osteoclastic cell types (Hattersley and Chambers, 1991). Neonatal and fetal organ culture studies have generally indicated that TGF-β inhibits osteoclast differentiation from bone marrow monocytes, yet stimulates bone resorption by differentiated osteoclasts (Tashjian et al., 1985; Chenu et al., 1988; Pfeilschifter et al., 1988; Dieudonné et al., 1991; Hattersley and Chambers, 1991).

The normal role of TGF-β in bone development has been hard to infer from these studies. Besides its complex and variable effects on bone cell populations in vitro and in vivo, a given experimental result with TGF-β may be potentially relevant to many different aspects of skeletal morphogenesis, including the generation of bone shape, bone growth, or bone remodeling. Furthermore, the exogenous application of TGF-β does not mimic its route of production within bone. Osteoblasts produce TGF-β largely as a bone matrix-bound latent complex that may be unable to induce cellular responses unless first released from mineralized bone during osteoclastic bone resorption (Pfeilschifter and Mundy, 1987). Lastly, the short term nature of TGF-β administration in both in vitro and in vivo experiments precludes an evaluation of the skeletal actions of TGF-β at steady-state.

To gain more direct insight into the role of TGF-β in bone morphogenesis, we generated transgenic mice that overexpress active TGF-β2 specifically in bone. Increased synthesis of TGF-β2 in osteoblasts leads to a dramatic, age-dependent loss of bone mass. This phenotype is attributed to a primary defect in bone remodeling, associated with increased activities of both osteoblasts and osteoclasts. Our results implicate TGF-β and more specifically TGF-β2 as an important local regulator of bone remodeling in vivo and raise the possibility that altered TGF-β2 expression or responsiveness may underlie the local pathogenesis of osteoporosis, hyperparathyroidism, and other metabolic bone diseases.

MATERIALS and METHODS

Expression plasmid. PCR mutagenesis was performed on the human TGF-β2 cDNA (de Martin et al., 1987) to replace cysteine codons 226 and 228 in the TGF-β2 precursor with codons TCT and AGC for serine, and to introduce a 5' EcoRI site (preceding nucleotide 178) and a 3' BamHI site (following nucleotide 1426) to allow subcloning. The resulting fragment was sequenced to confirm that no other point mutations were introduced during PCR amplification. The expression plasmid pOc-β2C2S2, cloned into pcDNAII (Invitrogen), consisted of a 1.8 kb fragment of the rat osteocalcin promoter (Baker et al., 1992), followed by a 0.65 kb fragment spanning the rabbit β-globin second intron (O'Hare et al., 1981), the mutated 1.3 kb TGF-β2 cDNA fragment and a 0.63 kb fragment of the human growth hormone gene to allow polyadenylation. Mature human TGF-β2 expressed by pOc-β2C2S2 has 97% amino acid sequence identity to mouse TGF-β2 (Miller et al., 1989). To verify that this plasmid could express TGF-β2, it was transfected into ROS 17/2.8 osteosarcoma cells using the Ca_2PO_4 precipitation method. As a control, cells were transfected with a plasmid expressing β-galactosidase under control of the osteocalcin promoter. Tissue culture supernatant was collect 72 h after transfection, concentrated 10-fold on a Centricon C-10 column (Amicon), and assayed by TGF-β2 ELISA (Amersham).

Transgenic mice. DBA2 x C57BL/6 F1 (B6D2 F1) mice (Jackson Laboratories) were used to generate transgenic mice using standard techniques (Hogan et al., 1986). We injected the osteocalcin-TGF-β2 expression insert excised as a 4.4 kb BamHI fragment from pOc-β2C2S2, and purified by Geneclean (Bio

101). Transgenic mice were identified using Southern blot analysis of tail DNA (Laird et al., 1991) using the β-globin intron fragment as a hybridization probe. Transgenic lines were established and maintained on a B6D2 F1 background, and subsequent generations of transgenic animals were identified by non-radioactive dot blot using either the β-globin intron or growth hormone poly(A) fragments as probes. Non-radioactive hybridization reagents were purchased from Boehringer Mannheim and used as described (Engler et al., 1993) .

RNA analysis. Total bone RNA was isolated from 4-5 week-old animals. Femurs and humeri were dissected and cleaned of soft tissues. Epiphyses were cut off, and the bone marrow was flushed out with PBS. Bones were then crushed in a mortar in liquid nitrogen, and further homogenized on ice in a Omni 200 tissue homogenizer (Omni International) for 30 s in 4 ml Ultraspec RNA isolation reagent (Biotecx). RNA was purified according to the manufacturer's instructions, and treated with RQ1 DNAase (Promega) before further analysis. One mouse typically yielded 25-40 μg total bone RNA.

Total bone RNA from two mice from each transgenic line was analyzed for the presence of spliced transgene mRNA by reverse-transcriptase PCR (RT-PCR). Reverse-transcriptase (RT) reactions were performed on 500-800 ng RNA in a 20 μl of 1X PCR buffer (Gibco-BRL), 2.5 mM $MgCl_2$, 1 mM dNTPs, 100 pmol random hexanucleotides (Pharmacia), 1 mM DTT, 0.5 μl RNasin (Promega), and 1 ml MMTV reverse transcriptase (Gibco-BRL). Control reactions without reverse transcriptase were done in parallel. RT reactions were incubated for 10 min at room temperature, 30 min at 37°C, 30 min at

42°C, and then stored directly at 4°C. To detect the spliced transgene cDNA by PCR, the 5' primer (5'-TCCTGAGAACTTCAGG/CTCCTG-3') spanned the rabbit β-globin intron splices sites and the 3' primer (5'-CCTTGGCG-TAGTACTCTTCGTC-3') was located within the TGF-β2 cDNA, to yield an expected product of 378 bp. 1 µl of RT reaction was amplified by PCR cycling in a 50 µl reaction volume containing 1X PCR buffer (Gibco-BRL), 3 mM $MgCl_2$, 0.2 mM dNTPs, 0.1% Triton X-100, 10 pmol each primer, and 0.25 µl Taq polymerase (Gibco-BRL). 20 µl of the reaction was run on a 2% TBE agarose gel stained with ethidium bromide. To confirm that the resulting DNA bands corresponded to TGF-β2 cDNA, we performed Southern blot hybridization using a human TGF-β2 cDNA fragment as probe. As a control for RNA quality and successful RT reactions, 1 µl of each RT reaction was amplified using primers specific for the osteocalcin gene (Araki et al., 1993) in 1.5 mM $MgCl_2$.

Preparation of bone extracts. Bone extracts were prepared as described (Finkelman et al., 1991) with modifications, from 35 day-old transgenic and non-transgenic females. Femurs and humeri were cleaned of soft tissue and the epiphyses and bone marrow were removed. Bones were stored at -70°C. To prepare bone powder, bones were crushed in a mortar in liquid nitrogen and fat was removed as described (Finkelman et al., 1991), yielding 15-30 mg bone residue. Bone powder was then extracted for 36 h at 4°C in 300 µl extraction buffer (4 M guanidine hydrochloride, 10% EDTA, 30 mM Tris-HCl pH 7.4) containing 5 µg/ml aprotinin, 5 µg/ml leupeptin, and 1 mM PMSF, with constant rotation. After removal of the debris by 15 min centrifugation,

supernatants were collected and stored at 4°C and assayed for protein concentration using the Bradford assay (Biorad).

Determination TGF-β protein concentrations. TGF-β1 and TGF-β2 concentrations were quantitated using TGF-β1- and TGF-β2-specific ELISA kits (R&D Systems and Amersham, respectively), according to the manufacturers' instructions. All bone samples were assayed in duplicate.

In bone samples, TGF-β was already activated due to the protein extraction in guanidine-HCl and did not require further acid-activation prior to ELISA. However, to assay TGF-β in culture media and plasma, samples were acid-activated (Lawrence et al., 1985) by addition of 1/10th volume of 1.2 N HCl at room temperature and neutralized after 20 min by addition 1/5th volume 0.72 N NaOH, 0.5 M Hepes. 80 µl of plasma were assayed per mouse, with two mice per test group, and five control mice. Active and latent TGF-β2 levels in cell culture media were assayed using duplicate samples either treated or untreated with acid.

Serology, body weights. Serum was collected by eye bleeds from 3 sex-matched transgenic and 3 non-transgenic littermates per age group. Calcium, phosphorous, total protein, and creatinine were determined by automated protocols (California Veterinary Diagnostics, Inc., West Sacramento, Ca.). Heparinized tubes were used for the collection of plasma. Weights of juvenile mice were measured from several groups of 2-3 transgenic and non-transgenic sex-matched littermates.

X-ray analysis. After sacrifice by CO_2 inhalation, radiographs were taken on a Hewlett-Packard faxitron model 43805 N, using Kodak X-OMAT TL film.

Exposure was for 1 min at 35 kVp. For 35 day old mice, a total of 16 D4, 7 D5 mice and 13 control littermates were analyzed. For 5 to 11 month old males and virgin females, a total of 7 D4 and 8 D5 mice, as well as 20 control littermates and non-littermates were analyzed. Consistent results were obtained from mice of the same line and age.

Histology and TGF-β2 immunohistochemistry. For paraffin-embedded sections, bones were fixed at 4°C in 2% paraformaldehyde/PBS, and decalcified for 4 h in 22.5% formic acid, 10% sodium citrate at room temperature. 5 μm sections were stained with hematoxylin and eosin for routine analysis using established procedures (Sheehan and Hrapchak, 1980). For each age group, 2 to 3 bones per mouse from at least 2 to 5 mice of each line were analyzed. Serial cross sections of tibia were standardized in reference to the hypertrophic cartilage-metaphyseal junction, defined as the cross section with an area occupied by 50% hypertrophic cartilage and 50% primary spongiosa.

Anti-TGF-β2 immunohistochemistry was performed as modified from Pelton et al. (1991) using rabbit anti-TGF-β2 (kindly supplied by Dr. Leslie Gold, NYU Medical School) at a concentration of 2.5 μg/ml. An HRP-conjugated donkey anti-rabbit secondary antibody (Amersham) was used at a 1:100 dilution. Diaminobenzidine was used as substrate for the HRP reaction and the sections were counterstained with hematoxylin.

For osteoclast detection using histochemical staining for tartrate-resistant acid phosphatase (TRAP) activity, femurs fixed in 2% paraformaldehyde/PBS were decalcified for 3 d at 4°C in 10% EDTA, 0.1 M Tris pH 6.95, embedded in Tissue-Tek OCT compound, and sectioned at 10

μm. After equilibration in 0.2 M sodium acetate, 50 mM sodium tartrate pH 5.0 for 20 min at room temperature, sections were incubated for 17 min at 37°C in the same buffer containing 0.5 mg/ml naphthol AS-MX phosphate (Sigma) and 1.1 mg/ml Fast Red Violet LB salt (Sigma). Sections were counterstained in methyl green.

To detect bone mineralization, 4 μm undecalcified longitudinal sections of the tibia (see below) were stained by the von Kossa technique (Sheehan and Hrapchak, 1980) and counterstained with toluidine blue.

Quantitative and kinetic analyses. Trabecular surface density was calculated by a stereological method using transverse lines superimposed upon bone section micrographs (Weibel, 1969). From longitudinal sections of the proximal tibial metaphysis, data were collected from the entire area of the bone marrow cavity 200-1800 μm from the growth plate for 35 day old mice, and 0-1600 μm from the growth plate for 7-11 month old mice. Values represent the mean +/- standard deviation of the surface density calculated from at least 3 non-consecutive sections per mouse from 3 D4, 2 D5, and 3 non-transgenic littermate 35 day old mice, and 2 D4, 2 D5, and 4 control 7-11 month old mice.

Data for osteocyte density, and osteoblast and osteoprogenitor cell number were taken from cortical bone cross sections of the proximal tibia, 2.5-3.1 mm from the growth plate. Osteocyte density was calculated as the 3/2 power of the two-dimensional density in cross section, and osteoblast and osteoprogenitor cell number was calculated as the square of the one-dimensional density on the endosteal surface. Values represent the mean +/- standard deviation of 30-70 measurements per group of 2 D4 and 3 littermate

control mice. Standard deviations maintain the same percent error of the original lower-dimensional value. The rate of osteocyte differentiation was calculated as the product of the osteocyte density and the bone volume produced per day in a mm^2 unit area (the mineral apposition rate multiplied by the mm^2 unit area).

For the kinetic analyses, 31 day sex-matched transgenic and non-transgenic littermates were given intraperitoneal injections of 2.5 mg/kg calcein, followed by similar injections of 25 mg/kg tetracycline three days later. Mice were sacrificed at day 35, and their bones were fixed in 70% ethanol at 4°C. Prior to processing for undecalcified sectioning, bones were prestained using the Villanueva bone stain (osteochrome stain, Polysciences Inc.) for 3 d at 4°C. Matched bones were dehydrated and embedded with identical orientation in methylmethacrylate, sectioned at 4 μm, and viewed under UV light.

Since there was virtually no trabeculation in bones from D4 animals, including the vertebrae, data for the mineral apposition rate and mineralization lag time was taken from epiphyseal and diaphyseal endosteal surfaces of the tibia. Individual measurements for the mineral apposition rate were calculated as the distance between the double fluorochrome labels divided by three days, and for the mineralization lag time as the osteoid seam width divided by the mineral apposition rate at the same location. Values represent the mean +/- standard deviation of 40-80 measurements per group of 2 D4 and 2 littermate control mice.

Cleared skeletal preparations. Cleared skeletons stained with alizarin red or alcian blue staining of were prepared as adapted from Kaufman (Kaufman,

1992). We analyzed four litters of D4 males x B6D2 F1 females crosses, giving a total of 19 transgenic and 16 non-transgenic embryonic day 15.5 and 2 day old offspring.

RESULTS

TGF-β2 expression under the control of the osteocalcin promoter

We designed the plasmid pOc-β2C2S2 to drive the osteoblast-specific expression of biologically active TGF-β2 in transgenic mice (Fig. 1a). Among the three isoforms of TGF-β, we elected to express TGF-β2 because it is normally expressed by osteoblasts and is thought to be more active than TGF-β1 in inducing cartilage and bone formation (Seyedin et al., 1985; Joyce et al., 1990). TGF-β is normally made in a latent or biologically inactive form due to non-covalent interactions between its large precursor segments and the mature TGF-β homodimer (Centrella et al., 1994). To assure the secretion and availability of active TGF-β2, we introduced two point mutations that resulted in the replacement of cysteines at positions 226 and 228 in the TGF-β2 precursor segment by serines. Similar mutations of the corresponding cysteines in the TGF-β1 precursor (at positions 233 and 235) have been shown to lead to the spontaneous activation of a fraction of the TGF-β secreted by transfected cells in culture, presumably as a result of destabilization of the interactions between the precursor segments and the active TGF-β dimer (Brunner et al., 1989).

To achieve specific transgene expression in bone, we used a 1.8 kbp fragment of the rat osteocalcin promoter previously shown to direct osteoblast-specific expression (Baker et al., 1992). Osteocalcin is an abundant bone matrix protein specifically expressed by mature osteoblasts, but not by osteoprogenitor cells (Bronckers et al., 1985; Groot et al., 1986). We verified the expression of TGF-β2 from pOc-β2C2S2 following transfection of the plasmid into the osteocalcin-expressing osteosarcoma cell line ROS 17/2.8.

Figure 1. Generation and biochemical characterization of transgenic mice.

(A) Schematic presentation of the plasmid pOc-β2C2S2 expressing the human TGF-β2 with cysteines at positions 226 and 228 within the precursor segment replaced by serines. The direction of transcription and the position of the primers for RT-PCR analysis are indicated.

(B) RT-PCR analysis of transgene mRNA expression from bone RNA. The RT-PCR generated cDNA fragment was subjected to Southern blot analysis using a human TGF-β2 cDNA probe. The four lines that express the transgene mRNA are shown, and (a) and (b) represent two different mice of each line. Abbreviations: NT, non-transgenic; RT, reverse-transcriptase.

(C) Quantitation of TGF-β2 levels in bone matrix of 35 day old female mice. TGF-β2 concentrations were measured by TGF-β2 ELISA and normalized to total extracted protein concentration. The graph represents the mean and standard deviations of duplicate measurements of two animals per transgenic line and four non-transgenic littermates.

A

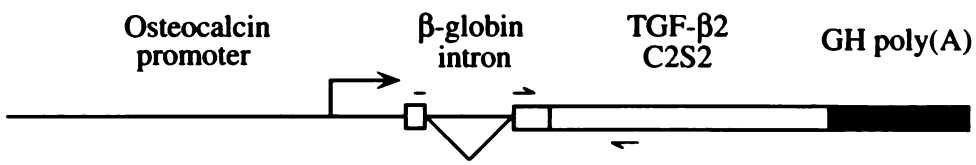
Osteocalcin promoter
β-globin intron
TGF-β2 C2S2
GH poly(A)

B

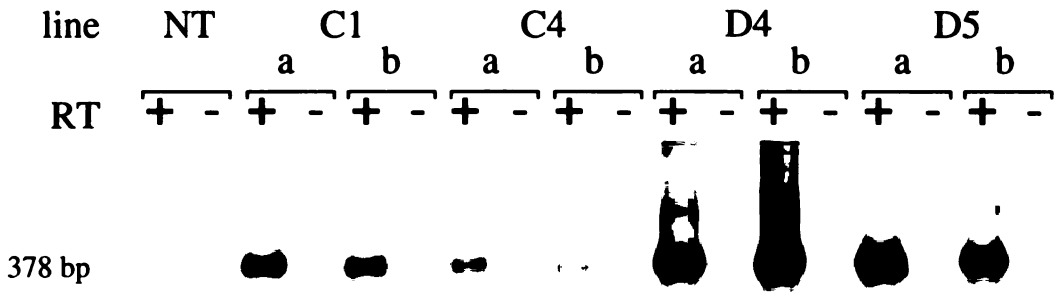
line
NT
C1
C4
D4
D5
a
b
RT
+ -
378 bp

C

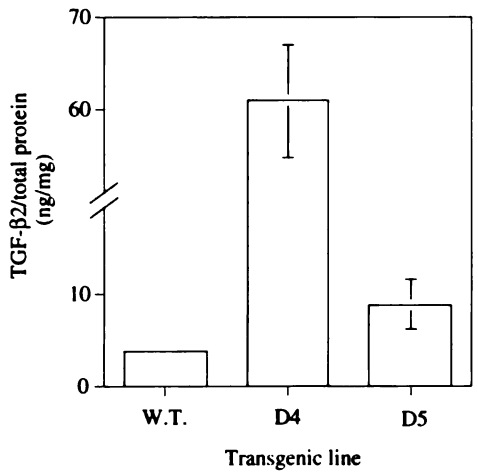
70
60
10
0
TGF-β2/total protein (ng/mg)
W.T.
D4
D5
Transgenic line

The double cysteine to serine mutation caused spontaneous activation of about 10% of the total amount of secreted TGF-β2 (data not shown).

Transgenic mice overexpressing TGF-β2 in osteoblasts

We established eight independent transgenic lines in which the transgene of pOc-β2C2S2 was stably integrated into the genome (data not shown). Four of these lines expressed the transgene mRNA as evaluated by RT-PCR of bone mRNA (Fig. 1b). The two mouse lines with the highest mRNA levels, D4 and D5, were chosen for detailed characterization. In contrast to the D5 line, we were unable to generate homozygous D4 animals, presumably as a result of intrauterine or perinatal death. We assessed transgene expression at the protein level using a specific ELISA to quantitate the TGF-β2 extractable from bone. Bone powder extracts from hemizygous D4 and D5 mice contained 16- and 2.5-fold more TGF-β2 than bone extracts from non-transgenic mice, as normalized to total extracted protein (Fig. 1c). The use of guanidine hydrochloride, which activates TGF-β2 in this extraction procedure, did not allow us to determine what fraction of the extracted TGF-β2 was active in situ. A TGF-β1-specific ELISA revealed that control bones contained 7.5-fold more TGF-β1 than TGF-β2 (data not shown). The level of TGF-β1 was unaltered in extracts of D5 bones, but was about 40% lower in D4 bones.

To localize the cellular sites of synthesis of TGF-β2 within bone, we stained longitudinal sections of the tibia of 35-day old D4 mice with a TGF-β2-specific antibody. Sections of transgenic bone showed a distinct increase in the TGF-β2 immunoreactivity of osteoblasts as compared with control sections (Fig. 2). The increased immunoreactivity was very pronounced in

Figure 2. Immunohistochemical detection of TGF-β2 expression in bone. Sections are through the proximal epiphysis of the tibia from 35-day old non-transgenic littermate (A) and D4 transgenic (B, C) females. (C) serves as a control of (B) in which the primary antibody against TGF-β2 is omitted from the staining procedure. The use of diaminobenzidine as a substrate results in brown staining for TGF-β2. Sections are counterstained with hematoxylin (blue). Transgenic bone shows strong TGF-β2 immunoreactivity in osteoblasts lining the endosteal surfaces (open arrows) in contrast to the low level of immunoreactivity within similar osteoblasts in non-transgenic bone (A). Endogenous TGF-β2 staining is seen in articular chondrocytes (a) and megakaryocytes (closed arrows). A low level of staining is seen in the bone marrow of both sections. Note also the increased number of plump, mature osteoblasts lining the surfaces of transgenic bone (B). Scale bar shows 100 μm. Abbreviations: a, articular chondrocytes; b, bone.

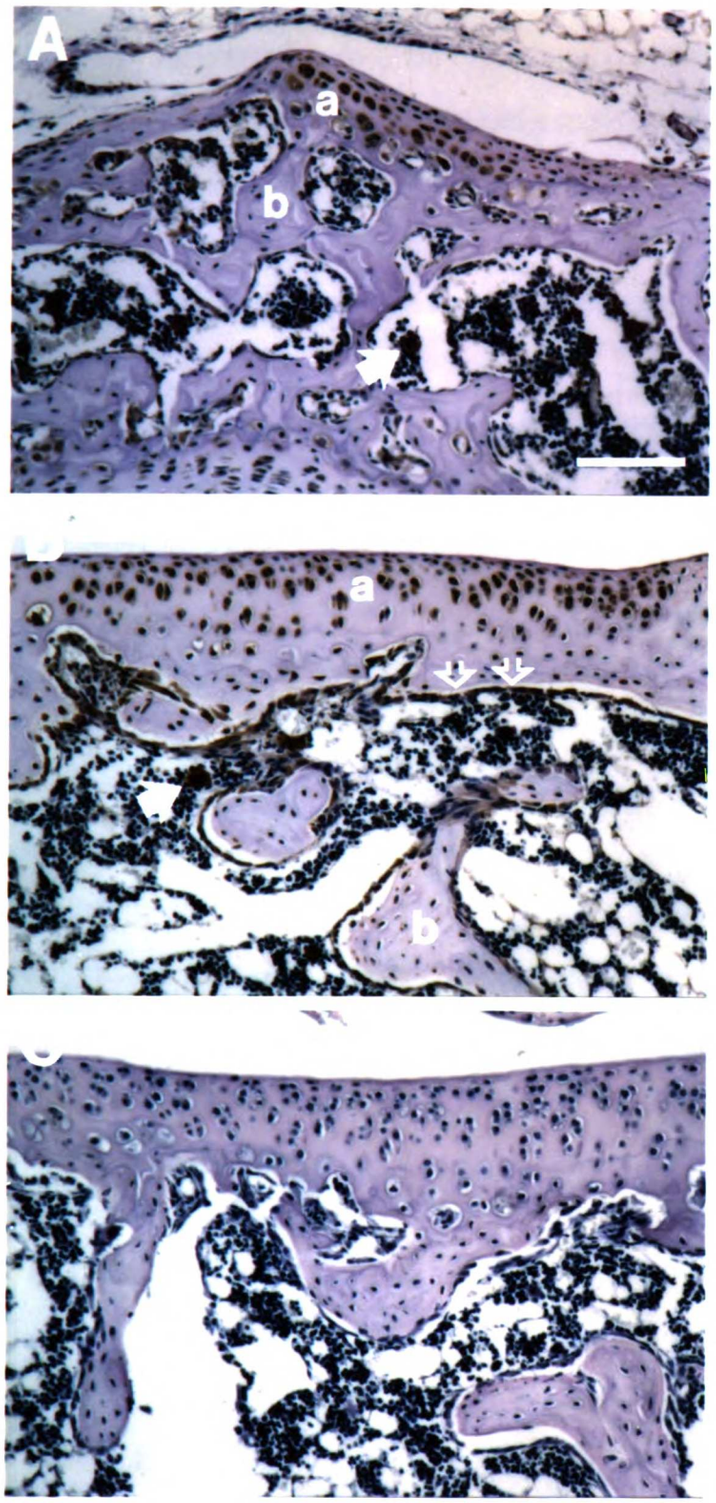

the osteoblasts lining epiphyseal bone surfaces (Fig. 2b, open arrows), but not in osteoblasts within the metaphysis (data not shown). In accordance with the osteoblast-specific expression of the osteocalcin promoter, there was no increase in the low level of endogenous TGF-β2 staining in bone marrow cells. In addition, both transgenic and control sections showed similar levels of strong endogenous TGF-β2 immunostaining in megakaryocytes (Fig. 2a and b, arrows), osteoclasts and articular chondrocytes, and moderate immunostaining in hypertrophic chondrocytes (Fig. 2 and data not shown).

Macroscopic evaluation of the skeletal phenotype

X-ray analysis revealed multiple skeletal defects in young mice of the high-expressing D4 line (Fig. 3). At 35 days of age, hemizygous D4 mice had a dramatic decrease in bone density (osteopenia) compared to normal littermates, as revealed by the generally radiolucent appearance of the entire skeleton (compare Fig. 3b and d with a and c) and the dramatic reduction in trabecular bone particularly evident in the metaphyses of long bones (Fig. 3a and b, arrows). Furthermore, the cortices of long bones were thinner than normal and frequently contained multiple internal radiolucent defects (Fig. 3b, arrowheads). Fracture calluses were regularly observed in long bones (Fig. 3b, asterisk), and callus-like focal lesions were frequently observed in the extremities, particularly at the distal ends of the radius, ulna, tibia, and fibula (data not shown). Based on their location and ultimate healing with time, these distal lesions most likely corresponded to stress fractures. The increased fragility of transgenic bones was also evident by the ease with which they were broken during dissection. By 7 months, hemizygous D4 mice were extremely osteopenic, with a glassy appearance of the entire skeleton

Figure 3. X-ray analysis of transgenic mice.

(A) and (B) Radiographs of the pelvis, tibia and femur of 35-day old non-transgenic littermate (A) and D4 transgenic (B) males. Transgenic bone is generally more radiolucent, and long bones show a dramatic reduction of metaphyseal trabeculation (arrows) and thinned cortices pockmarked with multiple radiolucent defects (arrowheads). There is also a fracture of the tibia and fibula (asterisk), with a clear fracture callus formed around the tibia. Scale bar shows 0.4 mm.

(C and D) Radiographs of the upper thorax of 35-day old non-transgenic littermate (C) and D4 (D) males. Only distal vestiges of clavicles are visible in the transgenic skeleton (arrows). As with (B), transgenic bone is more radiolucent than normal, and intracortical defects in the humerus are also apparent. The wild-type mouse shows an anterior arch of the atlas, a variable feature of normal mice. Scale bar shows 0.5 mm.

(E-G) Radiographs of the pelvis, proximal tibia, and femur of 7 month old non-transgenic (E) and D4 (F) and D5 transgenic (G) males. D4 bone (F) has an overall glassy appearance with a virtual absence of metaphyseal trabeculation, markedly reduced epiphyseal trabeculation and a thinned cortex. Radiographic changes are much milder in D5 mice than in D4 mice and only a marked reduction in metaphyseal and epiphyseal trabeculation is apparent (G). Arrows show areas of metaphyseal trabeculation in the distal femur. Scale bar shows 0.4 mm.

(compare Fig. 3f with 3e), a virtual absence of trabecular bone inside long bones (arrows), and a strikingly lower level of trabecular bone in the vertebrae. Soft tissue calcifications were apparent in the necks of aging D4 mice (1 yr old). Lastly, whereas all other bones had generally normal shapes and sizes, all D4 mice lacked normal clavicles and only small vestiges of their distal ends were apparent (Fig. 3c and d, arrows). This aspect of the D4 phenotype will be described in more detail below.

The D5 line had a considerably milder phenotype than the D4 line, consistent with its much lower level of TGF-β2 overexpression. Young (35 d) hemizygous and homozygous D5 mice did not have any obvious defects detectable by X-ray analysis; however, by 7 months of age, hemizygous D5 mice had a dramatic reduction of trabecular bone in the metaphyses of long bones (Fig. 3g, arrow) and in the vertebral bodies, particularly of the lower thoracic and upper lumbar regions (data not shown). The skeletal abnormalities in both lines were similar in males and virgin females.

Aside from these abnormalities, transgenic mice appeared generally healthy. The mortality rate and fertility of transgenic animals was similar to wild-type. All visceral organs appeared grossly normal at autopsy. Thirty five day old mice had normal body weights, tooth eruption was not delayed, and teeth appeared normal. Importantly, the lengths of long bones, an indication of longitudinal growth, were also normal. Only with increasing age did the body weight of D4 mice decrease in comparison to normal littermates (approximately 60% of normal in 6 month old D4 mice).

Based on various blood serum tests, there was no indication of a general metabolic disease in the high overexpressing D4 line. No differences in serum calcium and phosphorus levels were apparent between 35-day old

transgenic and control mice, while 6 month old transgenic animals had normal serum phosphorus, low serum calcium and normal serum protein levels (data not shown). These results indicate that D4 mice did not have primary hyperparathyroidism or a humoral hypercalcemia syndrome yet had a low circulating calcium level at older ages. Normal serum creatinine levels at 6 months of age excluded renal failure. Plasma TGF-β2 levels were normal in D5 mice, but were elevated three- to four-fold in 35-day old D4 mice, to about 2 ng/ml. At this level, circulating TGF-β is not physiologically relevant since it is inactivated by the abundant serum protein α2-macroglobulin (O'Connor and Wakefield, 1987; Huang et al., 1988). Taken together, our analyses support the notion that the observed skeletal abnormalities resulted from the localized overexpression of TGF-β2 and not from a general endocrine disturbance. It is likely that the hypocalcemia, low body weight and soft tissue calcifications observed in the older D4 mice were secondary manifestations of prolonged bone disease.

Histological appearance of transgenic bone

The progressive loss of bone mass in our overexpressing lines noted by X-ray was also apparent histologically (Fig. 4). When compared to sections of non-transgenic littermate controls at 35 days (Fig. 4a), longitudinal sections through the proximal tibia of D4 mice (Fig. 4b) revealed a thin cortex and a dramatic loss of trabeculation. In the metaphysis, trabecular surface density was reduced 70%, from 13.6 (+/- 1.4) mm^2/mm^3 in controls to 4.2 (+/- 2.5) mm^2/mm^3. Surprisingly, the epiphyseal growth plate, which is responsible for longitudinal growth, appeared normal. Similar longitudinal sections of the tibia from 7-month old D4 mice revealed a complete absence of

Figure 4. Age-dependent changes in histological appearance of transgenic bone.

(A-C) Longitudinal sections through the proximal tibia of 35 day old wild-type (A), D4 (B), and homozygous D5 (C) males. As compared with non-transgenic bone (A), D4 bone shows a thinned cortex and reduced trabeculation, dramatically in the metaphysis and moderately in the epiphysis (B). In the metaphysis, transgenic trabecular bone is apparent only in the immediate area of the growth plate, whereas in non-transgenic bone it extends down the length of the bone marrow cavity towards the diaphysis (arrows). In contrast to D4 bone, D5 bone (C) appears histologically normal at this age. The epiphyseal growth plates in both the D4 and D5 sections appear normal.

(D-F) Longitudinal sections through the proximal tibia of 7 month old wild-type (D), D4 (E), and hemizygous D5 (F) males. Cortical bone thinning and the extreme reduction in trabecular bone mass at this age is evident in D4 bone (E), as compared with non-transgenic bone (D), with a complete loss of trabeculation in the metaphysis and a dramatic reduction of trabeculation in the epiphysis. The residual growth plate cartilage is also more eroded in the D4 section (arrow) than in non-transgenic bone. In contrast to the normal phenotype in D5 bone at 35 days, 7 month old bone shows a complete loss of metaphyseal trabeculation and a moderate reduction in epiphyseal trabeculation (F), although clearly not as severe as in D4 bone.

Abbreviations: e, epiphysis; g, growth plate; m, metaphysis; d, diaphysis; c, cortical bone. Decalcified, paraffin-embedded sections were stained with hematoxylin and eosin. Scale bar shows 400 μm.

A
B
C
D
E
F
c
e
g
m
d

metaphyseal trabeculation (with a reduction in surface density from 5.2 (+/- 1.3) mm^2/mm^3 in controls to 0 mm^2/mm^3), very little remaining epiphyseal trabeculation, and extremely thin cortical bone (compare Fig. 4e with 4d). In contrast to the D4 line, hemizygous and homozygous D5 mice had only very mild alterations in phenotype at day 35 (Fig. 4c, with a metaphyseal surface density similar to controls at 15.1 (+/- 1.8) mm^2/mm^3), yet 7-month old hemizygous mice showed a complete absence of metaphyseal trabeculation (0 mm^2/mm^3 surface density), and dramatically reduced epiphyseal trabeculation (Fig. 4f).

The histological appearance of transgenic bone suggested an increase in osteoclastic resorption. The epiphyseal plates of 7 month old D4 mice were more eroded than those of control mice (Fig 4e, arrow). At 35 days, corresponding cross-sections of the tibia at equivalent distances from the growth plate (Fig. 5) showed that cortical bone was more porous than normal and contained large resorption lacunae lined by osteoblasts (Fig. 5b, arrows). Furthermore, endosteal resorption was more pronounced, and periosteal resorption, characteristic of the metaphysis, was apparent in more diaphyseal sections of transgenic bone (Fig. 5b and d). In equivalent diaphyseal sections of normal bone, the periosteum had already assumed its characteristically quiescent appearance (Fig. 5a and c). Surprisingly, no striking differences in the number of osteoclasts were observed between normal and D4 mice, as assessed by the osteoclast-specific histochemical stain for tartrate-resistant acid phosphatase activity (Fig. 6).

Histological sections of 35 day old D4 bone (Fig. 5d) also revealed marked increases in osteocyte density (a three-fold increase from 62,000 (+/- 14,000) cells/mm^3 to 197,000 (+/- 34,000) cells/mm^3) and osteoprogenitor cell

Figure 5. Histological appearance of transgenic bone.

(A and B) Cross sections of the tibia of 35 day old non-transgenic littermate (A), and D4 transgenic (B) males, 3.0-3.1 mm distal to the proximal epiphyseal growth plate. In contrast to smooth endosteal and periosteal surfaces characteristic of diaphyseal bone in non-transgenic bone, D4 bone shows extensive periosteal and more pronounced endosteal resorption. In addition, cortical bone is more porous than normal (arrows), and the periosteal and endosteal surfaces of D4 bone are extremely fibrotic. Scale bar shows 400 μm.

(C-E) Cross sections of the tibia of 35 day old non-transgenic (C), and D4 (D), and homozygous D5 (E) males, 3.0-3.1 mm distal to the proximal epiphyseal growth plate. Sections show equivalent areas of the tibia; (C) and (D) are high power views of areas in (A) and (B). The dramatic increase in cellularity of D4 bone (D) as compared with normal bone (C) is evident from the increased density of osteocytes within bone matrix and the increased number of fibroblastic osteoprogenitor cells (op) which give rise to the osteoblasts (ob) lining the endosteal and periosteal surfaces. Abundant extracellular matrix contributes to the fibrotic appearance of the endosteum and periosteum. A resorption lacuna extending deep within cortical bone is marked (closed arrow). Areas of prior resorption refilled with new bone matrix (light pink) are apparent at the bone surface under the periosteum, where a scalloped cement line demarcates new from old bone (open arrow). Similar areas are also apparent deep within cortical bone and on non-resorbed endosteal surfaces. In contrast to D4, D5 bone (E) shows no detectable histological alterations from wild-type. Scale bars show 100 μm.

Abbreviations: b, cortical bone, m, bone marrow, e, endosteum, p, periosteum. Decalcified, paraffin-embedded sections were stained with hematoxylin and eosin.

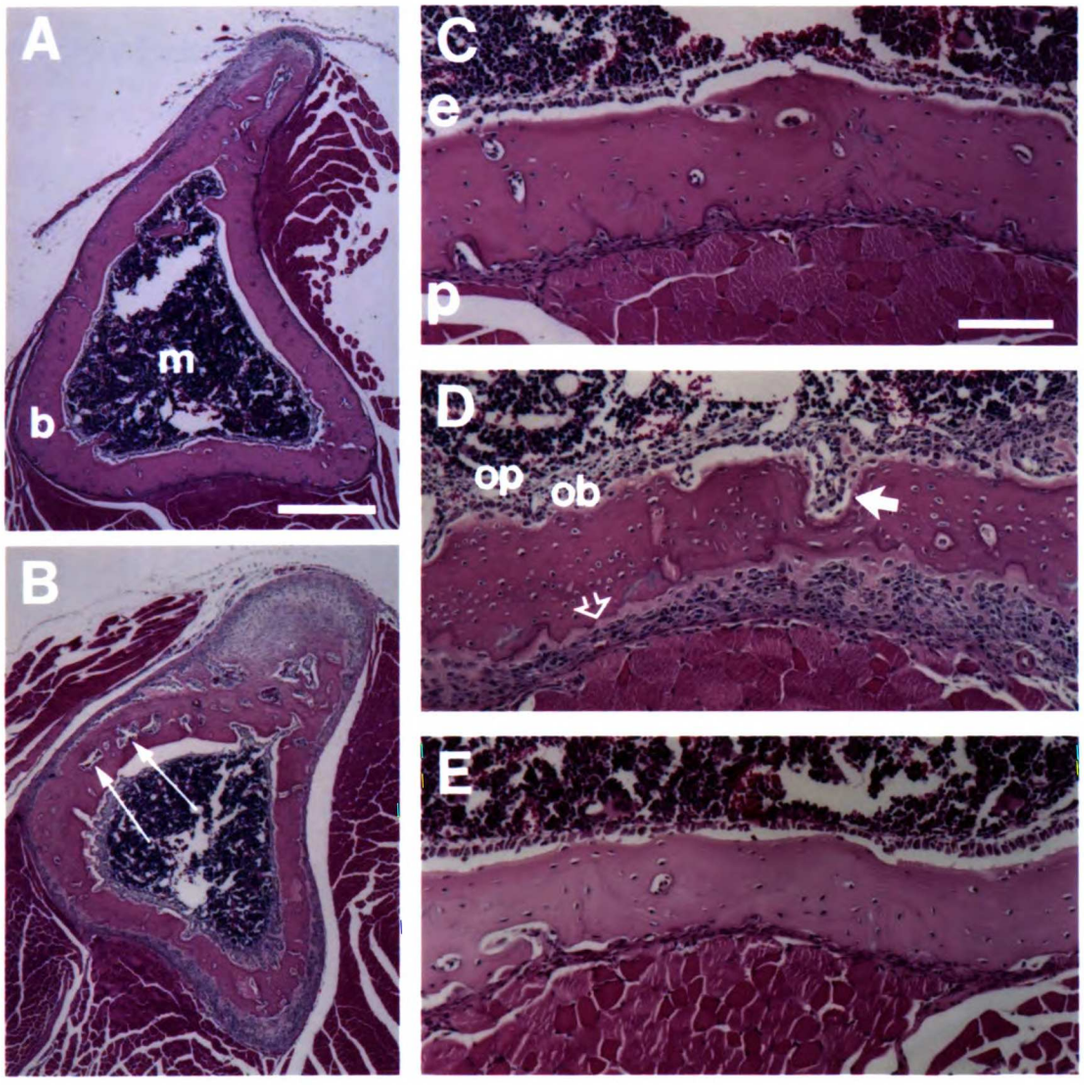

Figure 6. Histochemical identification of osteoclasts.

Sections of metaphyseal trabeculation and growth plate of femurs from 35 day old non-transgenic littermate (A) and D4 (B) females, stained for tartrate-resistant acid phosphatase activity (red), an osteoclast-specific marker. The numbers of osteoclasts in sections of control and transgenic bone are similar. Sections are counterstained with methyl green. Scale bar shows 200 μm.

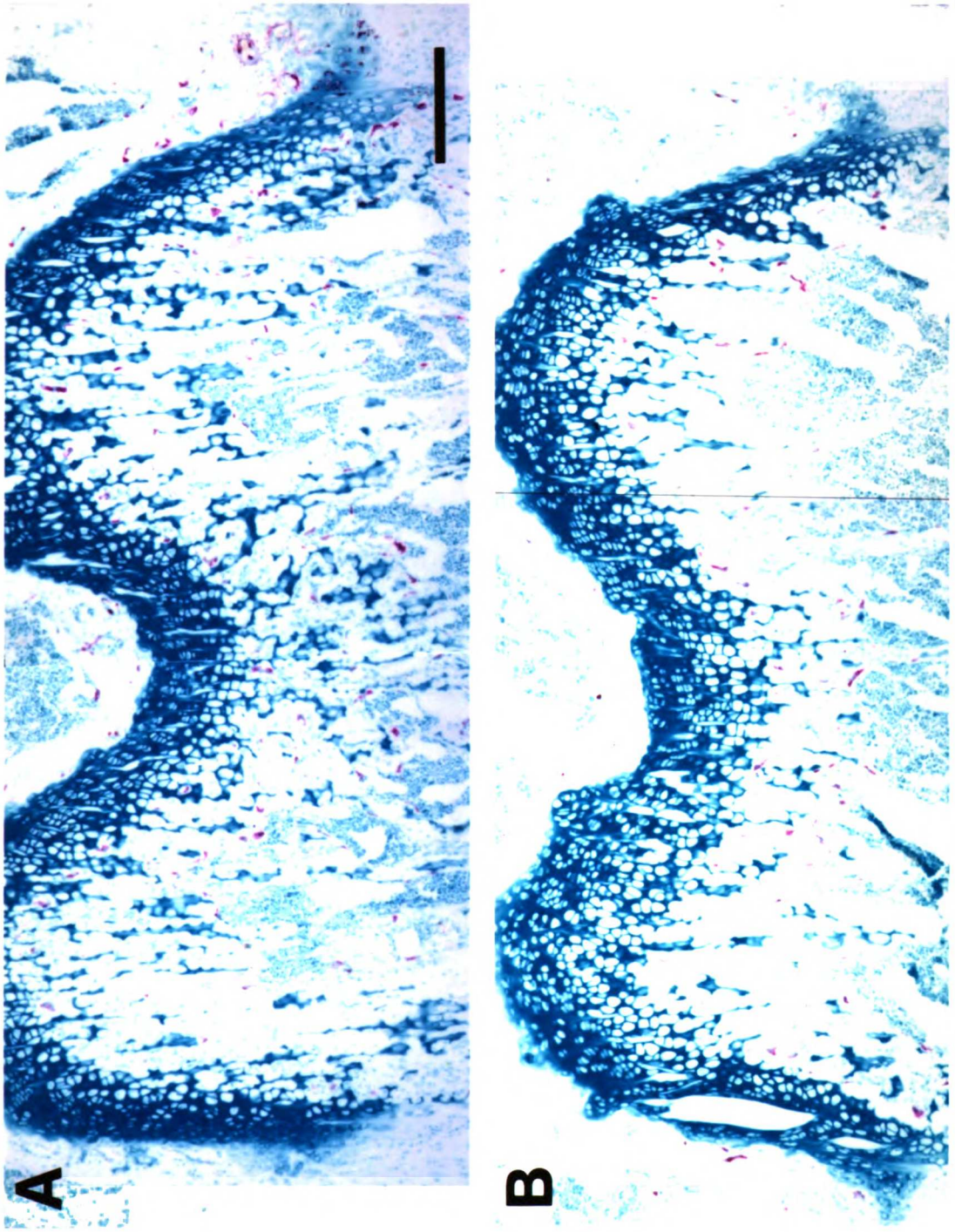
A
B

number (a five-fold increase from 22,000 (+/- 8,000) cells/mm^2 bone surface to 120,000 (+/- 47,000) cells/mm^2), suggesting increased rates of osteoblastic differentiation and osteoprogenitor cell proliferation. The increased cell number along with the associated increase in extracellular matrix gave many cortical bone surfaces a distinctly fibrotic appearance. Osteoblast cell number itself remained constant at 28,000 (+/- 7,000) cells/mm^2 bone surface in transgenic bone compared to 25,000 (+/- 6,000) cells/mm^2 in controls. On epiphyseal and trabecular surfaces, however, osteoblasts appeared more cuboidal than their non-transgenic counterparts (Fig. 2b, open arrows), consistent with active bone matrix synthesis. Osteocyte density was also increased in bone from 7 month old mice, however bone surfaces at this age were not fibrotic.

The mineralization of D4 bone was also abnormal. Bone matrix synthesized within resorption lacunae frequently appeared lightly stained in decalcified sections of cortical bone from both 35 day (Fig. 5b and d) and 7 month old mice. This matrix was unmineralized, as shown by undecalcified sections stained serially with hematoxylin or by the von Kossa technique, which reveals calcium deposits as dark brown or black (Fig. 7). Large pockets of unmineralized matrix extended deep within cortical bone (light blue areas in Fig. 7b), and probably corresponded to the radiolucent intracortical defects noted by X-ray analysis. In addition, the osteoid seam, i.e. the new, as yet unmineralized layer of bone matrix deposited by osteoblasts, was wider on many non-resorbed endosteal surfaces in the epiphysis and diaphysis (see Fig. 8d). In contrast, the mineralization appeared normal in metaphyseal trabecular bone, where osteoid seams were absent in both transgenic and wild-type sections (Fig. 7c and d). Under polarized light, unmineralized

Figure 7. Mineralization of transgenic bone.

Undecalcified sections of tibia from 35-day old non-transgenic littermate (A, C) and D4 (B, D) females, stained by the von Kossa technique for calcium deposits (dark brown or black), and counterstained with toluidine blue. Longitudinal sections through the diaphysis reveal large unmineralized areas of cortical bone (osteoid, light blue) in transgenic bone (B), whereas wild-type bone is entirely mineralized (A). However, there is no difference in the minimal amount of osteoid present in the metaphyseal trabeculation adjacent to the growth plate (C, D). Scale bar shows 100 μm for (A) and (B), 50 μm for (C) and (D).

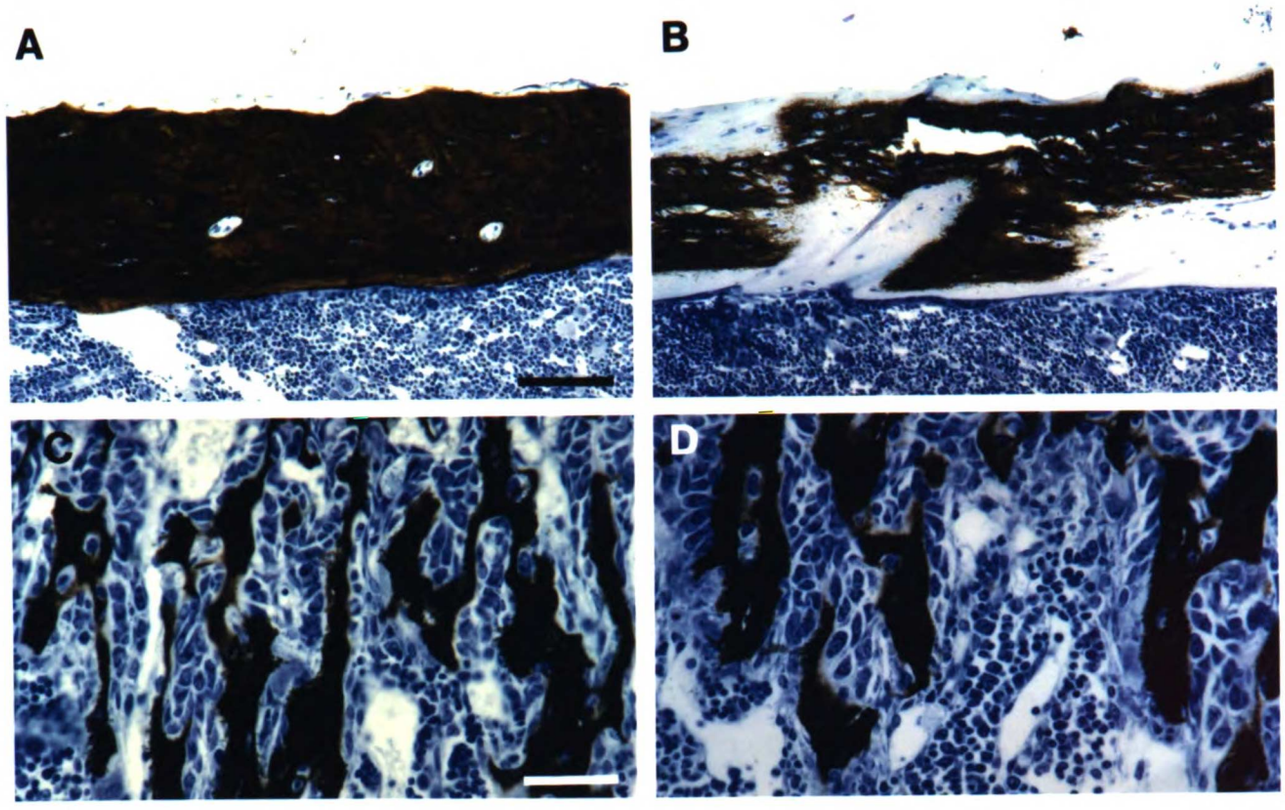

matrix displayed the typical pattern of birefringence associated with lamellar collagen fiber arrangement (not shown).

The histological alterations seen in the long bones of D4 mice were also evident in cross sections of parietal bones of the skull, which develop via direct ossification rather than endochondral ossification (data not shown). In contrast to the D4 line, skeletal sections of hemizygous and homozygous D5 mice showed no microscopic histological alterations (see Fig. 5e for a histological section of 35 day old bone), except for a slightly more porous appearance of cortical bone (not shown).

Kinetic analysis of bone turnover

We performed a kinetic analysis of bone turnover to directly assess the synthetic activity of osteoblasts in D4 bone. Two fluorochromes that incorporate into bone matrix at sites of mineralization were injected into young mice: calcein at 31 days of age, and tetracycline three days later, followed by sacrifice of the animal the next day. Undecalcified bone sections viewed under UV light visualized the incorporated fluorochromes as green and yellow fluorescent lines labeling sites of mineralization at the times of their injection. The distance between the two lines is thus a measure of the mineral apposition rate, which correlates with the local rate of bone matrix deposition by osteoblasts (Parfitt, 1983). Counterstaining of the sections with the Villanueva bone stain simultaneously visualized unmineralized osteoid by its red fluorescence.

In long bones of 35 day old control mice, the two fluorochrome labels formed smooth, contiguous and sharp lines (Fig. 8a and c). In contrast, labels in transgenic bone were diffuse and irregular, and frequently interrupted by

Figure 8. Kinetic analysis of bone turnover.

Undecalcified longitudinal sections of tibia from 35 day old non-transgenic littermate (A, C) and D4 (B, D) males viewed under UV light. Injection of calcein on day 31 and tetracycline on day 34 stains sequential sites of mineralization green and yellow, respectively. Counterstaining the sections with the Villanueva bone stain reveals unmineralized osteoid as bright red. (A, B) Longitudinal sections through cortical bone of the diaphysis. Unlike the homogenous appearance and complete mineralization of non-transgenic bone (A), transgenic bone has many pockets of unmineralized osteoid (B, bright red). These areas are not bordered by either fluorochrome label, indicating that they were not mineralizing over the course of the experiment. In contrast, the non-resorbed endosteal surfaces of both transgenic and non-transgenic bone are mineralizing as revealed by the their double labels (arrows). Note the increased distance between the fluorochrome labels in transgenic bone. Scale bar shows 100 μm.

(C, D) Higher power view of longitudinal sections through the epiphysis adjacent to the growth plate (gp, deep purple). Fluorochrome labels in the transgenic section (D) are diffuse and irregular as compared with their smooth appearance in non-transgenic bone (C). The distance between the labels as well as the width of the unmineralized osteoid layer (bright red, arrowheads) is increased over the entire length of the transgenic bone surface, indicating increased osteoblastic activity. Scale bar shows 100 μm.

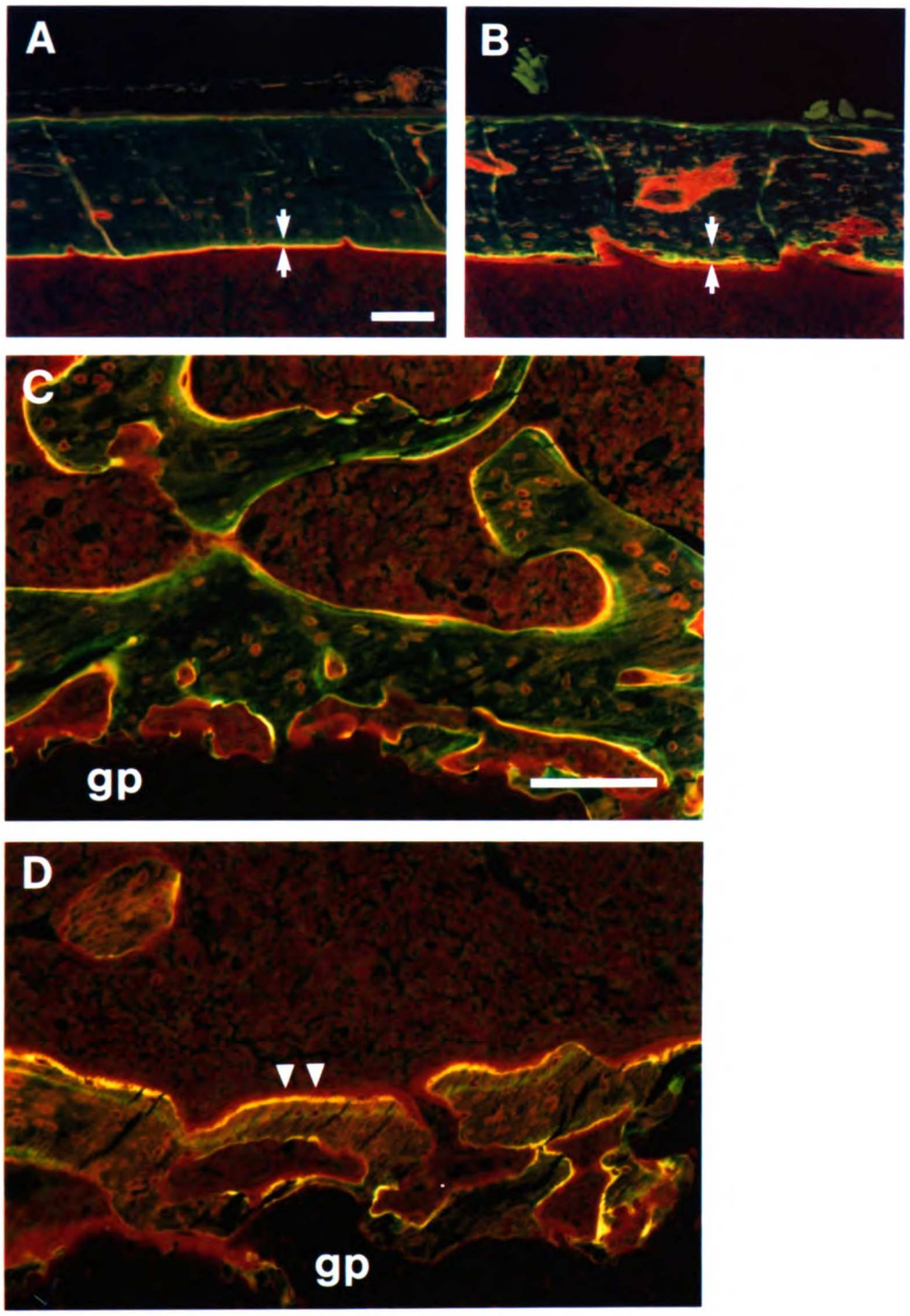

osteoid-filled resorption lacunae (Fig. 8b and d). The distance between the two labels on many surfaces was also distinctly increased in comparison to normal bone (compare Fig. 8a and b (arrows), and Fig. 8c and d), corresponding to a 1.7-fold increase in the mineral apposition rate (from 2.3 (+/- 0.3) μm/day in controls to 4.0 (+/- 1.0) μm/day). Almost all non-resorbed endosteal surfaces of normal bones were labeled with both fluorochromes, reflecting the overall growth of the skeleton at day 35, and the extent and distribution of these surfaces was similar in bones from D4 mice. However, the pockets of unmineralized matrix within cortical bone were not labeled with either fluorochrome, indicating a severe mineralization defect of the new bone matrix synthesized within resorption lacunae (red areas, Fig, 8b). While the unmineralized osteoid seam at endosteal surfaces was wider than normal (Fig. 8d, arrowheads), correlation of the osteoid seam width with the mineral apposition rate did not reveal a significant change in lag time of mineralization following osteoid deposition (2.2 (+/- 0.7) days in controls, 2.4 (+/- 1.0) days in transgenic animals). Thus, the mineralization defect was restricted to matrix synthesized within resorption lacunae.

Absence of clavicles and delayed ossification.

To further evaluate the skeletal development of D4 mice, we prepared cleared skeletons at different stages of development (Fig. 9). Skeletons were stained with alizarin red to visualize mineralized bone, or alcian blue to visualize cartilage. At embryonic day 15.5, D4 clavicles were already clearly hypoplastic compared to normal embryos (compare Fig. 9d and a, arrows). Since clavicle development initiates at day 14-14.5 (Tran and Hall, 1989), this difference indicates a primary defect in clavicle formation, rather than

Figure 9. Cleared skeletal preparations of embryos and newborn mice. Non-transgenic littermate (A-C) and D4 transgenic (D-F) embryos and newborns stained with alizarin red to visualize mineralized bone or alcian blue to visualize cartilage.

(A, D) Neck area of embryonic day 15.5 non-transgenic (A) and transgenic (D) embryos stained with alizarin red to reveal mineralized bone. Clavicles are fully formed in the wild-type embryo but appear as only distal rudiments in the transgenic embryo (arrows). m, mandible.

(B, E) Neck area of 2 day old non-transgenic (B) and transgenic (D) pups stained with alcian blue. Mineralized bone is white and cartilage is blue. No cartilage rudiment links the hypoplastic clavicle in the transgenic pup with the sternum. Arrowheads show the cartilage cap at the proximal end of the clavicle, which arises through a secondary induction event (Tran and Hall, 1989). s, sternum.

(C, F) Forelimb paws of 2 day old non-transgenic (C) and transgenic (F) pups stained with alizarin red. The delay in ossification of the transgenic skeleton is apparent when corresponding ossification centers are compared in transgenic and non-transgenic paws. Furthermore, other skeletal elements have started to ossify in the control paw but not in the transgenic paw (arrows).

C
F
B
S
E
S
A
m
D
m

secondary resorption. As expected for the normal pattern of clavicle development through intramembranous rather than endochondral ossification (Tran and Hall, 1989), no cartilage rudiment was observed connecting the clavicle vestige with the sternum (Fig. 9b and e).

Alizarin red staining also revealed a general delay in mineralization of the D4 skeleton, as illustrated by the ossification pattern in the hands of 2-day old mice (Fig. 9c and f). Whereas the lengths of corresponding digits were identical in transgenic and control mice, the mineralization of individual transgenic bones clearly lagged behind corresponding bones of normal mice. In addition, some bones of transgenic mice were not yet mineralized when compared to control counterparts (arrows). Importantly, the cartilaginous skeleton of transgenic embryos appeared normal, as evident from alcian blue stained preparations. With the exception of the clavicles, all other bones of D4 mice appeared normal in size and shape.

DISCUSSION

TGF-β is deposited in bone matrix and all three TGF-β isoforms are expressed by bone cells in vivo. In vitro and in vivo studies have shown that TGF-β can affect the activity of both osteoblasts and osteoclasts. However, the complexity of these results has made it difficult to define the normal role of TGF-β in bone development and turnover. To provide a physiological context to study the skeletal actions of TGF-β, we generated transgenic mice in which TGF-β2 is overexpressed specifically by osteoblasts. We characterized two independent lines: D5 with a 2.5-fold and D4 with a 16-fold increase in the amount of TGF-β2 extractable from bone matrix.

The primary phenotype of both lines was progressive, age-dependent loss of bone mass, and the severity of the phenotype correlated with the expression level of the transgene. D5 mice had no reduction of bone mass at day 35, but showed a complete loss of metaphyseal trabeculation and dramatically reduced epiphyseal trabeculation by 7 months. In contrast, bone loss in the D4 line was already striking at day 35 and extreme by 7 months. These mice also showed a defect in clavicle development, a generalized delay in the ossification of the skeleton, and a severe mineralization defect of newly synthesized bone matrix. Skeletal integrity was so compromised in the D4 line that spontaneous fractures occurred. Our inability to generate homozygous mice of this line may be related to its severe phenotype.

The progressive, age-dependent nature of the bone loss phenotype suggested a defect in bone remodeling. This was substantiated by histological and kinetic analyses of the D4 line indicating increased activities of both osteoblasts and osteoclasts in transgenic bone. The increases in

mineral apposition rate and osteoid seam width on many bone surfaces indicated an increased rate of bone matrix deposition by osteoblasts. Osteocyte density and osteoprogenitor cell number were also increased, consistent with an increased proliferation of osteoprogenitor cells and an increased rate of osteoblast differentiation. Based on the osteocyte density and mineral apposition rate, we estimate that the rate of differentiation of osteoblasts into osteocytes is increased 5.6-fold in transgenic bone, from about 140 cells/day/mm^2 bone surface in controls, to 790 cells/day/mm^2. Since bone matrix within resorption lacunae did not mineralize over the time course of the fluorochrome labeling experiment, we could not directly assess the rate of its production. However, it is likely that this matrix is produced at a rate equal to, if not greater than the matrix produced on non-resorbed surfaces, because refilled lacunae usually appeared flush with the level of neighboring non-resorbed surfaces. Increased osteoclastic activity was apparent from the increased size of cortical resorption lacunae, the pronounced degree of periosteal and endosteal resorption, and the thinned epiphyseal plates of older mice, and can be inferred from the age-dependent overall decrease of bone mass in the presence of increased osteoblastic activity.

The role of TGF-β in bone development and turnover

Our analysis indicates that overexpression of TGF-β2 increases the activities of osteoblasts and osteoclasts with a consequent increase in bone turnover. These results strongly suggest that TGF-β, or specifically TGF-β2, is a positive regulator of bone remodeling in vivo. Unlike the heterogeneous results of previous in vitro and in vivo studies, our transgenic model shows

that the activities of both cell types increase at steady-state when TGF-β2 is deposited into bone matrix in analogous fashion to endogenous TGF-β. The phenotype also shows that the increase in bone turnover results in a net imbalance between bone resorption and formation, resulting in progressive, age-dependent bone loss, and therefore suggests that TGF-β may regulate the coordination of osteoblast and osteoclast activities. Lastly, the mineralization defect observed in these mice suggests that TGF-β2 may negatively regulate bone matrix mineralization in vivo.

Based on the documented responses of osteoblasts and osteoclasts to TGF-β in vivo and in vitro, the increased turnover likely results from the independent actions of TGF-β on both cell types. It is therefore unlikely that TGF-β drives only one step of bone remodeling; instead, we speculate that TGF-β increases the rate of remodeling by potentiating the actions of other molecular mechanisms that directly coordinate progression through the remodeling cycle. Spatial variations in endogenous TGF-β expression levels may contribute to regional or developmental differences in remodeling or local rates of mineralization within a bone.

A priori, it was not clear that overexpression of TGF-β2 in osteoblasts would lead to a defect in bone turnover. Skeletal development and maintenance involve multiple levels of spatial and temporal control (Frost, 1985), and one might expect an individual growth and differentiation factor to affect several of these levels. Emerging evidence, however, suggests that the role of individual growth factors may be restricted to specific levels of skeletal organization. For example, fibroblast growth factors coordinate proportional bone growth, while the TGF-β related factors BMP-5 and GDF-5 are required to determine the shape of several skeletal elements (reviewed in

Erlebacher et al., 1995). Although TGF-β expression levels during chondrogenesis could indirectly modify bone shape, TGF-β2 overexpression by osteoblasts does not affect bone growth, the skeletal proportions, or bone morphogenesis per se (except the clavicle).

TGF-β2 from bone matrix was increased 2.5-fold in D5 mice. Since TGF-β2 is about 7.5 times less abundant than TGF-β1 in normal bone matrix, the progressive bone loss of these mice suggests that bone turnover may be sensitive over the long term to only minimal changes in total TGF-β content. Additionally, TGF-β2 may induce different cellular or more potent responses than TGF-β1. This latter possibility is consistent with the higher activity of TGF-β2 in inducing cartilage and bone formation (Joyce et al., 1990). Such differences in the actions of TGF-β2 and TGF-β1 could correlate with differential receptor binding or expression in bone cells.

Regional differences in the bone phenotype

The histological changes varied depending on the area of bone. Based on the kinetic analysis and the von Kossa staining, osteoblastic activity was most perturbed in the epiphysis and diaphysis, yet appeared normal in the metaphysis. These local differences likely result from differences in the local level of expression of the TGF-β2 transgene. Indeed, endogenous osteocalcin expression in osteoblasts is higher in the epiphysis and diaphysis than in the metaphysis of long bones (Bronckers et al., 1985; Vermeulen et al., 1989), and expression from the transgenic promoter is accordingly higher in the diaphysis than in the metaphysis (Baker et al., 1992). As a result, increased osteoblastic expression of TGF-β2 in transgenic bone was more prevalent in the epiphysis than in the metaphysis. The spatial correlation between

transgene expression and its phenotypic effects strongly suggests that the actions of TGF-β2 on osteoblasts are restricted to its site of production within bone. Furthermore, the observation that defective mineralization was restricted to the matrix within resorption lacunae supports the hypothesis that the TGF-β within bone matrix exerts its localized effects on osteoblasts after release and activation during osteoclastic resorption (Pfeilschifter and Mundy, 1987).

In contrast to osteoblasts, the increase in osteoclastic activity in transgenic bone showed less regional differences. Trabecular bone mass in the metaphysis was dramatically decreased even though transgene expression was considerably less there than in the epiphysis and diaphysis. This suggests that osteoclastic activity is induced at lower local TGF-β2 concentrations than osteoblastic activity. The similar numbers of osteoclasts in normal and transgenic bone further suggests that increased resorption was due to increased resorbing activity per osteoclast, a possibility consistent with the large size of resorption lacunae in transgenic bone.

Relationship of the transgenic phenotype to human bone diseases

Cleidocranial dysplasia:. A notable feature of D4 mice is their defect in clavicle development and general delay in ossification. Impaired clavicle development is a hallmark of the human autosomal dominant disorder cleidocranial dysplasia (Marie and Sainton, 1897; Jones, 1988) as well as the cleidocranial dysplasia (Ccd) mouse mutation (Sillence et al., 1987). The Ccd phenotype also includes delayed ossification of a number of bones, and although the developmental basis of human cleidocranial dysplasia has not been well studied, delayed mineralization of the sutures and pubic bone has

been noted. The severe hypoplasia or absence of clavicles in all three cases stands in contrast with the normal appearance of most other bones. However, clavicles are remarkable in that they are the only bones outside the skull which develop via intramembranous ossification and not through cartilage templates (Tran and Hall, 1989). Furthermore, clavicle development strongly depends upon mechanical stimulation, which may in turn depend upon the articulation of the clavicle with the sternum (Pai, 1965; Hall, 1986). Thus, clavicle development may be uniquely sensitive to delayed ossification or to a TGF-β2-induced perturbation in nearby muscle development (Massagué et al., 1986; Olson et al., 1986). The increased osteoblastic expression of TGF-β2 in D4 transgenic mice may provide a starting point to study the developmental abnormalities associated with human cleidocranial dysplasia and the mouse Ccd phenotype.

Hyperparathyroidism: The phenotype of the high TGF-β2 expressing D4 line showed a remarkable similarity to the skeletal abnormalities associated with hyperparathyroidism, a disease resulting from increased circulating levels of parathyroid hormone (PTH) (Malluche and Faugere, 1990; Kronenberg, 1993). Common features include generalized osteopenia, increased density of osteocytes, increased osteoclastic resorption, and high turnover kinetics. Increased amounts of unmineralized osteoid apparent in our transgenic mice are also commonly seen in hyperparathyroidism, especially when associated with renal failure (renal osteodystrophy), and fibrotic bone surfaces reflect a severe hyperparathyroid state termed osteitis fibrosa.

PTH is thought to maintain systemic calcium homeostasis in part by regulating osteoclastic bone resorption via an indirect mechanism involving osteoblasts (Rodan and Martin, 1981; McSheehy and Chambers, 1986;

Kronenberg, 1993). How increased PTH levels lead to the skeletal defects in hyperparathyroidism is unknown. The similarity of the D4 phenotype with hyperparathyroidism may link the local effects of TGF-β2 to the systemic actions of PTH. The osteoblast-dependent PTH stimulation of osteoclastic activity in vitro is simulated by TGF-β (Hattersley and Chambers, 1991), and PTH induces TGF-β expression by osteoblasts (Oursler et al., 1991). In addition, PTH alters the response of osteoblasts to TGF-β in culture, perhaps by altering the TGF-β receptor expression pattern of these cells (Centrella et al., 1988). Conversely, TGF-β upregulates the expression of PTH receptors in osteoblasts (Schneider et al., 1992; Seitz et al., 1992), raising the possibility that increased TGF-β expression mimics the histological phenotype of hyperparathyroidism by sensitizing osteoblasts to physiological levels of PTH. It is highly unlikely that the severe D4 phenotype resulted from increased levels of PTH or PTH-related peptide, since transgenic mice showed no evidence of hypercalcemia or hypophosphatemia (Kronenberg, 1993; Strewler and Nissenson, 1993).

Osteoporosis. Finally, the mild phenotype of the D5 line, with its progressive, age-dependent bone loss with little or no alteration in the microscopic appearance of bone, closely resembles osteoporosis, a prevalent disease thought to result from an imbalance between osteoclastic and osteoblastic activities during bone remodeling (reviewed in Manolagas and Jilka, 1995). In addition, bone from 7 month old D4 mice were extremely osteoporotic, aside from the increased osteocyte density and mineralization defect, which are strictly speaking not features of osteoporotic bone. Furthermore, a hallmark of osteoporosis is the increased propensity towards fracturing. Spontaneous

fractures were indeed commonly seen in D4 mice, and we infer that D5 mice may therefore be more prone to fractures as well.

Despite the association of osteoporosis with changes in the hormonal regulation of bone turnover, such as reduced estrogen in the postmenopausal state, the local mediators which alter bone remodeling and lead to the imbalance between osteoclastic and osteoblastic activities at the histological level remain largely unknown. Considering the epidemiological and histological heterogeneity of osteoporosis (Meunier et al., 1980; Parfitt et al., 1980; Whyte et al., 1982), and the multiplicity of cytokines and growth factors that affect osteoblasts and osteoclast function in vitro (Mundy, 1993), it is likely that several factors influence bone turnover and contribute to the pathogenesis of osteoporosis. Thus, transgenic overexpression of interleukin-4 by T-cells leads to an osteoporotic phenotype with decreased osteoblastic function, suggesting that this factor could play a role in low-turnover osteoporosis (Lewis et al., 1993). Furthermore, mice deficient mice in interleukin-6 (IL-6) expression have revealed a requirement for this cytokine in the bone loss that follows ovariectomy, which resembles postmenopausal osteoporosis (Poli et al., 1994). Interestingly, IL-6 deficient mice have an increased rate of bone turnover but no discernible bone loss prior to ovariectomy.

Our transgenic mice show that increased osteoblastic expression of TGF-β2, a normal product of osteoblasts in vivo, causes both an increase in bone remodeling and an imbalance in osteoclastic and osteoblastic activity leading to progressive bone loss, a phenotype similar to high-turnover osteoporosis. A potential link between postmenopausal osteoporosis and TGF-β has previously been made with the finding that ovariectomy in rats

leads to a 40% specific reduction in TGF-β extractable from bone matrix (Finkelman et al., 1992). However, it is unclear how this reduction is causally related to the high turnover state following ovariectomy (Wronski et al., 1985; Wronski et al., 1986), since we see a similar reduction in TGF-β1 content of bone matrix in our mice overexpressing a high level of TGF-β2. The remarkable association of an osteoporosis-like phenotype with only a mild, i.e. 2.5-fold increase in TGF-β2 expression by osteoblasts that only minimally affects the total TGF-β content of bone, suggests that small alterations in the expression of TGF-β in bone, or in the responsiveness of bone cells to TGF-β, could contribute to the remodeling defects underlying osteoporosis and other metabolic bone diseases.

ACKNOWLEDGMENTS

We are grateful to Richard Weiner and Suzanne Moenter for their instruction in generating transgenic mice, use of their microinjection setup, and much helpful advice. We would like to thank Nilda Urbana and Ilse Sauerwald for excellent histological assistance, Andrew Baker and Timothy Stewart for providing the rat osteocalcin promoter, the UCSF Pathology department for use of their faxitron, Catharina Mathews for helpful discussions and access to the fluorescence microscope used in the kinetic analyses, Jian-Qin Ye for technical help, Paivi Miettinen for discussions and comments on the manuscript, and Zena Werb, Caroline Damsky, and Arnold Kahn for critical reading of the manuscript. This work was supported by NIH grants RO1-AR41126 and P50-DE-10306. A. E. is a member of the Medical Scientist Training Program supported by grant NIGMS GM07618.

Chapter 4:

Stimulation of osteoblastic differentiation by TGF-β at sites of bone resorption

ABSTRACT

Bone remodeling depends upon the close spatial and temporal coupling of bone formation by osteoblasts to bone resorption by osteoclasts, although the molecular basis of this interaction is unknown. We have previously shown that the osteoblastic overexpression of TGF-β2 in transgenic mice leads to deregulated bone remodeling and a dramatic age-dependent loss of bone mass resembling high-turnover osteoporosis. These mice provide a unique model for studying the skeletal physiology of TGF-β and the coordination of osteoblast and osteoclast activities in vivo. We now apply a combination of anatomical, genetic and pharmacological techniques to dissect the physiological responses of osteoblasts to TGF-β. To detect autocrine effects, we use a new transgenic mouse line that expresses a cytoplasmically-truncated (dominant-negative) type II receptor in osteoblasts. To detect paracrine effects mediated through osteoclasts, we use osteoclast-deficient *c-fos*$^{-/-}$ mice and the in vivo administration of alendronate, a specific inhibitor bone resorption. Our results show that a primary, direct effect of TGF-β on osteoblasts is to increase the steady-state rate of osteoblastic differentiation from osteoprogenitor cell to osteocyte, as assessed by BrdU pulse/chase labeling. We also find that osteoclasts significantly contribute to this stimulatory effect at sites of bone resorption, potentially by releasing bone matrix-bound latent TGF-β. These results suggest that a major role of TGF-β in skeletal tissues is to mediate the stimulation of osteoblast differentiation at sites of osteoclast activity, and that this mechanism might at least partially underlie the proper coupling of bone formation to resorption required for skeletal homeostasis.

INTRODUCTION

During development and adult life, bone undergoes continuous remodeling through the coordinated processes of bone formation and bone resorption. Bone is formed by osteoblasts, which are of mesenchymal origin, and resorbed by osteoclasts, which are derived from the hematopoetic system. In the adult skeleton, constant bone mass is maintained through the close microanatomical coupling of osteoblastic and osteoclastic activities (for a review see (Parfitt, 1994)). Deregulation of this coupling underlies the pathological loss of bone mass seen in osteoporosis and other metabolic bone diseases. Since new bone formation requires the continuous generation of new osteoblasts, osteoclastic resorption is not only coupled to the activity of osteoblasts, but also to the differentiation of osteoblasts from osteoprogenitor cells. In spite of their importance for our understanding of normal bone metabolism and the pathogenesis of metabolic bone diseases, the molecular mechanisms that govern the coordination of these processes are largely unknown.

One secreted factor that modulates the differentiation of osteoblasts and the proliferation of osteoprogenitor cells is transforming growth factor-β (TGF-β) (for reviews see Bonewald and Dallas, 1994; Centrella et al., 1994). Both osteoblasts and osteoclasts secrete TGF-β, and all TGF-β isoforms (TGF-β1, -β2 and -β3) are present in their latent form within bone matrix (Pelton et al., 1991; Robey et al., 1987; Sandberg et al., 1988; Seyedin et al., 1985). Since bone explants release TGF-β during bone resorption (Pfeilschifter and Mundy, 1987), and osteoclasts have the ability to activate latent TGF-β (Oreffo et al., 1989; Oursler, 1994), it has been suggested that

TGF-β might play a role in the coupling of bone formation to bone resorption. Thus, TGF-β deposited in bone matrix by osteoblasts might be released and activated at sites of resorption by osteoclasts, which in turn leads to the induction of nearby osteoblastic differentiation. However, this model requires experimental verification in vivo, which so far has been difficult. For example, it has not been clear that TGF-β directly induces osteoblastic differentiation in the adult skeleton, and there have been no good in vivo experimental systems to detect the release of TGF-β from bone matrix during bone resorption, or to assess the physiological relevance of bone matrix-derived TGF-β towards osteoblastic differentiation.

We have previously generated transgenic mice that overexpress TGF-β2 from the osteocalcin promoter, which is osteoblast-specific (Erlebacher and Derynck, 1996). Transgenic mice showed a dramatic, age-dependent loss of bone mass similar to that seen in osteoporosis and hyperparathyroidism, yet showed relatively few defects in skeletal development or growth. In the transgenic line with the highest level of TGF-β2 expression, i.e. the D4 line, the phenotype was associated with three major histological alterations consistent with increased rates of bone remodeling: an increase in the density of bone matrix-embedded osteocytes, an increase in the rate of bone formation by osteoblasts, and an increase in the rate of bone resorption by osteoclasts.

These mice provide a unique model for studying the skeletal actions of TGF-β in the context of bone remodeling in vivo. The work described here was founded initially on our attempts to understand the two endpoint osteoblastic responses to TGF-β2 overexpression in D4 mice, namely the increase in osteocyte density and the increase in bone formation. We were

interested in these two phenotypic changes not only because of their inherent relevance to skeletal homeostasis (especially in the case of the increased rate of bone formation), but also because it was likely that they would reveal deeper aspects of TGF-β physiology in bone. For example, we reasoned that understanding the increase in osteocyte density, since this increase reflected a hyperplastic perturbation of terminal osteoblastic differentiation, might give insight into the overall regulation of osteoblastic differentiation by TGF-β.

Our analysis, however, was initially limited by the need to discern the primary effects of TGF-β overexpression from their secondary consequences. Thus, applying a combination of anatomical, genetic, and pharmacological approaches, we found that the increase in bone formation caused by TGF-β2 overexpression, contrary to expectation, was a secondary consequence of the increased bone resorption in transgenic animals. In contrast, the increase in osteocyte density was a direct effect of TGF-β2 on osteoblasts. Following this lead, we found that the effect was caused by an increase in the steady-state rate of osteoblastic differentiation, and that it was greatly enhanced by osteoclastic activity at sites of bone resorption. Our results show that TGF-β increases the rate of osteoblastic differentiation during bone remodeling, which in turn may contribute to the coupling of bone formation to resorption.

MATERIALS AND METHODS

Transgenic mice. The generation of D4 mice that overexpress TGF-β2 from the osteocalcin promoter has been described (Erlebacher and Derynck, 1996). The generation and characterization of E1 mice, which express a cytoplasmically truncated type II TGF-β receptor from the osteocalcin promoter will be described elsewhere (Filvaroff et al., in preparation). Both lines were generated and maintained on a (DBA/2 X C57BL/6J) F1 background (Jackson Laboratories, Bar Harbor, Maine). D4 mice were either identified by the distinct appearance of their calvariae (Erlebacher and Derynck, unpublished observations), or by PCR of tail DNA using the primers 5'-GTGCTGGTTGTTGTGCTGCTC-3' within the β-globin sequences of the transgene, and 5'-CCTTGGCGTAGTACTCTTCGTC-3' within the TGF-β2 cDNA (Erlebacher and Derynck, 1996). E1 mice were genotyped by PCR of tail DNA as described (Filvaroff et al., in preparation). D4/E1 mice were generated by crossing D4 hemizygotes with E1 hemizygotes or D4/E1 hemizygotes, and offspring were genotyped by PCR of tail DNA. TGF-β2 expression levels were measured using a TGF-β2-specific ELISA (R&D Systems, Minneapolis, MN) on bone powder extracts prepared from mice at day 35, as described (Erlebacher and Derynck, 1996). Mice homozygous for the D4 transgene were embryonic lethal (Erlebacher and Derynck, 1996) and were therefore not included in these analyses.

Mice heterozygous for an inactivated allele of *c-fos* (Johnson et al., 1992) were generously provided by Randall Johnson, and were on a (129/SvJ X C57BL/6J) F1 background. The inactivated *c-fos* allele was tracked by PCR of tail DNA as described (Johnson, et al., 1992). To generate *c-fos*$^{-/-}$ and

c-fos$^{-/-}$/D4 mice, *c-fos*$^{+/-}$ mice were crossed with D4 mice, and the resultant F1 *c-fos*$^{+/-}$/D4 mice and *c-fos*$^{+/-}$ mice were then intercrossed. All day 16 measurements of osteocyte density, mineral apposition rate, serum calcium and phosphorus levels, and growth rate were performed on the littermates of this cross. Mice homozygous for the targeted *c-fos* allele were identified by their failure to undergo tooth eruption (Johnson, et al., 1992; Wang et al., 1992), and the D4 transgene was detected by PCR of tail DNA. *c-fos*$^{-/-}$ mice and control littermates maintained past weaning were fed a liquid diet of dissolved powdered milk and rice cereal. Serum calcium and phosphorus levels were determined from retro-orbital bleeds using colorimetric assays (Sigma Chemical Co., St. Louis, MO).

Scanning electron microscopy. Femurs from 16 day and 35 day mice were deorganified in 5.25% sodium hypochlorite (Chlorox), coated with gold, and viewed at 10 kV with a Jeol JSM-840A scanning electron microscope (Tokyo, Japan). At least three D4 and three wild-type mice were analyzed at each time point.

Osteocyte density measurements. Osteocyte density was determined using hematoxylin and eosin-stained 5 μm sections of bones that were fixed in 2% paraformaldehyde/PBS, decalcified, and embedded in paraffin as described previously (Erlebacher and Derynck, 1996). Cortical bone measurements were based on cross sections of the femur at the level of the third trochanter, using at least two sections per mouse spaced at least 200 μm apart. Three photomicrographs per section were taken at a magnification of 200X, covering the dorsal, ventral and medial aspects of the diaphysis, and the number of

osteocytes spanning the entire cortical width, or located in the subperiosteal cortex, was counted. Bone surfaces were then outlined with a black pen, the micrographs were scanned into a computer using Adobe Photoshop (Mountain View, CA), and cross-sectional bone areas were determined using NIH Image (Wayne Rasband, U.S. National Institutes of Health). Osteocyte densities (osteocytes per mm^2) per micrograph were summed for each mouse and converted into three-dimensional densities as described (Sissons and O'Connor, 1977), assuming a 15 μm diameter for an osteocyte. Graphed values represent the mean +/- standard deviation for the mice in an experimental group. At day 16, the measurements of the osteocyte densities in the subperiosteal 25 μm of cortical bone were determined for 5 wild-type and 4 D4 transgenic mice, and measurements spanning the entire cortical width were from 3 *c-fos*$^{-/-}$ and 3 *c-fos*$^{-/-}$/D4 mice. Measurements spanning the entire cortical width at day 35 were from 6 wild-type, 5 D4, 5 E1, and 6 D4/E1 transgenic mice. Measurements at day 35 of the subperiosteal 36 μm of cortical bone, which corresponds to the prior 14 days of radial growth as estimated from the day 35 mineral apposition rate, were from 6 wild-type and 5 D4 mice that were untreated, and from 6 wild-type and 6 D4 transgenic mice that were treated with alendronate and had undergone parathyroidectomy.

We measured the osteocyte density in the distal femoral epiphysis at day 35 using essentially the same procedure. Six photomicrographs of cancellous bone were taken per mouse from two longitudinal 5 μm sections spaced at least 200 μm apart. In experiments analyzing the effect of the truncated type II TGF-β receptor, measurements were from 6 wild-type, 5 D4, 5 E1, and 6 D4/E1 mice. In experiments analyzing the effects of alendronate and parathyroidectomy, measurements were from 6 wild-type and 5 D4

untreated mice (as measured in the truncated receptor experiment), 2 wild-type and 4 D4 mice treated with vehicle and parathyroidectomy, 3 wild-type and 3 D4 mice treated with alendronate and sham operation, and 6 wild-type and 6 D4 mice treated with alendronate and parathyroidectomy. Statistical significance was determined by ANOVA and the Bonferroni t-test for multiple comparisons.

Mineral apposition rate measurements. The mineral apposition rate was determined from 4.5 μm sections of undecalcified bone fixed in 70% ethanol, stained en bloc in the Villanueva bone stain (osteochrome stain, Polysciences Inc., Niles, IL) and embedded in methylmethacrylate. For analyses at day 16, mice were injected with 10 mg/kg calcein (Sigma) on day 12 (or on day 10 for some *c-fos*$^{-/-}$ and *c-fos*$^{-/-}$/D4 mice), and on day 15 with 25 mg/kg tetracycline (Sigma). For day 35 analyses, mice were injected on day 30 with calcein and at day 34 with tetracycline.

The mineral apposition rate was measured from photomicrographs of sections of bone viewed under UV light at a magnification of 200X. For the periosteal mineral apposition rate, 6-12 photographs per mouse covering the dorsal and medial aspects of the femur at the level of the third trochanter were taken from at least two sections spaced 200 μm apart. For the epiphyseal mineral apposition rate, 12 photographs per mouse were taken of the distal femoral epiphysis from at least two sections spaced 200 μm apart. 50-100 individual measurements per mouse were taken along double-labeled surfaces at a spacing of about 40 μm. The mineral apposition rate for each mouse was calculated as the average of the distances between the fluorochrome labels divided by the time between their injection. The

standard error of the mean of these measurements per mouse was always lower than 10% their average value. Graphed values represent the mean +/- standard deviation for the mice in an experimental group. Mineralization lag time was calculated as the average of individual measurements of the osteoid seam width divided by the mineral apposition rate measured at the same location.

In experiments analyzing the effect of the truncated type II TGF-β receptor, measurements of the mineral apposition rate in the femoral epiphysis at day 35 were from 5 wild-type, 4 D4, 5 E1, and 4 D4/E1 mice. In experiments analyzing the effects of alendronate and parathyroidectomy, measurements from the femoral epiphysis were from 5 wild-type and 4 D4 untreated mice (as calculated in the truncated receptor experiment), 4 wild-type and 5 D4 mice treated with vehicle and parathyroidectomy, 3 wild-type and 3 D4 mice treated with alendronate and sham operation, and 5 wild-type and 5 D4 mice treated with alendronate and parathyroidectomy. Periosteal measurements in this experiment were from 4 wild-type and 4 D4 untreated mice, and 3 wild-type and 3 D4 mice treated with alendronate and parathyroidectomy. Periosteal mineral apposition rate at day 16 was measured from 7 wild-type, 7 D4, 8 *c-fos*$^{-/-}$, and 8 *c-fos*$^{-/-}$/D4 mice. Statistical significance was determined by ANOVA and the Bonferroni t-test for multiple comparisons.

Alendronate treatment and parathyroidectomy. Alendronate was generously provided by Gideon Rodan (Merck Research Laboratories, West Point, PA), or prepared as the soluble component of Fosamax (Alendronate Sodium Tablets, Merck & Co., Inc., West Point, PA) when dissolved in PBS.

Both sources gave identical results. Mice were given intraperitoneal injections of 0.3 mg/kg alendronate or vehicle (PBS) every other day from days 15 to 35. Alendronate treatment during this period of rapid growth caused a mild osteopetrosis, slightly reduced serum phosphorus levels, but no effect on serum calcium levels. Thus, it is likely that alendronate-treated mice were mildly hyperparathyroid secondary to a net increased demand by the growing skeletal for calcium.

Parathyroidectomy or sham operations were performed on day 21, following weaning. Mice were anesthetized with intramuscular injections of 100 mg/kg ketamine (Sigma), 5 mg/kg xylazine (Sigma), and 1.25 mg/kg acetopromazine (Sigma), and the parathyroid glands were removed by blunt dissection as described (Meyer et al., 1989). Incision sites were sutured shut and sealed with collodion (Mallinckrodt Baker Inc., Paris, KY). Sham operation mimicked the entire operation without the actual removal of the parathyroid glands. Untreated mice were fed a normal diet containing 0.7-0.8% calcium and 0.6% phosphorus; sham-operated and parathyroidectomized mice were fed a high calcium diet containing 1.46% calcium and 0.99% phosphorus (Purina Test Diets, Purina Mills, Inc., Richmond, IN) following surgery in order to minimize the risk of hypocalcemia. Mice were given intraperitoneal injections on day 30 with calcein and on day 34 with tetracycline for analysis of the mineral apposition rate. Mice were fasted overnight on day 34 and retro-orbital bleeds were taken immediately prior to sacrifice on day 35. Bones were dissected and fixed and stored in 70% ethanol at 4^{o} C. For analysis of the osteocyte density, bones were refixed in 2% paraformaldehyde/PBS prior to further processing (see above).

Day 35 serum calcium and phosphorus levels, determined by colorimetric assay (Sigma), were used to score for successful parathyroidectomies. The prior overnight fast was included to minimize the dietary absorption of calcium. Sham-operated, fasted mice had a serum calcium of 9.5 +/- 0.4 mg/dl (n=21) and a serum phosphorus of 7.6 +/- 1.0 mg/dl (n=21); we defined a successful parathyroidectomy as one resulting in a serum calcium level two standard deviations below the mean, and a serum phosphorus level one standard deviation above the mean. Thus, only mice with a serum calcium under 8.7 mg/dl and a serum phosphorus over 8.6 mg/dl were included for further analysis. These mice formed a clearly defined group relative to sham-operated mice and mice where the surgery was unsuccessful.

Analysis of osteoblast differentiation with bromodeoxyuridine (BrdU). Mice were given two intraperitoneal injections of BrdU (Boehringer Mannheim, Indianapolis, IN) spaced eight hours apart on day 12 or day 16. Mice injected on day 12 were sacrificed 96 h after the second injection, and mice injected on day 16 were sacrificed 4 h after the second injection. Bones were fixed overnight at 4°C in 4% paraformaldehyde/PBS, decalcified for 5 days in 10% EDTA, 0.1 M Tris pH 7.0 at 4°C, and embedded in paraffin. 5 μm cross-sections were taken at the level of the third trochanter, and stained for labeled nuclei using a BrdU staining kit (Zymed Laboratories Inc., South San Francisco, CA). Periosteal osteoblasts were identified as cuboidal cells abutting the bone surface. For each mouse, labeled periosteal osteoblast and subperiosteal osteocyte nuclei were counted from six sections spaced at least 50 μm apart, covering the dorsal, ventral and medial aspects of the diaphysis.

A total of 300-800 osteoblasts were scored per mouse. Graphed values represent the mean +/- standard deviation for the mice in an experimental group. For mice injected on day 12, measurements were from 4 wild-type, 4 D4, 4 E1, and 4 D4/E1 mice. For mice injected on day 16, measurements were from 2 wild-type and 4 D4 mice. Statistical significance was determined by ANOVA and the Bonferroni t-test for multiple comparisons.

Effects of alendronate on plasma TGF-β levels. For the plasma level of TGF-β2 at day 35, mice were injected intraperitoneally with 0.3 mg/kg alendronate or PBS vehicle every other day for a 3 total of injections prior to retro-orbital blood collection at day 35. Heparinized tubes were used for the collection of plasma, and samples were acid-activated as described (Erlebacher and Derynck, 1996) prior to TGF-β2 measurement by a TGF-β2 ELISA (R&D Systems, Minneapolis, MN). For the plasma level of TGF-β2 at 3 months, mice were injected for three consecutive days with 3 mg/kg alendronate or PBS vehicle prior to the collection of plasma and TGF-β2 ELISA as described above. At 3 months, a total of 7 wild-type mice treated with vehicle, 6 wild-type mice treated with alendronate, 6 D4 mice treated with vehicle, and 10 D4 mice treated with alendronate were analyzed. Statistical significance was determined using Student's t-test.

RESULTS

Increased osteocyte density in mice with osteoblastic overexpression of TGF-β2 does not require osteoclastic bone resorption.

Our first goal was to determine whether the increase in osteocyte density caused by TGF-β2 overexpression represented a direct effect of overexpressed TGF-β2 on osteoblasts, or whether it was the secondary consequence of another aspect of the deregulated bone remodeling in D4 mice. Because of the close functional relationships between osteoblastic differentiation, bone formation, and osteoclastic bone resorption, we assessed whether the increased osteocyte density depended on bone resorption by osteoclasts. This evaluation was pursued using anatomical and genetic approaches.

As an anatomical approach, we assessed the osteocyte density of bone at a location which is naturally devoid of osteoclastic activity, i.e. under the periosteum of the diaphysis of a long bone. More specifically, we measured the osteocyte density of subperiosteal cortical bone in the diaphysis of the femur of 16-day-old mice in the region opposite to the third trochanter (Fig. 1c). The bone surface at this location undergoes intramembranous ossification in the absence of bone resorption by osteoclasts, which is easily detected by scanning electron microscopy (Boyde, 1972). Thus, the diaphyseal surfaces of both wild-type and D4 mice clearly lacked characteristic resorption pits (lacunae), in contrast to the continuous resorptive surface of the distal metaphysis (Fig. 1a, b, and d).

Scanning electron micrographs also showed that the diaphyseal osteocyte density, as assessed by the density of surface osteocyte lacunae, was

Figure 1. Scanning electron microscopy of bone surfaces.
Periosteal surfaces of wild-type (A) and D4 transgenic (B) femurs corresponding to the area of the diaphysis bracketed in panel C. The third trochanter is located at the top of both micrographs. Osteoclastic resorption lacunae are absent from the diaphyseal surfaces of both bones, and are only visible distal to the third trochanter in the transition to the distal metaphysis (asterisk in panel A). The transition zone between diaphysis and metaphysis in the D4 bone (boxed in panel B) is shown at higher magnification in panel D. The resorptive surface of the metaphysis (r) is clearly distinct from the diaphysis, which has the characteristic appearance of forming and mineralizing bone (f). These micrographs also revealed a dramatic increase in the size of the vasculature in D4 bone compared to wild-type. One vascular pore is indicated with an arrow in panel D. The mineralizing surface in D4 bone appears somewhat disorganized compared to the wild-type surface, consistent with the irregular cross-sectional appearance of fluorochrome labels in D4 bone (Erlebacher and Derynck, 1996). Osteocyte lacunae are indicated with arrowheads in panel D. Scale bars show 200 μm in A and B, 100 μm in D.

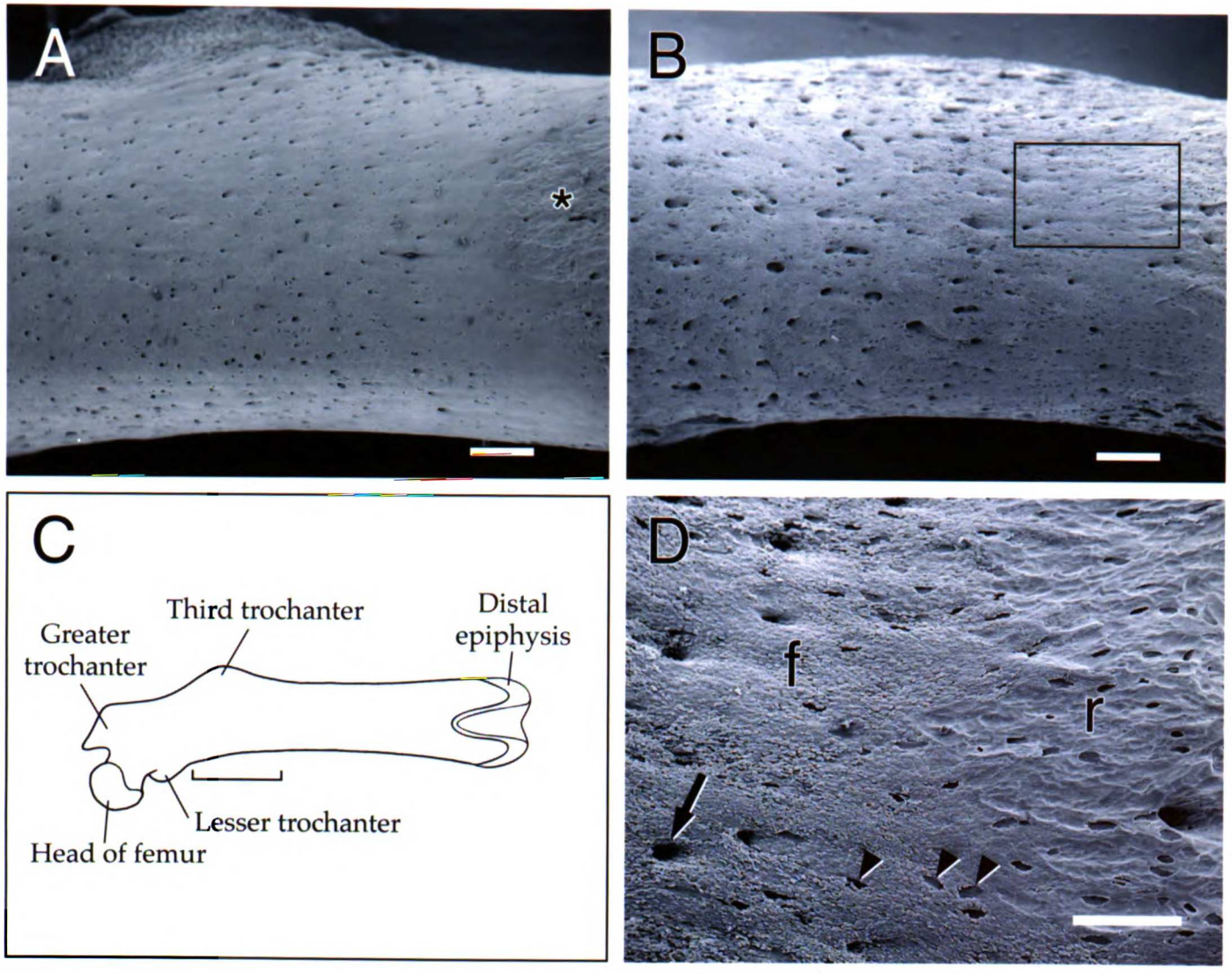

clearly higher in D4 transgenic bones than in normal bones at 16 days of age (Fig. 1a and b). This increase was also apparent histologically in cross-sections of diaphyseal bone (Fig. 2a and b). In these sections, we quantitated the osteocyte density in the subperiosteal 25 μm of cortical bone (bracketed in Fig. 2a), which corresponds to about 5.8 days of continuous radial growth up to day 16 (see below). As shown in Fig. 2e, the subperiosteal osteocyte density in D4 mice was about 1.6-fold higher than in wild-type controls. A similar increase in osteocyte density was also observed at day 35 (see below).

To genetically evaluate the role of osteoclastic bone resorption in the increase of osteocyte density caused by TGF-β2 overexpression, we crossed D4 mice with *c-fos*$^{-/-}$ mice which have an osteopetrotic phenotype due to a complete block in osteoclastic differentiation (Grigoriadis et al., 1994). However, despite the complete absence of osteoclasts in *c-fos*$^{-/-}$/D4 mice, their osteocyte density in cortical bone was still increased when compared to *c-fos*$^{-/-}$ and wild-type controls (Fig. 2c, d and e). These results are therefore consistent with our anatomical and histological analyses, and taken together strongly suggest that the increase in osteocyte density in D4 transgenic mice does not require osteoclastic bone resorption.

Increased osteocyte density in D4 bones requires osteoblastic responsiveness to TGF-β.

To conversely test whether the increase in osteocyte density depended directly upon the osteoblastic responsiveness to TGF-β, we used a newly generated strain of transgenic mice (the E1 line), that overexpress a cytoplasmically truncated version of the type II TGF-β receptor from the osteocalcin promoter (Filvaroff et al., in preparation). Overexpression of this

Figure 2. Osteocyte density in the absence of bone resorption.
(A and B) Hematoxylin and eosin stained sections of cortical bone from the femoral diaphyses of wild-type (A) and D4 transgenic (B) mice at day 16. The sections are at the level of the third trochanter, where bone resorption is absent on periosteal surfaces. The brackets in panel A demarcate the 25 μm of subperiosteal cortex in which we quantitated the osteocyte density in wild-type and D4 mice. (C and D) Similar sections of cortical bone from femurs of *c-fos*$^{-/-}$ (C) and *c-fos*$^{-/-}$/D4 mice at day 16 (D). The dense, slightly ossified calcified cartilage that fills the bone marrow spaces of *c-fos*$^{-/-}$ mice can be seen towards the bottom of both micrographs. (E) Osteocyte densities in the subperiosteal cortex of femurs from wild-type and D4 mice, and in the entire cortex of femurs from *c-fos*$^{-/-}$ and *c-fos*$^{-/-}$/D4 mice.

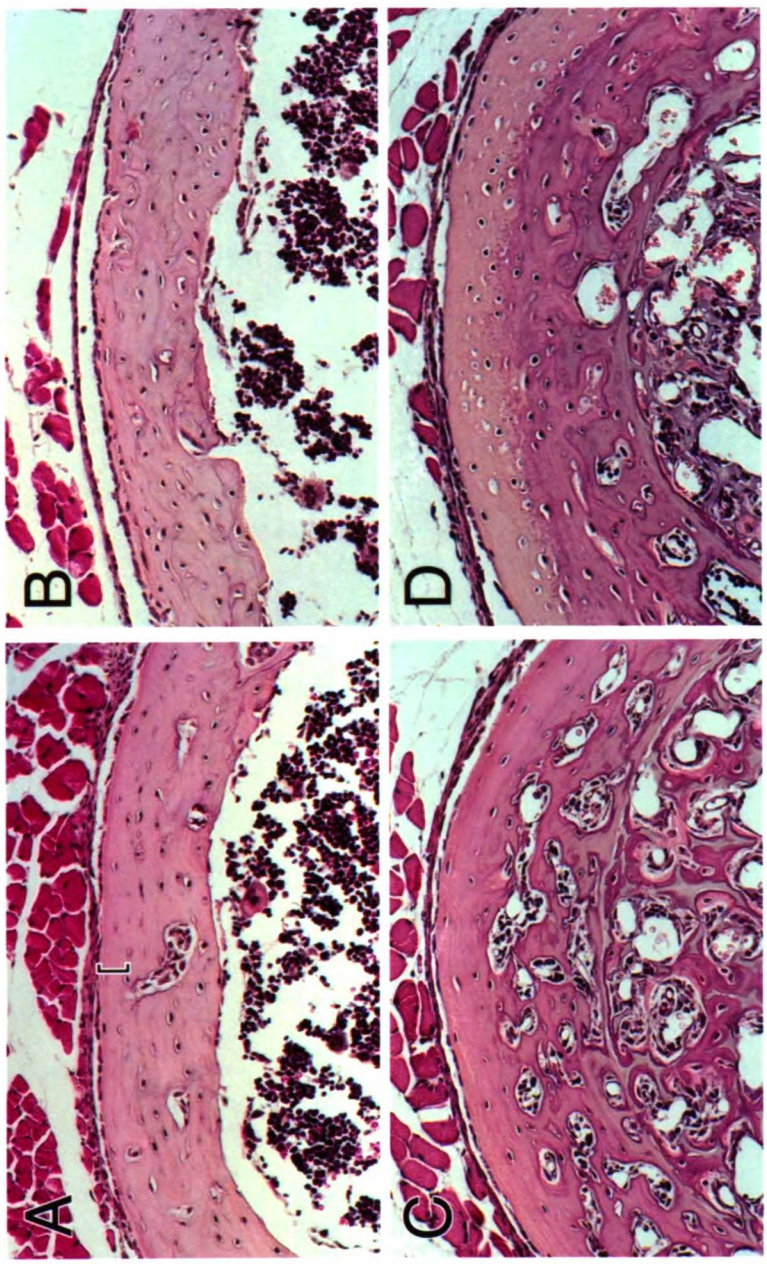
A
B
C
D

E

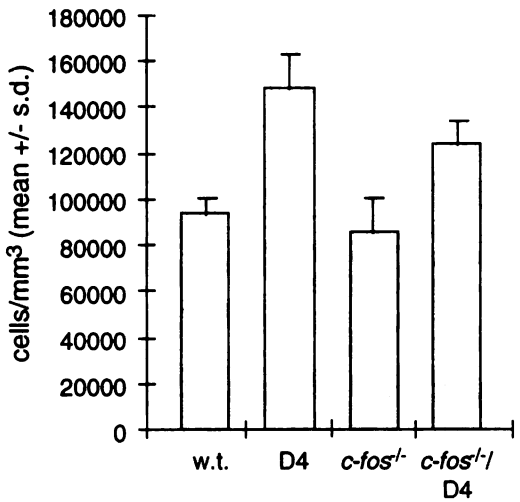
180000
160000
140000
120000
100000
80000
60000
40000
20000
0
cells/mm3 (mean +/- s.d.)
w.t.
D4
c-fos-/-
c-fos-/-/ D4

truncated receptor in cell culture has been shown to interfere with endogenous TGF-β signaling in a dominant negative fashion (Chen et al., 1993), and since the osteocalcin promoter is osteoblast-specific (Baker et al., 1992), we expected this transgenic line to have impaired TGF-β signaling in osteoblasts.

We crossed our D4 mice with the E1 transgenic mice to generate double transgenic D4/E1 mice that overexpress both the TGF-β2 and the truncated type II TGF-β receptor transgenes. Expression of the truncated receptor transgene in D4/E1 mice did not inhibit the expression of the TGF-β2 transgene, because the high level of TGF-β2 extractable from the bone matrix of D4 mice was not reduced in D4/E1 mice (data not shown). However, expression of the truncated receptor in D4/E1 mice dramatically reduced the high osteocyte density seen in D4 mice alone to almost wild-type levels. This effect was seen in both cortical bone where resorption is absent (Fig. 3a), as well as in the femoral epiphyses, where resorption is present (Fig. 3b). Furthermore, the osteocyte density in the femoral epiphyses of E1 mice was mildly (25%) reduced below the wild-type level, yet was not significantly different from wild-type mice in cortical bone (Fig. 3a and b). In contrast to the decrease in osteocyte density in D4/E1 mice, expression of the truncated receptor did not significantly affect the increased mineral apposition rate (see below) or the overall loss of cancellous bone mass caused by TGF-β2 overexpression. Furthermore, the hypoplastic clavicles and patent anterior fontanelles noted in D4 mice (Erlebacher and Derynck, 1996; unpublished observations) were also still present in D4/E1 doubly transgenic mice. Thus, these results strongly suggest that osteoblastic responsiveness to TGF-β is specifically required for both the increase in osteocyte density caused by

Figure 3. Effect of osteoblastic expression of a dominant-negative type II TGF-β receptor on osteocyte density in wild-type and D4 mice at day 35. Transgenic E1 mice overexpressing a truncated TGF-β receptor in osteoblasts were crossed to D4 mice overexpressing osteoblastic TGF-β2 to generate doubly transgenic D4/E1 mice. (A) Osteocyte density in the distal epiphysis of the femur, a site of bone resorption. The osteocyte density in E1 mice (*) was significantly reduced compared to wild-type ($P<0.005$). (B) Osteocyte density in cortical bone from the femoral diaphysis at the level of the third trochanter, where periosteal bone resorption is absent.

A

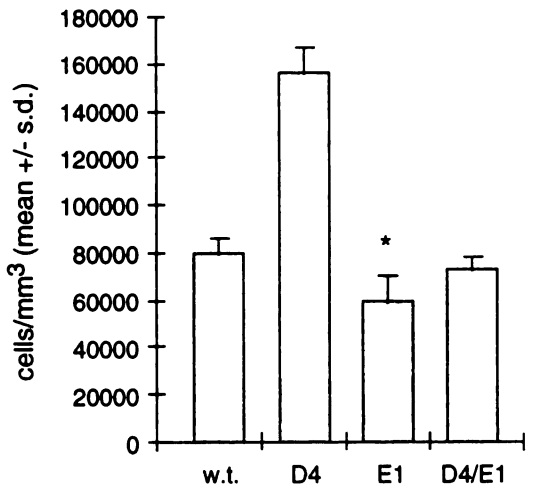
180000
160000
140000
120000
100000
80000
60000
40000
20000
0
cells/mm3 (mean +/- s.d.)
*
w.t.
D4
E1
D4/E1

B

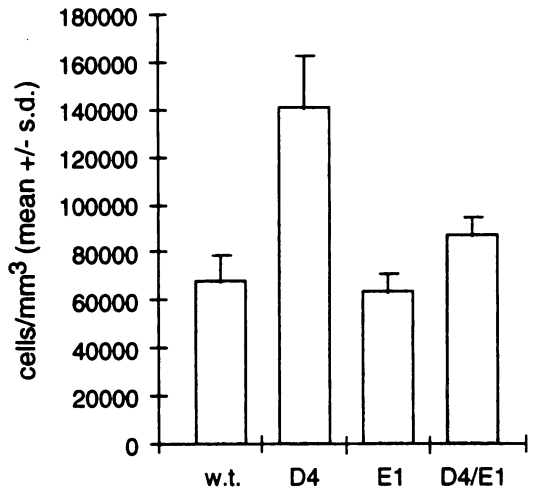
180000
160000
140000
120000
100000
80000
60000
40000
20000
0
cells/mm3 (mean +/- s.d.)
w.t.
D4
E1
D4/E1

osteoblastic overexpression of TGF-β, as well as for the generation of wild-type osteocyte density at some anatomical locations.

Alendronate reduces epiphyseal osteocyte density and plasma TGF-β2 levels.

From the experiments described above, we concluded that the increase in osteocyte density caused by TGF-β2 overexpression was a direct effect of TGF-β on osteoblasts that could occur in the absence of osteoclastic bone resorption. However, these analyses do not rule out the possibility that osteoclastic bone resorption might contribute to the increased osteocyte density at sites where active resorption occurs. We therefore inhibited bone resorption by injecting mice with alendronate, a bisphosphonate that potently inhibits osteoclastic bone resorption in vivo (for a review see Rodan and Fleisch, 1996), for a three week period prior to sacrifice at day 35. We then measured the osteocyte density in the femoral epiphysis, a site of ongoing resorption where osteocyte density was 1.9-fold higher in D4 mice than in wild-type mice. Since this treatment produced a mild osteopetrosis with serological changes in calcium and phosphorus levels consistent with secondary hyperparathyroidism (data not shown), we included in parallel experimental groups of mice that had undergone parathyroidectomy at day 21. As shown in Fig. 4a, alendronate treatment resulted in a moderate decrease in epiphyseal osteocyte density in D4 mice, but not in wild-type mice. Parathyroidectomy did not significantly affect osteocyte density. In contrast to its effects in the femoral epiphysis, and consistent with our results on diaphyseal osteocyte density at day 16, alendronate did not affect the subperiosteal osteocyte density (Fig. 4b). Thus, alendronate decreased the

Figure 4. Effect of alendronate and parathyroidectomy on osteocyte density in wild-type and D4 mice at day 35.

Mice were treated with alendronate or vehicle starting at day 15, and underwent parathyroidectomy or sham operation at day 21. (A) Osteocyte density in the distal epiphysis of the femur, a site of bone resorption. The reduction in osteocyte density in D4 mice caused by alendronate (*, $P<0.005$ compared to untreated mice) is much more striking after calculation of the osteocyte formation rate (Fig. 10). (B) Osteocyte density in the diaphyseal cortex of the femur at the level of the third trochanter, where periosteal bone resorption is absent. Osteocyte density was measured in only the subperiosteal 36 μm of cortical bone, which corresponds to periosteal bone made since day 21.

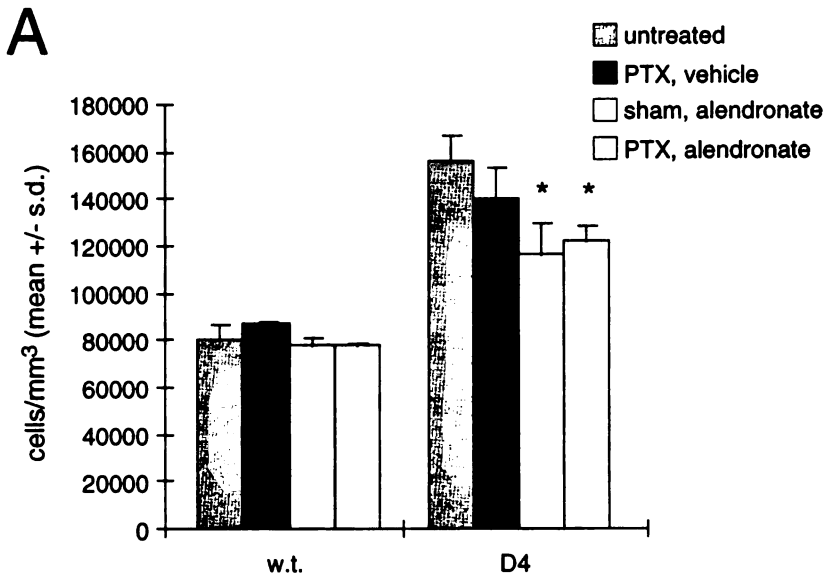
A
untreated
PTX, vehicle
sham, alendronate
PTX, alendronate
cells/mm3 (mean +/- s.d.)
180000
160000
140000
120000
100000
80000
60000
40000
20000
0
*
*
w.t.
D4

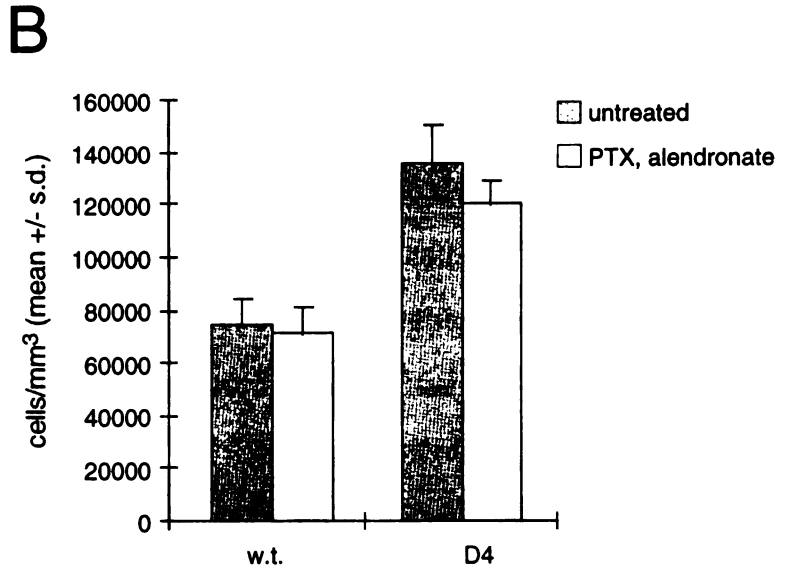
B
untreated
PTX, alendronate
cells/mm3 (mean +/- s.d.)
160000
140000
120000
100000
80000
60000
40000
20000
0
w.t.
D4

osteocyte density in D4 mice only at sites where osteoclastic bone resorption was present.

The observation that alendronate treatment decreased the epiphyseal osteocyte density in D4 mice suggested that bone resorption somehow locally enhanced the effect of TGF-β2 overexpression on osteocyte density. One possible mechanism, as previously suggested (Pfeilschifter and Mundy, 1987), is that osteoclastic bone resorption causes the release and activation of bone matrix-bound TGF-β, thereby increasing its local concentration on nearby bone surfaces. Since the level of bone matrix-bound TGF-β2 in D4 mice is considerably elevated over even the combined levels of TGF-β1 and -β2 in wild-type bone (Erlebacher and Derynck, 1996), its release from the matrix might conceivably lead to dramatic increases in the local concentration of TGF-β at bone surfaces. To evaluate this possibility, we measured the plasma level of TGF-β2 in D4 mice, which is elevated over wild-type (Erlebacher and Derynck, 1996), after treatment with alendronate. Injection of alendronate for one week starting at day 35 at the same dose as in our experiments above did not significantly reduce the level of plasma TGF-β2 (data not shown). However, three daily injections of a higher dose of alendronate in three month old mice resulted in reduced plasma TGF-β2 levels (Fig. 5). At this age, the direct contribution of the TGF-β2 secreted by osteoblasts to the plasma level of TGF-β2 is likely to be less than at day 35, when bone growth and remodeling are much more active. These results suggest that osteoclastic bone resorption can result in the release of bone matrix bound TGF-β and contribute to the elevated plasma levels of TGF-β.

Figure 5. The effect of alendronate on plasma TGF-β2 levels in wild-type and D4 mice.

Three month-old mice were injected daily for three days with 3 mg/kg alendronate or PBS vehicle prior to blood drawing, and plasma TGF-β2 levels were measured using a TGF-β2 ELISA.

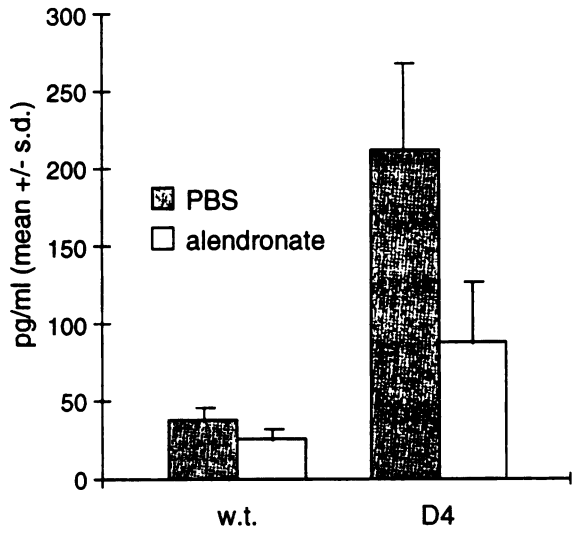
300
250
200
150
100
50
0
pg/ml (mean +/- s.d.)
PBS
alendronate
w.t.
D4

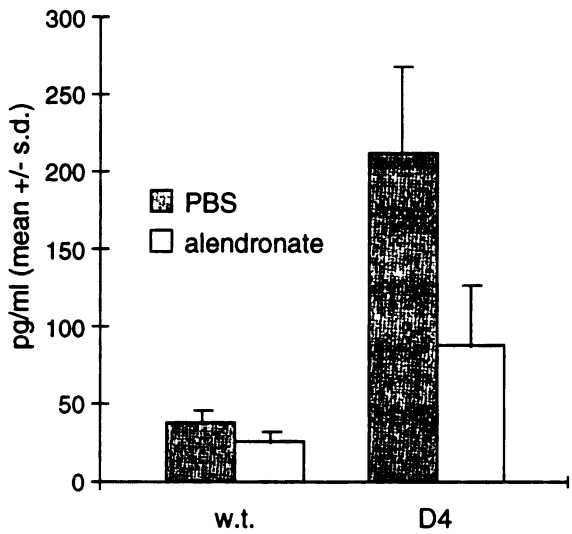
300
250
200
150
100
50
0
pg/ml (mean +/- s.d.)
PBS
alendronate
w.t.
D4

Kinetics of osteoblast differentiation.

Since it represented a direct effect of TGF-β on osteoblasts, we were interested in gaining further insight into the cause of the osteocyte density increase in D4 mice. In order to analyze the kinetics of osteoblast differentiation, 12-day-old mice were injected twice with bromodeoxyuridine (BrdU), which due to its short half-life in vivo (Packard, et al., 1973) labels dividing cells for two short periods. We then determined at day 16 the labeling index of mature periosteal osteoblasts on the femoral diaphysis, where resorption is absent. Mature osteoblasts, which are generally postmitotic in vivo (Young, 1962), were identified as comprising the monolayer of cuboidal cells abutting the bone surface (see Fig. 2a and b). These cells have been actively engaged in bone matrix synthesis since bone formation on their underlying surface has been continuous from day 12 to 16, with the same rate in both wild-type and D4 animals (see below). Fibroblastic osteoprogenitor cells, which are premitotic, were located more peripherally.

As shown in Fig. 6, the percentage of BrdU-labeled periosteal osteoblasts after the four day chase period was about 2.4-fold increased in D4 mice compared to wild-type mice. Furthermore, the percentage of labeled subperiosteal osteocytes per section was increased 8-fold from 0.5 (+/-0.6) in wild-type bone to 4.1 (+/-1.0) in D4 bone, which is proportionally much greater than would have been expected from the 1.6-fold increase in subperiosteal osteocyte density. Labeled osteoblasts and osteocytes could conceivably have been derived from osteoblasts dividing on day 12 that had either remained on the bone surface or subsequently matured into osteocytes. Alternatively, they could have been derived from osteoprogenitor cells dividing on day 12 that had subsequently differentiated. To distinguish

Figure 6. Kinetics of osteoblast differentiation in the femoral periosteum. Mice were injected with BrdU on day 12 and sacrificed on day 16. The number of labeled and total periosteal osteoblast nuclei was counted from immunostained sections of the femoral diaphysis at the level of the third trochanter. Overexpression of TGF-β2 in D4 mice increased the labeling index significantly over wild-type ($P<0.002$).

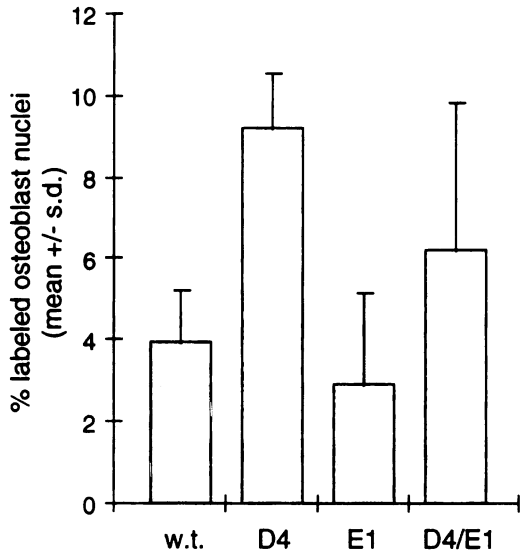
% labeled osteoblast nuclei
(mean +/- s.d.)
12
10
8
6
4
2
0
w.t.
D4
E1
D4/E1

between these possibilities, mice were given two pulses of BrdU and sacrificed the same day. With this schedule, D4 mice showed a low percentage of osteoblast labeling (1.6 +/-1.3) that was not significantly different from wild-type mice (0.45 +/-0.03), and sections showed no labeled osteocytes. This result is consistent with previous observations that mature osteoblasts rarely divide in vivo (Young, 1962). Furthermore, D4 and wild-type mice sacrificed two days after injection also showed low labeling indices (data not shown), indicating that a longer time period was required to generate appreciable numbers of labeled mature cells. Thus, the majority of BrdU-labeled osteoblasts and osteocytes after four days represent cells that had newly differentiated from osteoprogenitor cells that were dividing on day 12. Subtracting the same-day labeling index from the four-day labeling index, we estimate that osteoblastic overexpression of TGF-β2 increased the osteoblast birth rate about 2.2-fold, i.e. from a labeling index of 3.5 (+/-1.4) in wild-type bone to 7.6 (+/-1.9) in D4 bone.

In parallel to the experiments described above, we also analyzed the kinetics of osteoblast differentiation in our transgenic mice that overexpress the truncated type II TGF-β receptor in osteoblasts. Following BrdU-labeling at day 12 and analysis at day 16, the osteoblastic labeling index (Fig. 6) and the number of labeled subperiosteal osteocytes per section (not shown) were similar in E1 mice and wild-type mice. In D4/E1 doubly transgenic animals, these values were intermediate between wild-type and D4 mice, but showed variability between individual animals. Significantly, both results parallel the effect of truncated receptor overexpression on subperiosteal osteocyte density in wild-type and D4 mice (Fig. 3). Taken together, these kinetic studies are consistent with the notion that increased TGF-β2 expression in

osteoblasts stimulates the rate of osteoblastic differentiation, and that this stimulation underlies the increased osteocyte density in D4 mice.

Increased mineral apposition rate in D4 transgenic mice does not require osteoblastic TGF-β receptor function, yet is inhibited by alendronate.

One of the primary measures of the rate of bone deposition is the mineral apposition rate. This rate is experimentally determined through the sequential injection of two fluorochrome labels that are incorporated into bone matrix at sites of mineralization. Since the labels are injected with an interval of several days, they form clear parallel lines at sites of bone formation when viewed histologically. The mineral apposition rate is measured as the distance between the fluorochrome labels divided by the time between their injection (Parfitt et al., 1987).

We have previously shown that the mineral apposition rate on endosteal surfaces in the tibia was increased about 70% in D4 mice (Erlebacher and Derynck, 1996). Consistent with this observation, the mineral apposition rate measured on the endosteal surfaces of the femoral epiphysis at day 35 was 80% higher in D4 mice than in wild-type mice (Fig. 7). To evaluate whether this increase required TGF-β signaling in osteoblasts, we used the D4/E1 double transgenic mice which overexpress a cytoplasmically truncated type II TGF-β receptor in osteoblasts. In contrast to the dramatic effect of this truncated receptor on osteocyte density, the mineral apposition rate in D4/E1 mice showed the same 80% increase over wild-type mice as in D4 mice (Fig. 7). Furthermore, E1 mice showed no difference in their mineral apposition rate compared to wild-type mice. Thus, dominant negative interference with osteoblastic TGF-β receptor signaling did not affect the mineral apposition

Figure 7. The effect of osteoblastic expression of a dominant-negative type II TGF-β receptor on the mineral apposition rate in the femoral epiphyses of wild-type and D4 mice at day 35.

Transgenic E1 mice were crossed to D4 mice to generate doubly transgenic D4/E1 mice.

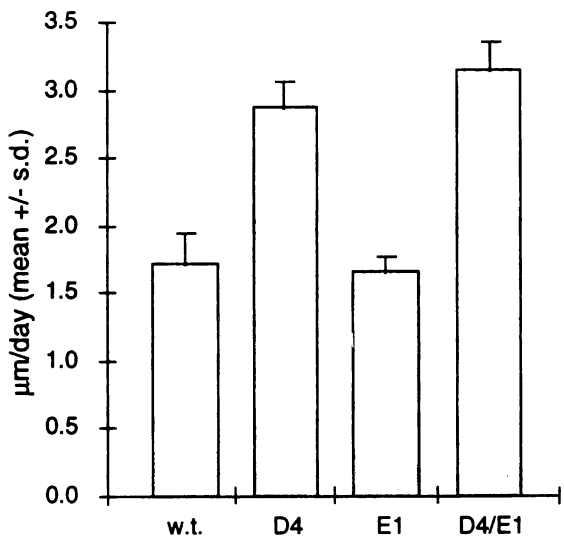
3.5
3.0
2.5
2.0
1.5
1.0
0.5
0.0
µm/day (mean +/- s.d.)
w.t.
D4
E1
D4/E1

rate, suggesting that its increase in D4 mice does not require osteoblastic responsiveness to TGF-β.

To assess whether the increased mineral apposition rate in D4 mice depended on osteoclastic bone resorption, we again tested the effect of alendronate administered over a three week period prior to sacrifice at day 35. In parallel, we included an experimental group that had undergone parathyroidectomy at day 21. Consistent with its inhibitory effect on bone resorption and, as a consequence, on overall bone formation (Rodan and Fleisch, 1996), alendronate decreased the percentage of fluorochrome-labeled bone surfaces from about 60% in the femoral epiphyses of both wild-type and D4 mice to about 30%. In addition, as shown in Fig. 8, treatment with alendronate dramatically reduced the epiphyseal mineral apposition rate in D4 bones to a level similar to wild-type, yet did not affect the mineral apposition rate in wild-type mice, which is consistent with previous results (Rodan and Fleisch, 1996). The decrease in mineral apposition rate in D4 mice was not due to impaired bone mineralization, since alendronate did not increase the lag time between osteoid deposition and its mineralization in wild-type or D4 mice (data not shown). Parathyroidectomy did not affect the mineral apposition rate in D4 or wild-type mice with or without alendronate treatment. Taken together, these observations suggest that the increase in mineral apposition rate in D4 mice does not depend on the responsiveness of osteoblasts to TGF-β yet requires osteoclastic bone resorption.

Figure 8. The effect of alendronate and parathyroidectomy on the epiphyseal mineral apposition rate in wild-type and D4 mice at day 35.
Mice were treated with alendronate or vehicle starting at day 15, and underwent parathyroidectomy or sham operation at day 21. The mineral apposition rate was determined in the distal epiphysis of the femur, a site of bone resorption.

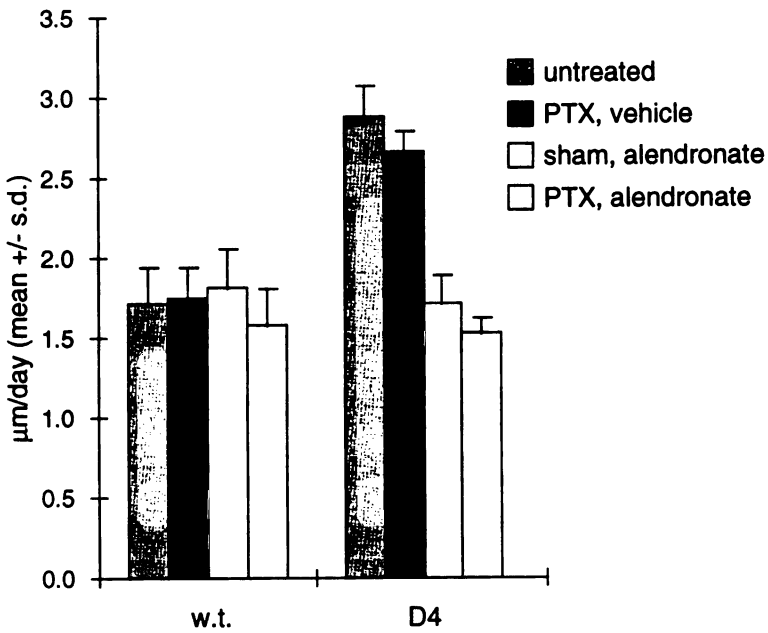
3.5
3.0
2.5
2.0
1.5
1.0
0.5
0.0
µm/day (mean +/- s.d.)
w.t.
D4
untreated
PTX, vehicle
sham, alendronate
PTX, alendronate

The mineral apposition rate in D4 mice is not increased on periosteal surfaces lacking bone resorption.

The conclusion that the increased mineral apposition rate in D4 mice depends on osteoclastic activity predicts that bone surfaces which lack osteoclastic resorption would not have an increased mineral apposition rate. We therefore examined the mineral apposition rate on the periosteal surface of the femoral diaphysis, a site devoid of osteoclastic activity (see above). As shown in Fig. 9, the periosteal mineral apposition rate in D4 mice was the same as in wild-type mice at both days 16 and 35 (Erlebacher and Derynck, 1996). The higher periosteal mineral apposition rate at day 16 is consistent with the faster growth rate of younger mice. Fluorochromes injected at this time formed continuous concentric rings parallel to the periosteum, showing that radial growth was continuous (data not shown). The periosteal mineral apposition rate of the tibia at day 16 was 50% greater than that of the femur (data not shown). Consistent with the absence of osteoclastic activity on the femoral diaphyseal periosteum, alendronate and parathyroidectomy treatment did not affect the mineral apposition rate in wild-type or D4 mice on periosteal surfaces (Fig. 9a).

Surprisingly, increasing TGF-β2 expression in osteoblasts in a *c-fos*$^{-/-}$ background, i.e. by crossing D4 mice with *c-fos*$^{-/-}$ mice, resulted in an increased periosteal mineral apposition rate compared to *c-fos*$^{-/-}$ controls (Fig. 9b). *c-fos*$^{-/-}$/D4 and *c-fos*$^{-/-}$ mice also showed lower serum calcium and phosphorus levels than wild-type mice (Table 1). However, the increase in periosteal mineral apposition rate in *c-fos*$^{-/-}$/D4 mice over *c-fos*$^{-/-}$ mice could not be ascribed to a differential defect in bone mineralization, since the lag time between osteoid deposition and its mineralization, i.e. the

Figure 9. Mineral apposition rate in the absence of bone resorption. The periosteal mineral apposition rate was determined from sections of cortical bone of the femoral diaphysis at day 35 (A) or day 16 (B). Sections were at the level of the third trochanter, where periosteal bone resorption is absent.

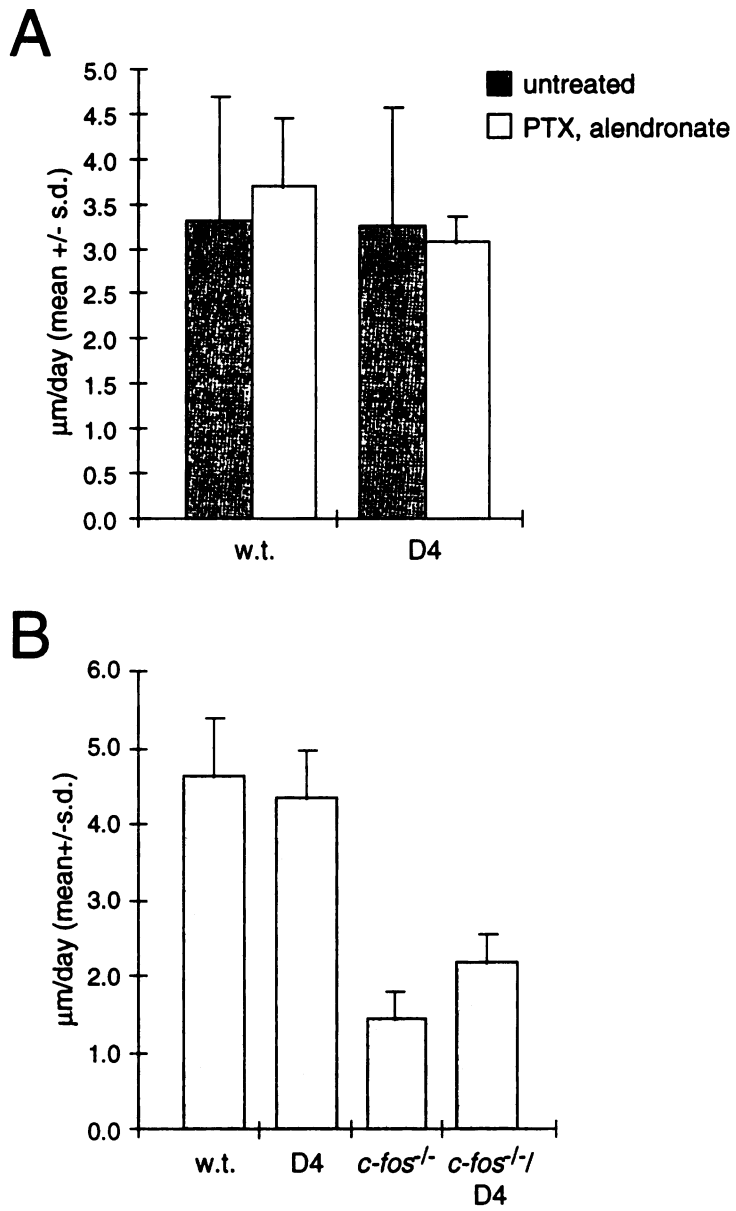
A
5.0
4.5
4.0
3.5
3.0
2.5
2.0
1.5
1.0
0.5
0.0
µm/day (mean +/- s.d.)
untreated
PTX, alendronate
w.t.
D4
B
6.0
5.0
4.0
3.0
2.0
1.0
0.0
µm/day (mean+/-s.d.)
w.t.
D4
c-fos-/-
c-fos-/-/
D4

Table 1. Growth parameters, serological values, and periosteal mineralization lag times in wild-type, D4, *c-fos*$^{-/-}$, and *c-fos*$^{-/-}$/D4 mice at day 16.

Significantly different from wild-type, *$P<0.01$; **$P<0.001$. The number of mice analysed is shown in parentheses.

Mouse	day 16 weight (g)	day 12 to day 16 growth rate (g/day)	Serum calcium (mg/dl)	Serum phosphorus (mg/dl)	Mineralization lag time (days)
wild-type	8.3+/-0.7 (17)	0.31+/-0.09 (17)	10.6+/-0.6 (12)	11.5+/-1.7 (12)	1.3+/-0.1 (7)
D4	7.7+/-1.0 (23)	0.29+/-0.06 (23)	10.7+/-0.5 (12)	10.6+/-1.2 (12)	1.5+/-0.4 (7)
c-fos$^{-/-}$	7.3+/-1.0 (13)*	0.07+/-0.05 (5)**	8.8+/-0.9 (5)**	6.0+/-0.9 (5)**	7.8+/-2.8 (8)**
c-fos$^{-/-}$/D4	7.1+/-1.5 (15)*	0.13+/-0.08 (7)**	9.4+/-0.6 (7)**	6.6+/-1.7 (7)**	8.7+/-3.5 (8)**

mineralization lag time (Table 1), was not significantly different between the two types of mice, although it was dramatically increased over normal. Thus, increased osteoblastic expression of TGF-β2 resulted in increased periosteal bone deposition in a *c-fos*$^{-/-}$ background, in contrast to the unaltered mineral apposition rate in a wild-type background. We were unable to accurately assess the mineral apposition rate of endosteal surfaces in *c-fos*$^{-/-}$ and *c-fos*$^{-/-}$/D4 mice because these surfaces lacked double fluorochrome labeling. The density of the slightly ossified calcified cartilage that fills the bone marrow cavities of *c-fos*$^{-/-}$ mice was unchanged in *c-fos*$^{-/-}$/D4 mice (data not shown).

Whereas TGF-β2 overexpression increased the periosteal mineral apposition rate in *c-fos*$^{-/-}$ mice, it should be emphasized that the mineral apposition rate in *c-fos*$^{-/-}$ mice was dramatically lower than in wild-type mice (Fig. 9b). Furthermore, *c-fos*$^{-/-}$ and *c-fos*$^{-/-}$/D4 mice were smaller and had a dramatically reduced growth rate compared to wild-type or D4 mice (Johnson et al., 1992, Table 1). TGF-β2 overexpression in osteoblasts did not affect the weights and growth rates of wild-type or *c-fos*$^{-/-}$ mice (Table 1). Lastly, *c-fos*$^{-/-}$/D4 mice evaluated at day 35 had a dramatically increased incidence of long bone fractures. As previously observed, D4 mice occasionally showed spontaneous fractures (Erlebacher and Derynck, 1996); however, five out of nine *c-fos*$^{-/-}$/D4 mice showed tibial fractures (with bilateral fractures observed in four cases), whereas none of the six *c-fos*$^{-/-}$ mice examined showed hind limb fractures.

DISCUSSION

TGF-β is abundant in bone matrix and all three TGF-β isoforms are expressed by bone cells in vivo. In vivo and in vitro studies have previously shown that TGF-β affects the activity and differentiation of both osteoblasts and osteoclasts (Bonewald and Dallas, 1994; Centrella, et al., 1994). However, the complexity of these data and the difficulty in applying their interpretations to the context of normal bone development and remodeling has made it difficult to define the physiological role of skeletal TGF-β. In the present study, we have used transgenic mice that overexpress TGF-β2 in bone to study the physiological responses of osteoblasts to TGF-β during bone remodeling in vivo. As starting points for our analysis, we focused on the two endpoint osteoblastic responses to TGF-β2 overexpression, namely the increase in bone formation as measured by the mineral apposition rate, and the increase in osteocyte density, which reflects a hyperplastic perturbation of osteoblast differentiation.

Increased osteocyte density results from a direct effect of TGF-β on osteoblasts.

Our previous results showed that increased expression of TGF-β in osteoblasts results in an increased osteocyte density (Erlebacher and Derynck, 1996). Two key results here strongly suggest that this increase does not depend on osteoclastic activity. First, TGF-β overexpression causes an increase in osteocyte density in the subperiosteal cortical bone of the diaphysis, a site devoid of osteoclasts. Second, the increase in osteocyte density persists in a genetic background where osteoclasts are completely

absent, i.e. in a *c-fos*$^{-/-}$ background. We also showed that the increased osteocyte density requires osteoblastic responsiveness to TGF-β. Thus, coexpression of a dominant negative type II TGF-β receptor in osteoblasts decreases the osteocyte density of D4 mice to a level similar to that of wild-type mice. Furthermore, expression of the dominant negative receptor alone reduced the osteocyte density below the wild-type level. From these results, we conclude that TGF-β increases osteocyte density as a direct effect on osteoblasts.

Whereas the increased osteocyte density corresponds to the endpoint response of overexpressed TGF-β, this parameter may not accurately reflect the rate of differentiation from osteoblast to osteocyte. Indeed, the relative rate of osteocyte formation should be assessed by multiplying the osteocyte density with the mineral apposition rate, which in turn correlates with the local rate of bone deposition. This index may therefore be a better measure of the effects of TGF-β on osteocyte differentiation. Thus, the 1.6-fold increase in subperiosteal osteocyte density in D4 mice compared to wild-type translates directly into a 1.6-fold increase in the osteocyte formation rate, since the periosteal mineral apposition rate is not altered in D4 mice. In contrast, the 1.9-fold increase in osteocyte density in the femoral epiphysis of D4 mice actually reflects a 3.3-fold increase in the osteocyte formation rate, because the mineral apposition rate at that site is increased 1.7-fold (Fig. 10a). Furthermore, while the truncated type II TGF-β receptor dramatically reduces the epiphyseal osteocyte density of D4 mice down to the wild-type level (Fig. 3), the epiphyseal osteocyte formation rate in D4/E1 mice is still elevated 1.7-fold over normal (Fig. 10a), since the local mineral apposition rate is increased (Fig. 7). This partial inhibitory effect of the dominant-

Figure 10. Osteocyte formation rates in the femoral epiphysis at day 35. (A) Effects of TGF-β2 overexpression and osteoblastic expression of a truncated type II TGF-β receptor on the epiphyseal osteocyte formation rate. Transgenic E1 mice were crossed to D4 mice to generate doubly transgenic D4/E1 mice. (B) Effect of alendronate on the epiphyseal osteocyte density. Alendronate dramatically inhibits the osteocyte formation rate increase in D4 mice because it inhibits both the osteocyte density increase as well as the mineral apposition rate increase caused by TGF-β2 overexpression.

A

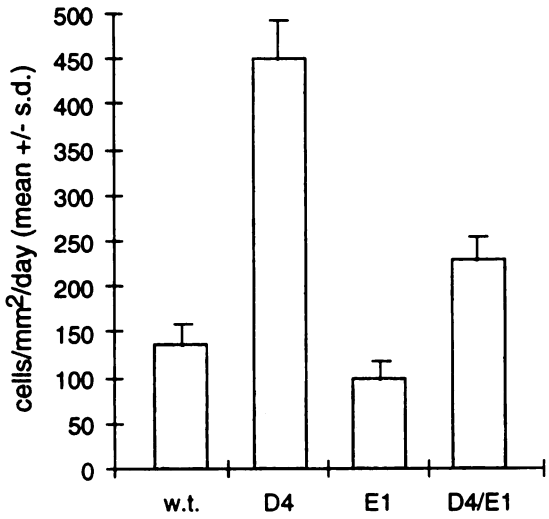
cells/mm2/day (mean +/- s.d.)
500
450
400
350
300
250
200
150
100
50
0
w.t.
D4
E1
D4/E1

B

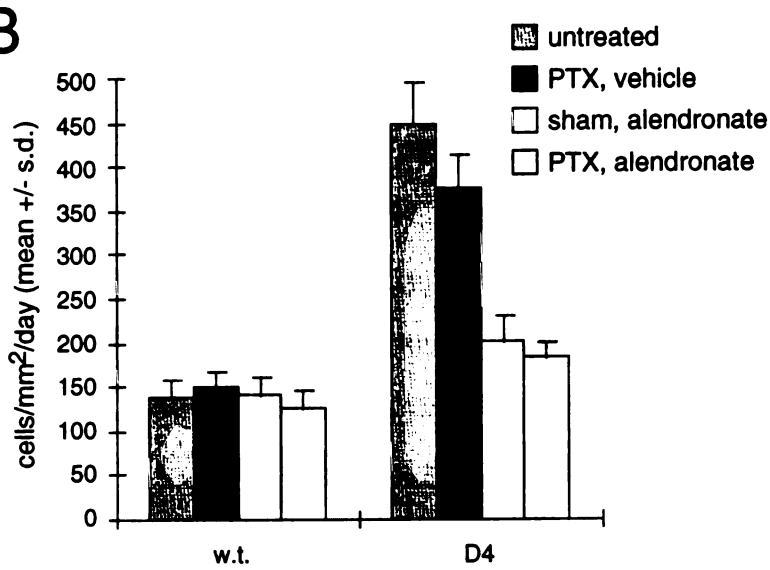
untreated
PTX, vehicle
sham, alendronate
PTX, alendronate
cells/mm2/day (mean +/- s.d.)
500
450
400
350
300
250
200
150
100
50
0
w.t.
D4

negative receptor is consistent with our expectation that it acts as a competitive inhibitor of TGF-β signaling. Lastly, the modest inhibitory effect of alendronate on absolute epiphyseal osteocyte density in D4 mice (Fig. 4a) actually underestimates a dramatic inhibition of the local osteocyte formation rate (Fig 10b), since alendronate dramatically inhibits the mineral apposition rate increase in D4 epiphyses (Fig 8). Alendronate, however, did not affect the periosteal osteocyte formation rate, since it had no effect on the periosteal mineral apposition rate or the subperiosteal osteocyte density.

The increased mineral apposition rate depends upon osteoclastic activity and not upon the direct response of osteoblasts to TGF-β.

Whereas the increased osteocyte density caused by TGF-β2 overexpression clearly depends on the direct response of osteoblasts to TGF-β and not on osteoclastic activity, the increased rate of bone formation by osteoblasts, as measured by the mineral apposition rate, is a function of bone resorption. This conclusion is based on several observations. First, osteoblastic overexpression of a truncated type II TGF-β receptor did not affect the mineral apposition rate in the femoral epiphysis of wild-type and D4 mice, even though it reduced the osteocyte density at this location in both mice. Second, increased TGF-β2 expression resulted in increased osteocyte density in subperiosteal cortical bone, but did not affect the periosteal mineral apposition rate. Lastly, alendronate treatment inhibited the increase in mineral apposition rate caused by overexpression of TGF-β2.

The dependence of the mineral apposition rate on osteoclast activity stands in contrast to the osteoblast-mediated effects of TGF-β2 on the osteocyte density. Given the different dose-dependent responses of many cell

types to TGF-β and the possibility that distinct TGF-β signals are differentially inhibited by dominant negative receptor interference (Chen, et al., 1993; Derynck and Feng, 1997), the increases in mineral apposition rate and osteocyte density could conceivably result from distinct effects of TGF-β2 on osteoblasts with different thresholds of response. However, the ability of the truncated receptor to inhibit the increase in epiphyseal osteocyte density, but not the increase in the epiphyseal mineral apposition rate, would then imply that higher TGF-β concentrations are required to increase the osteocyte density than to increase the mineral apposition rate. This is difficult to reconcile with the findings that TGF-β increases subperiosteal osteocyte density without changing the periosteal mineral apposition rate, or that the epiphyses of alendronate-treated D4 mice have a normal mineral apposition rate but an elevated osteocyte density. Instead, our results are much more consistent with the simple interpretation that increased TGF-β2 expression leads to an increase in the epiphyseal mineral apposition rate as a secondary response to its stimulation of bone resorption.

This conclusion falls into line with a number of other observations suggesting that TGF-β does not directly regulate the rate of bone formation during bone remodeling. Specifically, dominant negative interference with TGF-β receptor signaling in osteoblasts not only had no effect on the increased mineral apposition rate in D4 mice, but also had no effect on the mineral apposition rate in wild-type mice. Furthermore, TGF-β2 overexpression in D4 mice did not increase the fraction of total bone surface undergoing mineralization (see above), which is a parameter that reflects bone formation at the osteoblast population level. Reciprocally, expression of the truncated receptor in E1 mice does not reduce the mineralizing surface below

the wild-type level (Filvaroff et al., in preparation), and reducing the skeletal content of TGF-β1 in half by targeted inactivation of one TGF-β1 allele has no effect on either the mineral apposition rate nor the mineralizing surface (Erlebacher et al., in preparation). Thus, we can find no evidence, at either the local or tissue level, that TGF-β directly regulates the rate of bone formation. It is possible that the observed increases in bone formation following subperiosteal injections of TGF-β (Joyce et al., 1990; Noda and Camilliere, 1989) reflect part of a exaggerated tissue or microfracture repair process consistent with the role of TGF-β in wound healing (Border and Noble, 1994), but distinct from the skeletal actions of TGF-β under physiological conditions.

The increased mineral apposition rate in D4 mice might reflect a homeostatic response that maintains bone integrity past a critical threshold of resorption. The effect may therefore be similar to the increase in mineral apposition rate following treatment with continuous high doses of PTH, which also induces extensive bone resorption (Hock and Gera, 1992; Uzawa et al., 1995). Rather than depending directly on the level of osteoclastic activity, however, such a mechanism may be generally sensitive to impaired mechanical and structural properties of bone. Thus, mice with osteogenesis imperfecta show increases in periosteal bone formation as a compensatory response to their severely impaired skeletal integrity (Bonadio et al., 1993; Pereira et al., 1995).

The increase in bone formation as a result of impaired mechanical properties might also explain our findings that the periosteal mineral apposition rate in *c-fos*$^{-/-}$/D4 is increased over to *c-fos*$^{-/-}$ mice, even though D4 mice have the same periosteal mineral apposition rate as wild-type mice.

Osteopetrotic bones are structurally defective, as apparent from the increased fracture risk of humans with osteopetrosis (Rimoin and Lachman, 1993). Concurrent TGF-β2 overexpression probably adds to the structural defects by decreasing bone matrix quality, as *c-fos*$^{-/-}$/D4 mice have a dramatic increase in fracture incidence over *c-fos*$^{-/-}$ mice, even though both mice have the same total bone mass. Thus, the increased periosteal mineral apposition rate in *c-fos*$^{-/-}$/D4 mice may reflect a compensatory response to the severely impaired mechanical properties of *c-fos*$^{-/-}$/D4 bone.

TGF-β increases the steady-state rate of osteoblastic differentiation on forming bone surfaces.

The increase in osteocyte density, as clearly representing a direct effect of TGF-β on osteoblasts, provided a basis for further investigations into the skeletal physiology of TGF-β. Our BrdU labeling experiments showed that the increase in osteocyte density resulted at least partially, if not entirely, from an increased rate of osteoblastic differentiation. Four days after injection of BrdU, the fraction of newly differentiated periosteal osteoblasts was increased 2.2-fold over wild-type, and the number of labeled subperiosteal osteocytes in cortical bone was disproportionally increased relative to the increase in osteocyte density. Indeed, the 2.2-fold increase in periosteal osteoblast birth rate in D4 mice is of sufficient magnitude to explain the concurrent 1.6-fold increase in the osteocyte formation rate on the femoral periosteum, and the 1.6-fold resultant increase in the final osteocyte density. Overexpression of TGF-β2 may also affect the rate of apoptosis of osteoprogenitors and osteoblasts; however, we were unable to notice any

differences in the very low level of detectable apoptotic cells, as assessed by DAPI staining of the femoral periosteum at day 16 (data not shown).

Consistent with the increase in osteocyte density itself being a direct effect of TGF-β on osteoblasts, the increases in osteoblast and osteocyte labeling occurred in the absence of bone resorption, and both increases were partially inhibited by dominant negative interference with TGF-β signaling in osteoblasts. Thus, we conclude that TGF-β also increases the rate of osteoblastic differentiation as a direct effect on osteoblasts. Since the surface density of osteoblasts in D4 bone is not increased over wild-type on any bone surface analyzed at any age (Erlebacher and Derynck, 1996, Fig. 2a and b, and data not shown), we emphasize that the increase in differentiation rate reflects an ongoing steady-state phenomenon rather than the transient en masse maturation of a finite progenitor population. TGF-β has therefore a primarily kinetic effect on osteoblast differentiation on forming bone surfaces, increasing both the rate of mature osteoblast formation from osteoprogenitor cell and the rate of osteocyte formation from osteoblast, without causing a steady-state increase in the actual number of osteoblasts present at one time.

From these experiments, however, we cannot conclude whether TGF-β accelerates the maturation rate of osteoprogenitor cells that are already committed to terminal differentiation, or induces a larger number of osteoprogenitor cells to undergo differentiation. Since the expression of the truncated receptor from the osteocalcin promoter is strongly upregulated during post-mitotic osteoblast maturation (Bronckers et al., 1985; Groot et al., 1986), the direct effect of TGF-β on osteoblasts may be to induce a secondary signal that increases both the proliferation of osteoprogenitor cells and the frequency that they initiate further differentiation. We speculate that part of

this secondary signal may be PDGF, since PDGF selectively stimulates osteoprogenitor cell proliferation (Hock and Canalis, 1994) and mediates the TGF-β-stimulated proliferation of a number of mesenchymal cell types (Battegay et al., 1990).

Interestingly, the developmental phenotype of D4 mice (Erlebacher and Derynck, 1996) bears a striking resemblance to the phenotype of mice heterozygous for an inactivated allele of *Cbfa1*, a transcription factor required for normal ossification and osteoblast differentiation (Ducy et al., 1997; Komori et al., 1997; Otto et al., 1997). Both mice show the hypoplastic clavicles, patent anterior fontanelles, and general delay in ossification characteristic of cleidocranial dysplasia. This phenotypic similarity suggests that TGF-β may downregulate the embryonic expression of *Cbfa1*. Since the cleidocranial phenotype in D4 mice does not require osteoblastic responsiveness to TGF-β, its underlying mechanism is likely to be quite distinct from the direct stimulatory effects of TGF-β2 on the rate of osteoblastic differentiation in the mature skeleton.

We chose to analyze the kinetics of osteoblast differentiation in D4 mice on the day 16 femoral periosteum so as to avoid the confounding effects of differences in the mineral apposition rate and levels of bone resorption. However, we infer that TGF-β also stimulates the rate of osteoblast differentiation on endosteal surfaces, such in the femoral epiphysis where the osteocyte formation rate is 3.3-fold over wild-type. Since the osteocyte density in the femoral epiphysis is actually decreased below the wild-type level in E1 mice, we also infer that endogenous TGF-β signaling in osteoblasts is required to maintain the normal rate of osteoblastic differentiation at this location. Demonstrating this directly will require extensive kinetic analyses

since the osteocyte density in E1 mice is reduced in epiphysis by only a mild 25%.

In contrast to the epiphysis, however, dominant-negative interference with TGF-β signaling in osteoblasts did not significantly reduce the osteocyte density in cortical bone, which is consistent with the inability of the truncated receptor to reduce the osteoblast birth rate below the wild-type level on periosteal surfaces. These results may therefore reveal a relatively low level of endogenous TGF-β activity on periosteal surfaces compared to endosteal surfaces. We speculate that such apparent differences in the spatial distribution of TGF-β activity in bone may at least partially explain the higher rate of osteoblastic differentiation on endosteal surfaces compared to periosteal surfaces (Young, 1962). Localized or overall increases in TGF-β activity may be involved in the increased osteocyte density seen in several metabolic bone disease states such as osteoporosis (Mullender et al., 1996), hyperparathyroidism (Malluche and Faugere, 1990), and osteogenesis imperfecta (Bonadio, et al., 1993; Whyte, 1996). Since osteocytes potentially mediate skeletal responses to mechano-sensation (Aarden et al., 1994), regulating their density by TGF-β might have significant secondary effects on bone metabolism.

Contributions of osteoclasts to the increased rate of osteoblastic differentiation caused by TGF-β.

As discussed above, the increases in osteocyte density, the osteocyte formation rate, and the rate of osteoblastic differentiation on forming bone surfaces in D4 mice all depend upon the direct response of osteoblasts to TGF-β and do not require bone resorption. However, we also found that

alendronate dramatically reduced the osteocyte formation rate in D4 mice in the femoral epiphysis, a site of bone resorption (see above and Fig. 10b). This effect was clearly associated with osteoclastic activity and was not caused by a general inhibition of TGF-β signaling, since alendronate did not alter the increased osteocyte formation rate on periosteal surfaces. Thus, at sites of bone resorption, osteoclastic activity augments the direct effects of TGF-β2 on the osteocyte formation rate, and by extension the direct stimulatory effect of TGF-β2 on the overall rate of osteoblastic differentiation.

Since experiments with the truncated type II TGF-β receptor showed that the increase in epiphyseal osteocyte formation rate in D4 mice is largely, if not entirely, due to the direct local actions of TGF-β2 on osteoblasts, the similar inhibition of the osteocyte formation rate increase by alendronate reveals a substantial contribution by osteoclasts to the local level of TGF-β activity. It has been shown that osteoclasts may activate latent TGF-β (Oreffo, et al., 1989; Oursler, 1994), and osteoclasts could in principle increase osteoblastic responsiveness to TGF-β. Furthermore, osteoclastic bone resorption leads to the release of bone matrix-bound TGF-β in organ culture (Pfeilschifter and Mundy, 1987). Accordingly, we have shown that alendronate is able to decrease the plasma level of TGF-β2 in D4 mice, consistent with the osteoclast-mediated release of TGF-β from bone matrix.

The spatial and temporal coupling of osteoblastic differentiation to sites of osteoclastic activity is one of the central tenets of bone remodeling, yet the regulation of this process remains poorly understood at the molecular level. Since the direct stimulation of the rate of osteoblastic differentiation on forming bone surfaces by TGF-β can be further augmented by local osteoclastic activity, TGF-β may be an important molecular mediator that

contributes to the coupling of osteoblastic differentiation to sites of bone resorption. Since overexpression of TGF-β in transgenic mice also leads to an increase in bone resorption (Erlebacher and Derynck, 1996), TGF-β may be involved in more complex regulatory circuits that regulate and coordinate the activities of both osteoblasts and osteoclasts during bone remodeling. Deregulation of skeletal TGF-β expression, activation, and responsiveness may have important physiological consequences and contribute to pathological bone remodeling states.

ACKNOWLEDGMENTS

We thank Ilse Sauerwald and Nilda Ubana for their assistance with the histological analyses, and Margaret Mayes for her assistance with the scanning electron microscopy. We also thank Gideon Rodan for the alendronate and Randall Johnson for the *c-fos*$^{-/-}$ mice. We are grateful to Deborah Zimmerman, Alfred Kuo, Steve Gitelman, Bernard Halloran, Gideon Rodan, and Zena Werb for helpful discussions, and Jill Helms for use of the fluorescence microscope used in the kinetic analyses. This research was supported by grants DE10306 and AR41126 to R.D. and a postdoctoral fellowship from the American Heart Association to E.H.F. A.E. is a member of the Medical Scientist Training Program supported by grant NIGMS GM07618.

Chapter 5:

Osteoblastic contributions to TGF-β-induced osteoporosis

Postmenopausal osteoporosis is caused by a relative increase in the rate of bone resorption over the rate of bone formation. Rodent models of estrogen deficiency-induced osteoporosis have suggested that bone loss results from increased numbers of osteoclasts; however, this has been an inconsistent finding in postmenopausal women, and other aspects of the resorption process may be important. We have previously shown that the osteoblastic overexpression of TGF-β2 in transgenic mice leads to a high-turnover osteoporosis-like phenotype involving increases in both bone resorption and formation. While clearly dependent upon the presence of osteoclasts, the increase in bone resorption surprisingly does not correlate with increases in osteoclast number, turnover, or apparent activity as assessed histologically and biochemically. Rather, the increase in resorption requires osteoblastic responsiveness to TGF-β, and correlates with increased production of gelatinase A and with changes in bone matrix composition and cellularity. These results suggest that osteoblastic processes may have an important rate-limiting role in pathological bone resorption independent of changes in osteoclast behavior per se.

Osteoporosis, a disease of bone remodeling, ultimately stems at the tissue level from an excess of bone resorption by osteoclasts over bone formation by osteoblasts (for review see Manolagas and Jilka, 1995). At the cellular and molecular levels, however, the causes of osteoporosis are very unclear and likely to be heterogeneous (Eriksen et al., 1990; Meunier et al., 1980; Parfitt et al., 1980; Whyte et al., 1982). This is even the case with postmenopausal osteoporosis, where the primary defect is likely to be an overstimulation of bone resorption. Rodent models of estrogen deficiency caused by ovariectomy have focused attention on increased osteoclast

differentiation in turn leading to increased osteoclast numbers (for reviews see Kalu, 1991; Manolagas and Jilka, 1995). However, histomorphometric studies of women with postmenopausal osteoporosis have shown increased osteoclast numbers only inconsistently (Eriksen, et al., 1990; Meunier, et al., 1980; Parfitt, et al., 1980; Whyte, et al., 1982), and instead have implicated increased bone resorption per osteoclast (Eriksen, et al., 1990). Unfortunately, there are no animal models that mimic this latter situation.

In order to study the skeletal actions of transforming growth factor-β (TGF-β), which is abundant in bone, we have previously generated transgenic mice that overexpress TGF-β2 from the osteoblast-specific osteocalcin promoter (Erlebacher and Derynck, 1996). Surprisingly, these mice showed a dramatic loss of cancellous bone mass and an increased fracture incidence very similar to that seen in osteoporosis and other metabolic bone diseases. In the high expressing D4 line, bone loss was extreme by one month of age and was associated with several histological indications of rapid bone turnover.

Increases in bone resorption in D4 mice were evident at three anatomical locations. In the cortices of long bones, resorption lacunae were very pronounced, and when refilled created large intracortical patches of unmineralized bone (Erlebacher and Derynck, 1996, and see Fig. 2e). In the metaphyses and epiphyses of long bones, cancellous bone volume was dramatically reduced despite an increase in bone formation (Erlebacher and Derynck, 1996 and submitted). Lastly, the number of osteoclasts was dramatically increased on the endocranial surface of calvariae from 35 day-old D4 mice (Fig. 1c and f), although calvarial osteoclast number appeared normal prior to day 21 (Fig. 1a, b, d and e). Significantly, TGF-β2 overexpression did

Figure 1. Bone resorption in D4 transgenic mice overexpressing TGF-β2 in osteoblasts.

(a-f) Whole-mount TRAP-stained calvariae of wild-type (a-c) and D4 (d-f) mice at postnatal day 6 (a and d), day 16 (b and e), and day 35 (c and f). Increases in osteoclast number in C4 calvariae are only apparent at the 35 day time point.

(e) Bone resorption as measured by ^{45}Ca release from prelabeled postnatal day 6 calvariae. ^{45}Ca release in D4 mice is significantly increased over wild-type ($P<0.0001$), and ^{45}Ca release in both wild-type and D4 mice was inhibited by 10 ng/ml salmon calcitonin (sCT) ($P<0.0005$). The data shown represent the compilation of two independent experiments; the increase in ^{45}Ca release in D4 calvariae over wild-type was also seen in seven other independent experiments.

(f) Osteoclast density, osteoclast apoptosis, and percentage of osteoclasts with ruffled borders in the distal femoral metaphysis of 35 day-old mice. Values show mean +/- SEM of n=4-5 mice each (osteoclast number and ruffled border measurements) or n=7-8 mice each (apoptosis measurements).

A
B
C
D
E
F

G

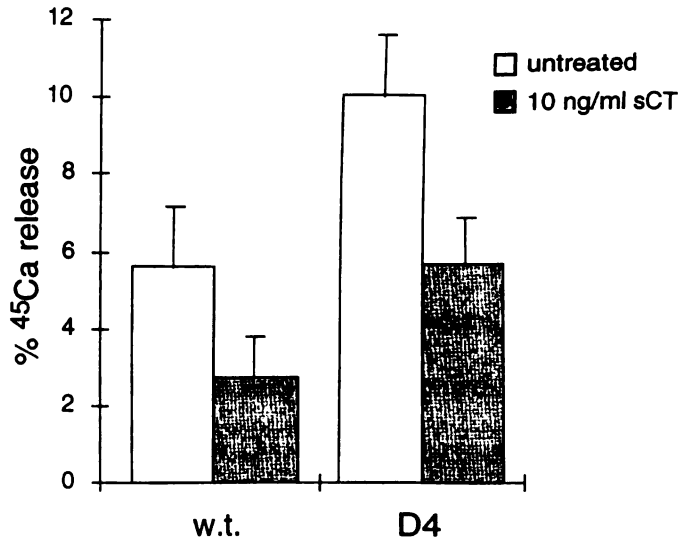

H

	Osteoclasts/ mm² bone area	Apoptotic osteoclasts (%)	Osteoclasts with ruffled borders (%)
wild-type	144 +/- 12	0.25 +/- 0.06	69.9 +/- 1.9
D4	155 +/- 23	0.30 +/- 0.10	73.6 +/- 2.2

not induce ectopic osteoclasts on bone surfaces normally devoid of osteoclastic activity. Thus, resorption lacunae were absent from the diaphyseal periostea of long bones despite the clear presence of increased TGF-β2 activity at these surfaces (Erlebacher et al., submitted), and no osteoclasts were seen on ectocranial surfaces of calvariae (data not shown) .

Although osteoclast number on the calvariae of D4 mice at day 6 was normal (Fig. 1a and d), bone resorption was still elevated 1.8-fold at this location as measured by the release of ^{45}Ca from prelabeled calvariae (Fig. 1g). This increase was at least partially dependent upon the actions of osteoclasts, as the release of ^{45}Ca was partially inhibited by 10 ng/ml salmon calcitonin in both wild-type and D4 mice. Reciprocally, osteoclast density per mm^2 bone surface in the femoral metaphysis at 35 days of age was unchanged in D4 mice compared to wild-type (Fig. 1h), in accord with previous results (Erlebacher and Derynck, 1996) and despite our inference that bone resorption is increased at this location as well. We also found no change in the percentage of apoptotic osteoclast nuclei in D4 bone (Fig. 1h), suggesting that the turnover of osteoclasts is not affected by TGF-β2 overexpression. Lastly, the percentage of osteoclasts with ruffled borders, as a histological measure of their activity, was not increased in D4 bone (Fig. 1h).

Taken together, these results show that the increase in bone resorption caused by TGF-β2 overexpression does not correlate with an increase in the number of osteoclasts, yet still requires their presence and activity. Furthermore, these results show that TGF-β2 does not induce ectopic osteoclasts, change their rate of turnover, or induce their activity as assessed histologically. While the increase in osteoclast number on the endocranial surface of the calvarium after day 21 may be an exception to this rule, it is also

very likely that this particular alteration stems from the unusual nature of calvarial development. The calvarium forms via intramembranous ossification, with osteoclasts disappearing from the endocranial surface of wild-type calvariae at around day 21 when they start to excavate bone marrow cavities from the peripheries of each individual calvarial bone (Erlebacher and Derynck, unpublished observations). Since bone turnover is very rapid in D4 mice, which results in calvariae that are much more porous than normal (data not shown), this developmental transition may be profoundly perturbed. By whatever mechanism, however, the increase in calvarial osteoclasts at day 35 provides a good endpoint marker for the pathological remodeling seen in D4 mice.

Since the increase in bone resorption in D4 mice is not caused by increased numbers of osteoclasts, we hypothesized that the defect may be caused by either an increase in the resorptive capacity per osteoclast, or by a non-osteoclastic process. To test the potential contribution of osteoblasts, we crossed our D4 mice to a new line of transgenic mice (E1 mice) that overexpress a cytoplasmically-truncated type II TGF-β receptor from the osteocalcin promoter (Filvaroff et al., in preparation). Since this truncated receptor has been shown to interfere with TGF-β signaling in vitro in a dominant-negative fashion, we expected these mice to have impaired osteoblastic responsiveness to TGF-β. Indeed, in doubly transgenic D4/E1 mice, the truncated receptor was able to dramatically and specifically rescue the increase in osteocyte density caused by TGF-β2 overexpression, validating this approach in vivo (Erlebacher et al., submitted).

Surprisingly, expression of the truncated TGF-β receptor in D4/E1 mice also dramatically rescued the increase in bone resorption caused by

TGF-β2 overexpression (Fig. 2). The number of osteoclasts in the calvariae of D4/E1 mice at day 35 was dramatically reduced compared to D4 mice alone, and approached the wild-type level (Fig. 2, a-d). Furthermore, the large areas of unmineralized bone in the cortices of long bones of D4 mice were absent from the bones of D4/E1 mice (Fig. 2, e and f), and cortices of D4/E1 long bones were macroscopically indistinguishable from wild-type. By X-ray analysis, however, coexpression of the truncated receptor did not inhibit the overall loss of cancellous bone mass in the metaphyses of long bones caused by TGF-β2 overexpression, although we cannot rule out quantitative changes (data not shown). Since expression of the truncated receptor alone in E1 mice causes an increase in cancellous bone mass (Filvaroff et al., in preparation), its inability to rescue the overexpression phenotype in the metaphysis presumably only reflects the high sensitivity of cancellous bone to even moderate increases in resorption. Significantly, expression of the truncated receptor in D4/E1 mice also prevented the spontaneous fractures seen in D4 mice.

These experiments showed that osteoblastic responsiveness to TGF-β was largely required for the skeletal pathologies and the increase in bone resorption caused by TGF-β2 overexpression. Since the increase in resorption was also osteoclast-dependent, we entertained three, non-exclusive hypotheses: 1) that TGF-β signaling in osteoblasts leads to the release of a secondary signal that stimulates the resorptive capacity of osteoclasts; 2) that TGF-β-induced alterations in the cellularity, composition or structure of bone matrix somehow allowed it to be more efficiently resorbed by osteoclasts; and 3) that TGF-β stimulates osteoblasts themselves to resorb bone in a osteoclast-dependent fashion, or to prepare bone matrix for more efficient removal by

Figure 2. Effects of coexpression of a truncated (dominant-negative) type II TGF-β receptor in osteoblasts on the resorption phenotype caused by TGF-β2 overexpression.

D4 mice overexpressing TGF-β2 in osteoblasts were crossed to E1 mice expressing a truncated receptor type II TGF-β receptor in osteoblasts to generate D4/E1 mice.

(a-d) Whole-mount TRAP-stained calvariae of wild-type (a), D4 (b), E1 (c), and D4/E1 (d) mice at day 35. The dramatic increase in osteoclast number in D4 calvariae is largely inhibited by osteoblast-specific coexpression of the dominant-negative TGF-β receptor.

(e and f) Cross-sections of the femoral diaphysis of D4 (e) and D4/E1 (f) 35 day-old mice at the level of the third trochanter (the structure towards the top of both bones). Bones had been prestained in the Villanueva bone stain which stains osteoid red. In the D4 sample, arrows indicate the large resorption lacunae and arrowheads indicate the large areas of unmineralized osteoid that result when these lacunae are refilled. Both defects are absent from sections of D4/E1 mice. The asterisk indicates a fracture of the D4 bone that was an artifact of the embedding process. Scale bar shows 250 μm.

A
B
C
D
E
F

osteoclasts.

While difficult to study directly, the composition of D4 bone is clearly quite different from wild-type. First, D4 bone shows an increase in the density of osteocytes that is largely prevented by coexpression of the truncated TGF-β receptor (Erlebacher et al., submitted). Osteocytes have been implicated in the remodeling responses of bone to mechanical loading (Aarden et al., 1994), and there is a correlation between osteocyte density and the local rate of remodeling (Cané et al., 1982). Increased osteocyte density has also been associated with human osteoporosis (Mullender et al., 1996). Second, independent of the increase in resorption itself, bone formed under the influence of TGF-β2 is mechanically defective, as shown by the high fracture incidence in mice carrying the D4 transgene on a *c-fos* $^{-/-}$ background, which prevents osteoclastic differentiation (Grigoriadis et al., 1994; Erlebacher et al., submitted). We have also found that D4 calvariae are very resistant to limited pepsin digestion, used as a means release collagen from its insoluble matrix, even though the hydroxyproline content of D4 bone is normal (data not shown). The mechanism for pepsin resistance might be increased levels of collagen cross-linking, and indeed TGF-β has been shown to induced the expression of the collagen cross-linking enzyme lysyl oxidase in a number of cell types including osteoblasts (Boak et al., 1994; Feres-Filho et al., 1995; Gacheru et al., 1997). Lastly, while the mineral content of D4 bone is normal aside from the large intracortical areas of unmineralized osteoid (data not shown), mineralization fronts in D4 bone are irregular, revealing a defect in the underlying organic scaffold (data not shown). This irregularity is prevented by coexpression of the truncated TGF-β receptor (data not shown).

In order to assess the resorptive capacity of osteoclasts and osteoblasts, we analyzed the expression of several enzymes thought to be involved in the process of bone resorption. On the osteoclast side, we looked at the expression of cathepsin K, the major cysteine proteinase responsible for bone resorption by osteoclasts (Gelb et al., 1996; Tezuka et al., 1994), tartrate resistant acid phosphatase (TRAP), an osteoclast-specific enzyme also required for bone resorption in vivo (Hayman et al., 1996), and gelatinase B (MMP-9), the major matrix metalloproteinase made by osteoclasts (Reponen et al., 1994). On the osteoblast side, we looked at collagenase-3 (MMP-13), and gelatinase A (MMP-2).

As shown in Figure 3a, there was no reproducible difference in the expression of either procathepsin K or mature cathepsin K by western blot analysis of bone extracts from wild-type, D4, E1, or D4/E1 mice. To determine the expression of TRAP, collagenase-3 and the two gelatinases, we analyzed the conditioned media of explants of metaphyseal bone, where osteoclast density was unchanged in D4 mice. We normalized protein loading of gels to secreted TRAP activity measured enzymatically. Equal TRAP activity led to equal total secreted protein loading (Fig. 3d), showing that the expression of TRAP was not different between the four groups of mice. By western blot analysis, there was also no difference in the expression of collagenase-3 between wild-type and D4 mice (Fig. 3b). While the apparent downregulation of collagenase-3 in E1 and especially D4/E1 mice was consistent in these bone explant experiments, both western and northern blot analysis of direct bone extracts showed no differences in expression between the four groups of mice (data not shown). Lastly, gelatinase B expression, as determined by gelatin zymography, was also unchanged (Fig. 3c).

Figure 3. Expression of bone-resorbing enzymes in the distal femoral metaphysis of wild-type, D4, E1, and D4/E1 mice at 35 days of age. D4 mice overexpressing TGF-β2 in osteoblasts were crossed to E1 mice expressing a truncated receptor type II TGF-β receptor in osteoblasts to generate D4/E1 mice. Two independent sets of mice are shown. The same samples were used in panels b, c, and d.

(a) Procathepsin K and cathepsin K expression as determined by western blot analysis of direct metaphyseal extracts. The band migrating a bit slower than procathepsin K is presumably preprocathepsin K.

(b) Procollagenase-3 and collagenase-3 expression as determined by western blot analysis of metaphyseal culture supernatants, loaded by equal TRAP activity.

(c) Gelatinase expression as determined by gelatin zymography of metaphyseal culture supernatants, loaded by equal TRAP activity.

(d) The profile of total secreted glycosylated proteins in the metaphyseal culture supernatants, loaded by equal TRAP activity.

(e-g) Densitometry of gelatinase band intensities. Progelatinase A (A), active gelatinase A (Aa), and active gelatinase B (Ba) optical densities for each lane were internally normalized one each other. Data show mean +/- s.d. for n=9 wild-type, n=12 D4, n=7 E1, and n=5 D4/E1 mice. (e) relative O.D. of (A+Aa)/Ba; * $P<0.0005$ compared to wild-type. (f) relative O.D. of Aa/Ba; * $P<0.00001$, ** $P<0.02$ compared to wild-type. (g) relative OD of Aa/A; * $P<0.02$ compared to wild-type.

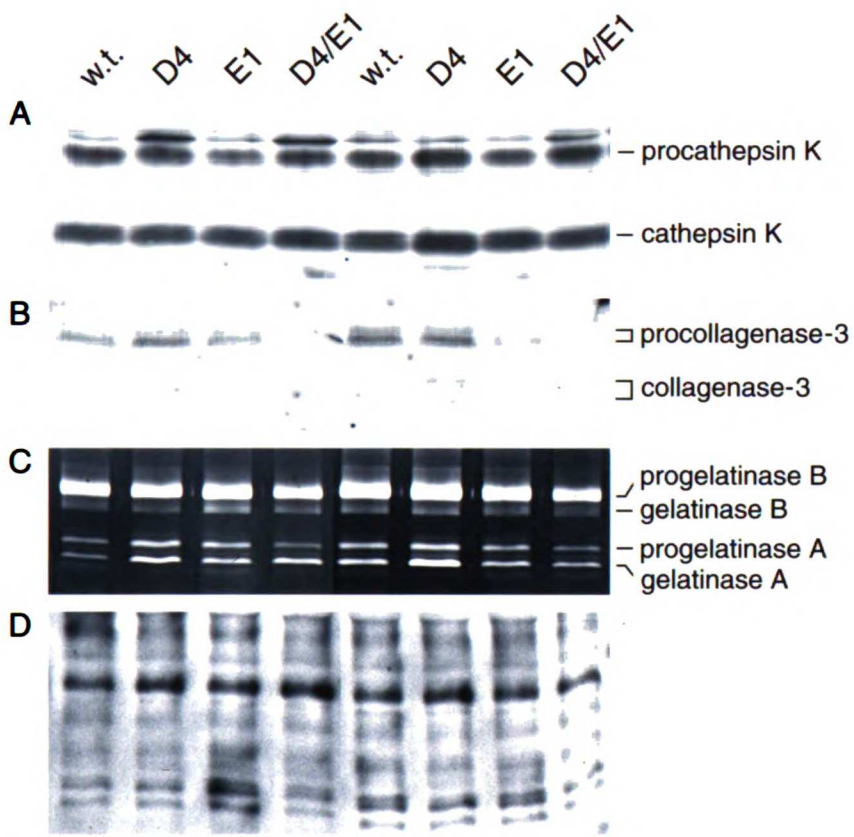
w.t.
D4
E1
D4/E1
w.t.
D4
E1
D4/E1
A
– procathepsin K
– cathepsin K
B
⊐ procollagenase-3
⊐ collagenase-3
C
progelatinase B
– gelatinase B
– progelatinase A
gelatinase A
D

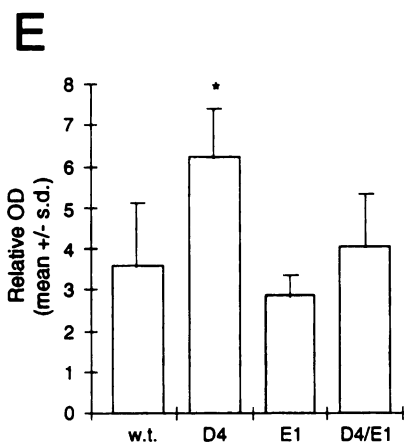
E
Relative OD
(mean +/- s.d.)
0
1
2
3
4
5
6
7
8
*
w.t.
D4
E1
D4/E1

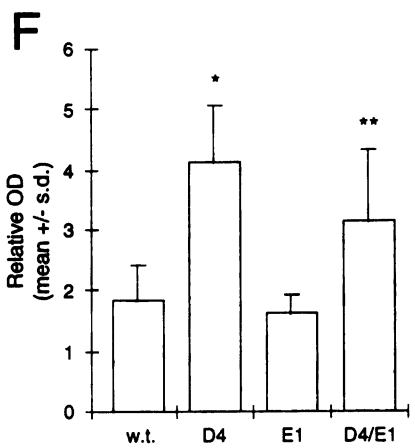
F
Relative OD
(mean +/- s.d.)
0
1
2
3
4
5
6
*
**
w.t.
D4
E1
D4/E1

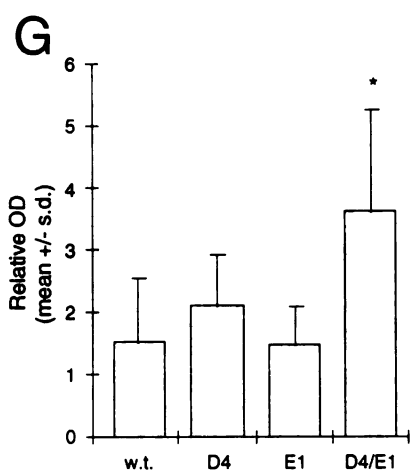
G
Relative OD
(mean +/- s.d.)
0
1
2
3
4
5
6
*
w.t.
D4
E1
D4/E1

Surprisingly, the amounts of both pro- and active gelatinase A was reproducibly increased in D4 mice compared to wild-type (Fig. 3c). This increase was largely prevented by coexpression of the truncated TGF-β receptor in D4/E1 mice, although there was a consistent preponderance of active gelatinase A. To quantitate these differences, we measured band intensities by gel densitometry and normalized internally to the level of active gelatinase B in each lane. As shown in Fig. 3e, the total amount of gelatinase A (pro- plus active) was 1.7-fold higher in D4 mice compared to wild-type, but there was no increase in total expression in D4/E1 mice. However, the amount of active gelatinase A was increased 2.2-fold in D4 mice and 1.7-fold in D4/E1 mice, with D4/E1 mice showing a reduction compared to D4 mice (Fig. 3f). The increase in active gelatinase A expression in D4/E1 mice was due to a 2.4-fold relative increase in amount of active gelatinase A to progelatinase A (Fig. 3g).

Thus, these expression studies showed that TGF-β2 overexpression had no effect on the expression on a number of bone resorbing enzymes, except for increasing the expression of gelatinase A. Significantly, this increase was inhibited by coexpression of the dominant-negative TGF-β receptor, correlating the amount of gelatinase A activity to the level of bone resorption. The observation that the stimulated production and activation of gelatinase A can be uncoupled suggests that TGF-β differentially regulates these two processes. Although threshold effects cannot be ruled out, our data suggest that direct osteoblastic responsiveness to TGF-β is required for progelatinase production, with its activation mediated by another cell type.

While the involvement of gelatinase A in bone resorption has not been directly demonstrated, this possibility is consistent with the observations that

gelatinase A has significant collagenolytic activity (Aimes and Quigley, 1995) and is produced in large quantities by osteoblasts (Kinoh et al., 1996; Lorenzo et al., 1992; Meikle et al., 1992; Rifas et al., 1989), and that matrix-metalloproteinases, including gelatinases, are required for bone resorption in vitro (Hill et al., 1995). Since gelatinase B knockout mice have no apparent defect in bone resorption (Thiennu Vu and Zena Werb, personal communication), gelatinase A is by default implicated as the potentially relevant bone-resorbing gelatinase in vivo. Gelatinase A might be involved in the osteoblastic removal of unmineralized osteoid thought to be required to allow osteoclasts access to the mineralized bone surface (Chambers et al., 1984), or for the migration of preosteoclasts to the bone surface (Blavier and Delaisse, 1995). Interestingly, an upregulation of gelatinase A in bone has recently been observed in ovariectomized rats (Mansell et al., 1997).

In summary, TGF-β2 overexpression in osteoblasts causes a dramatic increase in bone resorption that does not correlate with the number or turnover of osteoclasts, or with their expression of bone resorbing enzymes, yet requires their presence and activity. Rather, the increase in resorption requires direct osteoblastic responsiveness to TGF-β and correlates with changes in the cellularity and composition of bone matrix, and with the production of gelatinase A, which is produced by osteoblasts. While we cannot presently judge the relative contributions of these changes to the resorption phenotype, our data show that osteoblastic processes may be of primary importance in regulating rates of resorption, with osteoclasts acting as essentially passive contributors. Since we have also shown that osteoclastic activity increases the local level of functional TGF-β activity at sites of bone resorption, possibly through the release and activation of bone matrix bound

TGF-β (Erlebacher et al., submitted), our data also suggest that TGF-β-mediated communication between osteoclasts and osteoblasts might serve to maintain and propel groups of resorbing osteoclasts.

Histomorphometric studies of postmenopausal women with established osteoporosis have revealed increased osteoclast numbers only inconsistently (Eriksen, et al., 1990; Meunier, et al., 1980; Parfitt, et al., 1980; Whyte, et al., 1982). Thus, the transient increase in osteoclast number in rodents soon after ovariectomy has implicated increased osteoclast numbers in the early stages of postmenopausal osteoporosis before bone loss becomes clinically manifest (Kalu, 1991). However, increases in osteoclast differentiation in rodent models might obscure other aspects of bone resorption that are clearly relevant to postmenopausal bone loss in humans, such as increased resorption per osteoclast (Eriksen, et al., 1990). The high-turnover bone loss phenotype with no increase osteoclast number caused by TGF-β2 overexpression in transgenic mice isolates and highlights this aspect of pathological bone resorption, and implicates TGF-β in the pathogenesis of at least this component of human osteoporosis. It must be emphasized that the bone loss seen in our D4 line is not merely a consequence of its very high level of expression, although the severity of the defects in this line have allowed a more convenient analysis. Rather, we note that even low levels of TGF-β2 overexpression lead to bone loss with otherwise no detectable histological alterations, and expression of a dominant-negative TGF-β receptor in osteoblasts leads to an actual increase in cancellous bone mass (Filvaroff et al, in preparation). Furthermore, mice heterozygous for a targeted TGF-β1 allele have half the skeletal content of TGF-β1, yet also have increased cancellous bone mass (Erlebacher et al., in preparation). Thus, our

data taken together provides a rational basis for anti-TGF-β osteoporosis therapies. The possibility that altered bone matrix cellularity or composition might inherently allow for more efficient resorption also has clinical implications towards therapeutic strategies that intend to increase bone mass by stimulating new formation.

METHODS

Mice. D4 mice that overexpress TGF-β2 from the osteocalcin promoter have been described previously (Erlebacher and Derynck, 1996), and E1 mice that express a cytoplasmically-truncated type II TGF-β receptor from the osteocalcin promoter will be described (Filvaroff et al., in preparation). Both lines were established and maintained on a (DBA/2 X C57BL/6J) F1 background.

Histological analysis and TRAP histochemistry. Measurements of the osteoclast number per mm^2 bone area, percentage of apoptotic osteoclasts, and percentage of osteoclasts with ruffled borders were from histological sections of the distal femoral metaphyses of 35 day-old mice as previously described (Boyce et al., 1995; Hughes et al., 1996). Whole-mount TRAP-stained calvariae were prepared using a leukocyte acid phosphatase kit (Sigma Chemical Co., St. Louis, MO) with the coupling dye replaced by fast red violet LB (Sigma). Calvariae had been fixed in 2% paraformaldehyde, post-fixed in methanol for 1 h, then washed in water during removal of the dura mater. The methanol post-fixation completely removed non-cell associated TRAP staining. For the analysis of resorption and mineralization in cortical bone, undecalcified 4.5 μm diaphyseal cross-sections of femurs from 35-day-old mice were prepared as described from bones stained en bloc with the Villanueva bone stain (osteochrome stain, Polysciences Inc., Niles, IL) (Erlebacher et al., submitted). We estimated the volume of completely unmineralized osteoid in D4 bone from these sections by stereological methods (Weibel, 1969).

Bone explants and assays. The release of ^{45}Ca from prelabeled mouse calvariae was performed as described previously (Lerner, 1987; Ljunggren et al., 1991). Two-day-old pups were injected with 1.5 μCi $^{45}CaCl_2$, and parietal bones were dissected on day 6 in Leibowitz L-15 media. All subsequent incubations were in CMRL 1066 medium containing 1 μm indomethacin and 0.1% BSA. The amount of ^{45}Ca released into the medium by cellular processes during a 48 h test incubation was expressed as a percentage of the total amount present in the explant, subtracting the percentage released due to passive diffusion. Passive release was determined from parallel explants of devitalized parietal bones, and was not different between wild-type and D4 mice. 10 ng/ml salmon calcitonin (Sandoz Pharmaceuticals Corporation, East Hanover, NJ), was added to treated bones in throughout all incubations. Statistical analysis was performed using Student's t-test.

Metaphyses of long bones were prepared from the combined femurs and tibia from 35-day-old mice. Bones were dissected free of soft tissues in Leibowitz L-15 media, and epiphyses and growth plates of the distal femur and proximal tibia were flicked off using a scalpel blade. About 1 mm of the underlying primary spongiosa/metaphysis was then shaved off and crudely dissagregated, and these samples were washed 3X in Leibowitz L-15 media, using gentle trituration to dissagregate and remove bone marrow clumps. Samples were then cultured in 300 μl F-12 Ham's media containing 0.1% BSA for 24 h at 37° in a humidified 15% CO_2 incubator so as to maintain a pH less than 7.0 (Arnett et al., 1994). TRAP activity in the explant supernatant was measured immediately after the culture period using a series of dilutions in the linear range (0.1-2 μl) as previously described (Ek-Rylander et al., 1997). Profiles of the glycosylated proteins secreted by these explants, as an estimate

of total secreted protein, was determined by western blot analysis of explant supernatants equally loaded for TRAP activity, using concanavalin-A-biotin (Pierce, Rockford, IL) as a primary probe. For western blot analysis of collagenase-3 expression and gelatin zymography, 10% polyacrylamide gels were also equally loaded for supernatant TRAP activity. To detect collagenase-3 expression, we used goat-anti-mouse collagenase-3 antibodies generously provided by Dr. Chantal Peeters-Jooris (Université Catholique de Louvain, Belgium). For western blot analysis of cathepsin K expression, bone samples were prepared as above and immediately extracted in RIPA buffer containing 1 mM PMSF and 5 µg/ml aprotinin, leupeptin, benzamidine and pepstatin, with 20 mM EDTA added after removal of the bone particles. Western blot analysis was performed on these extracts normalizing the loading of 10% polyacrylamide gels to the total amount of extracted protein (determined by the D_C method, Biorad, Hercules, CA). Rabbit-anti-mouse cathepsin K antibodies were generously provided by Dr. Dieter Brömme (Mount Sinai School of Medicine, New York). Gelatin zymography was performed as described (Tournier et al., 1994), and quantitated by densitometry of scanned gels using NIH Image (Wayne Rasband, U.S. National Institutes of Health). Statistical significance was determined by ANOVA and the Bonferroni t-test for multiple comparisons.

Analysis of type I collagen and mineralization. Femurs and tibia from 35 day-old-mice were dissected free of soft tissues and flushed of bone marrow. Samples were crushed in liquid nitrogen, and weighed before and after decalcification in 10% EDTA, 0.1 M Tris pH 7.4. Determination of bone mineral content per wet weight in this fashion allowed the same bones to be

then analyzed for hydroxyproline content as previously described (Woessner, 1961). Prior to comparison with controls, the mineral content in D4 bone was corrected for the amount of completely unmineralized osteoid (see above). Calvariae from 35-day-old mice, similarly decalcified, were subjected to limited pepsin digestion as previously described (Rhodes and Miller, 1978). As determined from Coomasie blue-stained polyacrylamide gels, the total amount of type I collagen released from D4 bones was much less than that from wild-type bones. However, normalizing loading to equivalent amounts of released hydroxyproline gave identical type I collagen band intensities, showing that the collagen released from D4 bones was not degraded and contained a normal hydroxyproline content (data not shown).

Chapter 6:

Mice heterozygous for an inactivated allele of TGF-β1 have a 50% decrease in the skeletal content of TGF-β1 yet increased cancellous bone mass

ABSTRACT

Reductions in the skeletal content of TGF-β have been associated with pathological bone loss, although a causal relationship has not been established. To test whether a decreased content of TGF-β in bone matrix leads to bone loss, we have analyzed mice heterozygous for an inactivated allele of TGF-β1, the major TGF-β isoform in bone. Heterozygous mice all had a 50% reduction in the content of skeletal TGF-β1, and no compensatory upregulation of TGF-β2. Surprisingly, these mice showed an incompletely penetrant phenotype of dramatically increased cancellous bone mass in the distal femoral metaphysis, and no evidence of osteopenia. Histomorphometric analysis suggested that bone resorption was decreased in TGF-$\beta 1^{+/-}$ mice, while bone formation was unchanged. These results show that skeletal TGF-β1 deficiency does not inherently lead to bone loss; rather TGF-β1 deficiency increases cancellous bone mass contingent upon interactions with other modifying genetic loci.

INTRODUCTION

Transforming growth factor-β (TGF-β) has potent effects on the differentiation and activity of both osteoblasts and osteoclasts, the principle cell types in bone (for reviews see Bonewald and Dallas, 1994; Centrella et al., 1994). Bone matrix contains abundant latent quantities of all three TGF-β isoforms (TGF-β1, -β2, and -β3), and this reservoir may give rise to the majority of the TGF-β activity ultimately exposed to bone cells in vivo (Bonewald and Dallas, 1994). During bone remodeling, osteoclasts are thought to release and activate bone matrix-bound TGF-β, thus creating a local source of TGF-β activity at sites of bone resorption (Oreffo et al., 1989; Oursler, 1994; Pfeilschifter and Mundy, 1987).

Several results have suggested that TGF-β may have an overall anabolic effect on bone metabolism. In vitro, anabolic agents induce the osteoblastic production and activation of TGF-β (Oursler et al., 1991), and TGF-β has been shown to mediate the estrogen-induced apoptosis of osteoclasts (Hughes et al., 1996). Furthermore, subperiosteal injections of TGF-β induce robust bone formation in vivo (Joyce et al., 1990; Noda and Camilliere, 1989), consistent with its ability to stimulate the osteoblastic production of collagen and other bone matrix proteins in vitro (Centrella, et al., 1994). Lastly, skeletal TGF-β content, as measured by the amount of TGF-β extractable from bone matrix normalized to total extracted protein, positively correlates with the amount of cancellous bone in vivo. Thus, ovariectomized rats, which are used as a model for estrogen deficiency-induced osteopenia, show a 40% specific reduction in skeletal TGF-β1 content (Finkelman et al., 1992), and aging humans show a progressive skeletal loss of TGF-β (Nicolas et al., 1994).

Reciprocally, intermittent treatment of rats with parathyroid hormone causes a 2.5-fold increase in skeletal TGF-β1 content over a 12-week period, in parallel with a strong anabolic effect (Pfeilschifter et al., 1995). Lastly, the bone matrix of vitamin D-deficient rats, which has impaired osteoinductive and mitogenic activity, is 60% deficient in TGF-β (Finkelman et al., 1991).

These results, while suggestive, do not establish a firm causal link between skeletal TGF-β content and the amount of cancellous bone. It has also been difficult to show that TGF-β acts as an anabolic agent during bone remodeling in vivo, since the effects of TGF-β on bone cells in vitro are very variable, and the TGF-β-stimulated production of extracellular matrix components by osteoblasts in vivo and in vitro may reflect more an aspect of the exaggerated tissue repair processes commonly evoked by TGF-β (Border and Noble, 1994), rather than a true physiological response. We have also shown that the osteoblast-specific TGF-β2 overexpression in transgenic mice actually leads to an overall loss of cancellous bone mass associated with a high rate of bone turnover (Erlebacher and Derynck, 1996). High overexpression of TGF-β2 in one transgenic line led to a 40% decrease in skeletal TGF-β1 content, raising the possibility that such decreases might reflect homeostatic responses rather than primary events.

To test directly whether a specific deficiency in skeletal TGF-β1 leads to bone loss, we have analyzed the bones of mice carrying an inactivated allele of TGF-β1 (Shull et al., 1992). TGF-β1 is by far the primary TGF-β isoform in bone matrix, being at least 10-fold more abundant in rodent bone than TGF-β2 (Erlebacher and Derynck, 1996; Pfeilschifter, et al., 1995), so control of its production will largely determine the overall amount of skeletal TGF-β. Since TGF-β1-null mice die at an early age unless immunosuppressed

(Diebold et al., 1995; Kulkarni et al., 1993; Shull, et al., 1992), we chose to study mice heterozygous for the inactivated allele. We show that TGF-$\beta 1^{+/-}$ mice have a 50% reduction in their TGF-β1 skeletal content, consistent with the 50% reduction in TGF-β1 gene dosage. Surprisingly, these mice show no osteopenia but rather a incompletely-penetrant increase in cancellous bone mass.

MATERIALS AND METHODS

Mice and measurements of skeletal TGF-β content. A single male TGF-$\beta1^{+/-}$ founder mouse on a mixed 129/SvJ X CF1 background (Shull, et al., 1992) was purchased from Jackson Laboratories (Bar Harbor, MA) and mated to (129/SvJ X C57BL/6J) F1 females (Jackson Laboratories). Offspring were housed until 6 months of age without mating and identified by PCR of tail DNA as using primers as previously described (Diebold, et al., 1995). Mice were given intraperitoneal injections of 10 mg/kg calcein (Sigma, St. Louis MO) eleven days and then again one day before sacrifice. Sacrificed mice were weighed, and humeri were completely dissected of soft tissues. Bone powder extracts from these bones were prepared for the determination of skeletal TGF-β contents by TGF-β1 and TGF-β2 specific ELISAs (R&D Systems, Minneapolis, MN) as previously described (Erlebacher and Derynck, 1996). Hind limbs were trimmed of muscle and fixed and stored in 70% ethanol at 4° C. Skeletal TGF-β content measurements and X-ray analysis were performed on a total of n=20 TGF-$\beta1^{+/-}$ mice and n=26 TGF-$\beta1^{+/+}$ male and female littermates. CF1 (Charles Rivers Laboratories, Wilmington, MA) and 129/SvJ and C57BL/6J (Jackson Laboratories) inbred males were purchased at two months of age, and housed until sacrifice at 6 months of age.

X-ray analysis and bone densitometry. Hind limbs were radiographed as previously described (Erlebacher and Derynck, 1996). For each bone, densitometry was performed by scanning the radiograph into a computer using Adobe Photoshop (Mountain View, CA), and then generating a histogram of optical density values over the bone marrow area 2.4-6.0 mm

from the growth plate using NIH Image (Wayne Rasband, U.S. National Institutes of Health). In order to conservatively normalize for differences in cortical bone thickness and background intensity, we subtracted the minimum value of each histogram from its mean value to generate a final calculated relative optical density. The validity of this approach was confirmed by its comparison to corresponding stereological measurements of cancellous bone volumes from histological sections (see below). The volume of cancellous bone in the same 2.4-6.0 mm area from the growth plate measured histologically showed a good correlation with the bone density measured radiographically (r^2=0.71; P<0.005 [n=9]).

Histology and histomorphometry. Longitudinal 4.5 μm undecalcified sections were prepared from femurs fixed in 70% ethanol, stained en bloc in the Villanueva bone stain (osteochrome stain, Polysciences Inc., Niles, IL), and embedded in methymethacrylate. Some sections were stained for mineralized bone by the Von Kossa method and counterstained with nuclear fast red (Sheehan and Hrapchak, 1980). Histomorphometric analyses were performed on unstained sections viewed under UV light at a magnification of 200X. We measured the cancellous bone volume/total marrow space volume, mineralizing surface/total cancellous bone surface (MS/BS), and eroded surface/total cancellous bone surface (ES/BS) as described previously (Parfitt et al., 1987; Weibel, 1969), using a 200x200 μm grid reticule with 20 μm subdivisions to systematically scan over the entire bone marrow cavity. Thus, about 10 mm^2 total area was scanned per section covering the distal 7 mm of the femoral metaphysis. Average cancellous bone density values were calculated for each consecutive 200 μm-thick cross-sectional slice of the

femur. In order to compare cancellous bone volumes between different mice, these consecutive densities were summed over different distances from the growth plate. These values therefore represent the volume of cancellous bone in imaginary longitudinal core samples of the bone marrow cavity with unit cross-sectional area, and so will reflect differences both in absolute bone density as well as in how far the cancellous bone extends down the diaphysis. Final mineralizing surface and erosion surface measurements were calculated as individually measured values per reticular area summed over the entire relevant area of the bone marrow cavity. The mineral apposition rate was measured from photomicrographs of all visible double-labeled surfaces as described previously (Erlebacher and Derynck, 1996).

RESULTS

Skeletal content of TGF-β in TGF-β1$^{+/-}$ mice.

To generate TGF-β1$^{+/-}$ mice, a single male founder mouse, which was on a mixed 129/SvJ X CF1 background, was mated to (129/SvJ X C57BL/6) F1 females. At six months of age, offspring were sacrificed and the skeletal contents of TGF-β1 and TGF-β2 were determined from protein extracts of both humeri. As shown in Figure 1a, TGF-β$^{+/-}$ mice had almost a 50% reduction in the amount of extractable TGF-β1 compared to TGF-β$^{+/+}$ littermates, with very little variablity between independent mice. No differences in the skeletal content of TGF-β1 was noted between the males and females of each group. Furthermore, there was no compensatory upregulation in the skeletal content of TGF-β2 (Fig. 1b), which was ten-fold less abundant that TGF-β1. These results show that the TGF-β1 gene is haplo-insufficient with respect to its expression in osteoblasts, with 50% of the gene dose giving 50% production of protein.

X-ray analysis of TGF-β1$^{+/-}$ mice.

When the hind limbs of the same mice were analyzed radiographically, a surprising degree of variability was evident in the apparent amount of cancellous bone in the distal femoral metaphysis, our site of analysis. While most mice were very similar to one another, several TGF-β1$^{+/-}$ mice showed a dramatic increase in the amount of cancellous bone. We quantitated these differences as described below, but to first give a visual impression of the phenotype and the degree of variability, we show the extreme cases of high and low bone density for both TGF-β1$^{+/-}$ and TGF-β1$^{+/+}$ male mice in

Figure 1. Skeletal contents of TGF-β1 and TGF-β2 in 6 month-old TGF-$\beta1^{+/-}$ and TGF-$\beta1^{+/+}$ mice.

Graphed values show means +/- s.d. for n=20 TGF-$\beta1^{+/-}$ mice and n=26 TGF-$\beta1^{+/+}$ littermates.

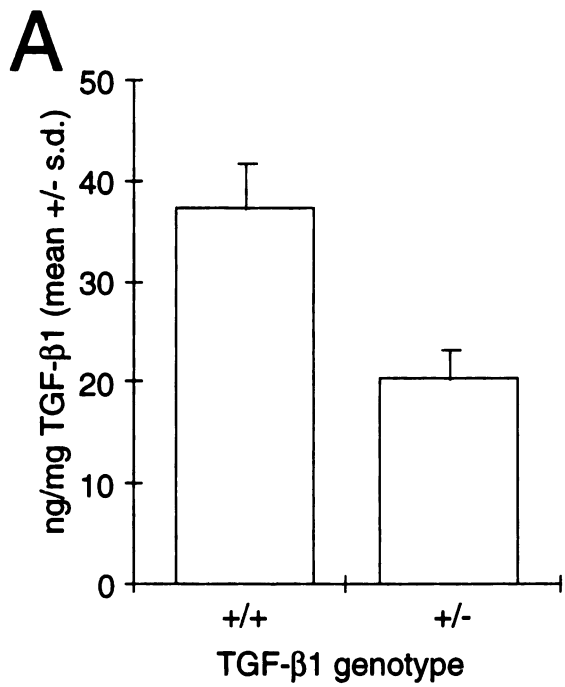
A
50
40
30
20
10
0
ng/mg TGF-β1 (mean +/- s.d.)
+/+
+/-
TGF-β1 genotype

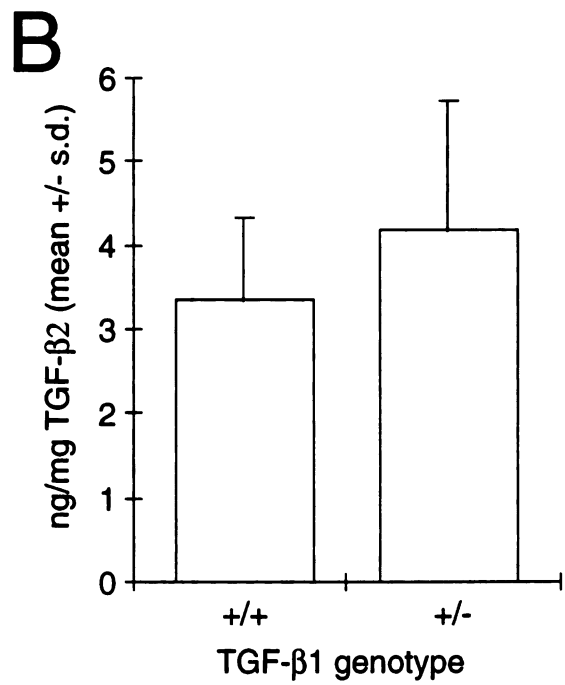
B
6
5
4
3
2
1
0
ng/mg TGF-β2 (mean +/- s.d.)
+/+
+/-
TGF-β1 genotype

Figure 2. Compared to all other groups of mice, phenotypic (i.e. high-density) TGF-β1 $^{+/-}$ mice (Fig. 2d-f) showed a dramatic extension of cancellous bone from the distal metaphysis towards mid-diaphysis (arrow in Fig. 2d), an apparent increase in the density of that cancellous bone, and a mild clubbing of the distal metaphysis. This phenotype was seen in both male and female mice. In contrast, non-phenotypic (i.e. low density) TGF-β1 $^{+/-}$ mice appeared very similar to their TGF-β1$^{+/+}$ littermates. Osteopenia was not observed in any of the TGF-β1$^{+/-}$ mice, and no other skeletal defects were noted.

We emphasize that the examples shown in Figure 2 are not statistically representative samplings of the TGF-β1$^{+/-}$ and TGF-β1$^{+/+}$ populations. Rather, the TGF-β1$^{+/+}$ mice with high density shown in Figure 2a-c were clear outliers of the total TGF-β1$^{+/+}$ population (n=26), whereas the TGF-β1$^{+/-}$ mice with high density (Fig. 2d-f) were representative of a larger distinct subgroup of mice (n= 8) within the total TGF-β1$^{+/-}$ population (n=20). Furthermore, the TGF-β1$^{+/+}$ mice with low density (Fig. 2g-i) were actually quite representative of almost all TGF-β1$^{+/+}$ mice. For further comparison, 6 month-old males representative of the three inbred lines that constitute the genetic makeup of the TGF-β1$^{+/-}$ mice and their TGF-β1$^{+/+}$ littermates are shown in Fig. 2m-o; these mice as well appeared very similar to the majority of the TGF-β1$^{+/+}$ offspring.

To quantitate these differences, densitometry was performed on radiographs of the metaphyseal marrow space in the area spanning 2.4 mm to 6.0 mm from the growth plate, which based upon our measurements of femoral growth rates reflects bone present since one month of age (data not shown). The results of these analyses are shown in Figure 3 and Table 1. As

Figure 2. X-ray analysis of TGF-$\beta 1^{+/-}$ and TGF-$\beta 1^{+/+}$ mice. Radiographs of distal femurs from 6 month-old males. 'Highest' and 'lowest' mice were chosen according to their cancellous bone densities as determined by densitometry, and do not intend to be a statistically representative sampling of the TGF-$\beta 1^{+/-}$ and TGF-$\beta 1^{+/+}$ populations. Six month-old inbred males (m-o) are shown for comparison.

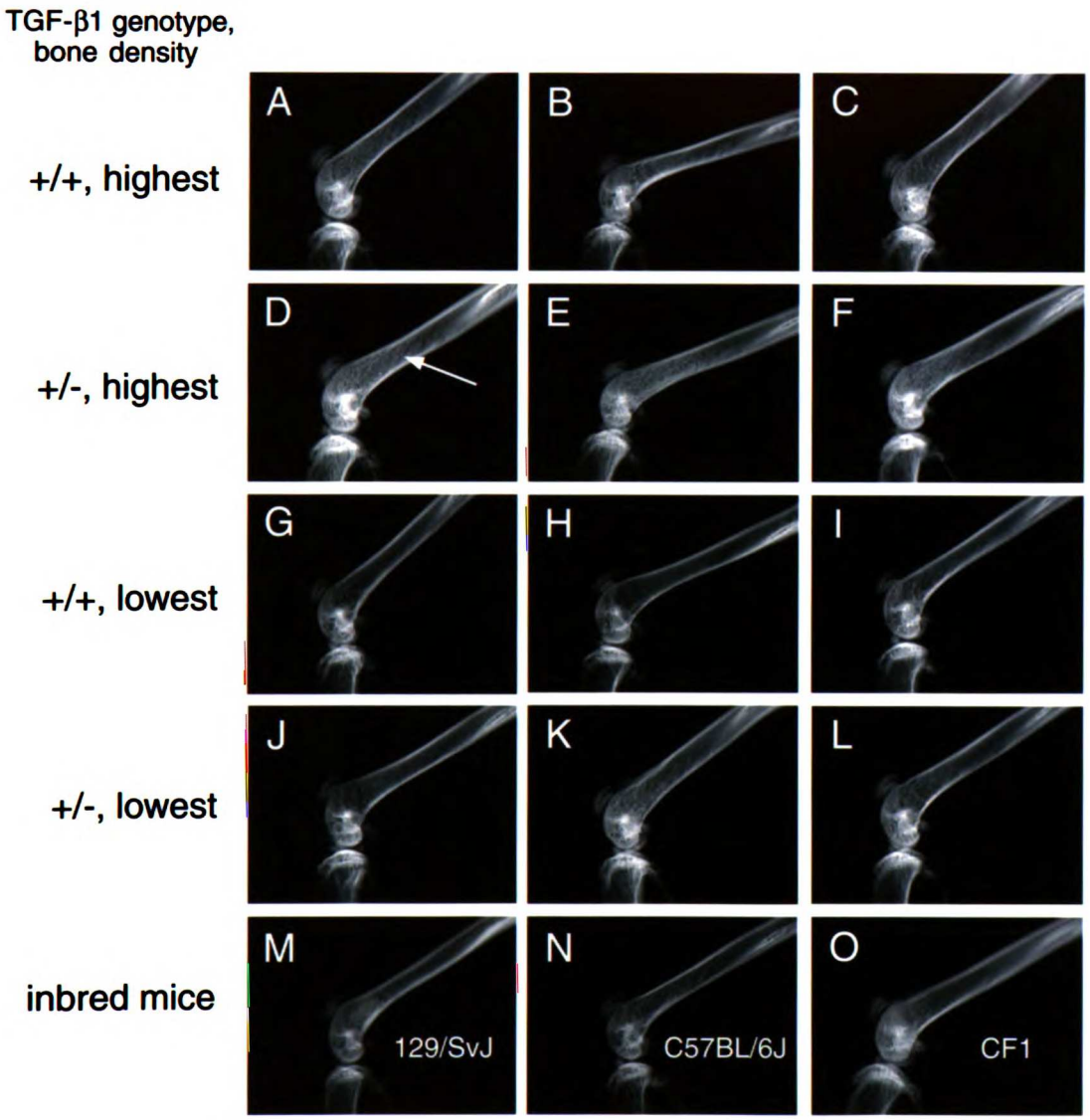
TGF-β1 genotype,
bone density
+/+, highest
+/-, highest
+/+, lowest
+/-, lowest
inbred mice
A
B
C
D
E
F
G
H
I
J
K
L
M
129/SvJ
N
C57BL/6J
O
CF1

Figure 3. Cancellous bone densities plotted versus individual TGF-β1 skeletal content.

Cancellous bone densities in the distal femoral metaphysis were determined as described in the Materials and Methods, and show individual values corresponding to the averages shown in Table 1. (a) 6 month-old males; (b) 6 month-old females; (c) combined plots for males and females normalized to body weight.

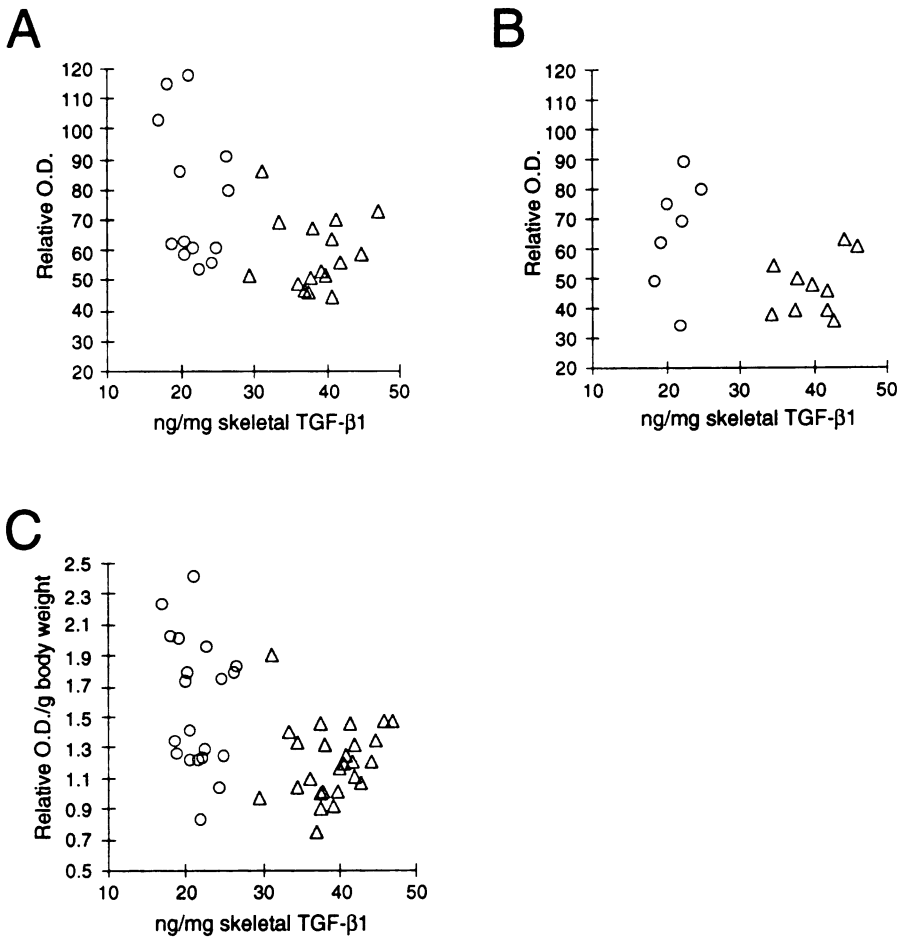
A
Relative O.D.
120
110
100
90
80
70
60
50
40
30
20
10
20
30
40
50
ng/mg skeletal TGF-β1
B
Relative O.D.
120
110
100
90
80
70
60
50
40
30
20
10
20
30
40
50
ng/mg skeletal TGF-β1
C
Relative O.D./g body weight
2.5
2.3
2.1
1.9
1.7
1.5
1.3
1.1
0.9
0.7
0.5
10
20
30
40
50
ng/mg skeletal TGF-β1

Table 1. Cancellous bone density in the distal femoral metaphysis.
Bone densities of 6 month-old TGF-$\beta 1^{+/-}$ and TGF-$\beta 1^{+/+}$ mice were determined as described in Materials and Methods. a, significantly different from sex-matched littermate controls; b, significantly different from combined male and female controls.

mouse	TGF-β1 genotype	sex	n	body weight (g)	relative bone density (O.D.)	*P* value	relative bone density/g body weight	*P* value
cross progeny	+/+	M	16	49.5+/-5.7	59+/-12		1.20+/-0.28	
	+/-	M	13	48.6+/-4.0	78+/-23	0.008[a]	1.60+/-0.44	0.007[a]
	+/+	F	10	38.9+/-5.6	47+/-10		1.22+/-0.17	
	+/-	F	7	42.4+/-7.9	65+/-19	0.02[a]	1.56+/-0.43	0.04[a]
cross progeny	+/+	M&F	26				1.21+/-0.24	
	+/-	M&F	20				1.58+/-0.43	0.0005[b]
129/SvJ	+/+	M	3	30.1+/-3.5	41+/-9		1.35+/-0.16	
C57BL/6J	+/+	M	3	42.2+/-2.3	47+/-6		1.10+/-0.09	
CF1	+/+	M	3	57.1+/-2.7	49+/-6		0.85+/-0.08	

plotted versus individual skeletal TGF-β1 content, about half of the TGF-$\beta1^{+/-}$ mice showed a dramatic increase in bone density (Figure 3a and b) well over the range of values seen in TGF-$\beta1^{+/+}$ mice, whereas the other half of TGF-$\beta1^{+/-}$ mice were similar to wild-type. The increase in density was apparent in both male and female TGF-$\beta1^{+/-}$ mice, and correlated well with visual appearance. On average, the bone density of TGF-$\beta1^{+/-}$ males and females was also significantly increased over same-sex control littermates (Table 1), but this analysis does not do justice to the bimodal appearance of the TGF-$\beta1^{+/-}$ distribution. Female mice of all groups on average showed lower bone densities than male mice, but normalizing the bone density to body weight eliminated this sex difference (Table 1). We therefore show a combined plot of all mice similarly normalized in Figure 3c. Importantly, this plot shows that the increase in bone density in TGF-$\beta1^{+/-}$ mice was in itself not correlated to body weight, which was on average unchanged compared to same-sex controls (Table 1).

Histological and histomorphometric analysis of TGF-$\beta1^{+/-}$ bone.

To assess the histological characteristics of TGF-$\beta1^{+/-}$ bone, we prepared longitudinal sections of the distal femur (Fig. 4.). The sections shown (panels a-h) correspond to the mice shown in Figure 2a, b, d, e, g, h, j and k, respectively. Again, as discussed above, we emphasize that these examples are not statistically representative samplings of the TGF-$\beta1^{+/-}$ and TGF-$\beta1^{+/+}$ populations, but were rather chosen to show the range of variability. However, the low density wild-type mice shown in panels e and f can be considered as fairly representative of the range of normal as discussed above.

Figure 4. Histology of TGF-$\beta 1^{+/-}$ and TGF-$\beta 1^{+/+}$ mice.
Longitudinal sections of the distal femur of 6 month-old males stained by the Von Kossa method. Sections are aligned according to the position of their growth plates. Sections (a-h) correspond to bones shown in panels a, b, d, e, g, h, j and k, respectively, of Figure 2. The lines demarcate the area of the diaphysis 2.4-3.4 mm from the growth plate from which the bone density was measured by radiographic densitometry. Based upon femoral length measurements, the growth plate was positioned at the 2.4 mm mark at one month of age.

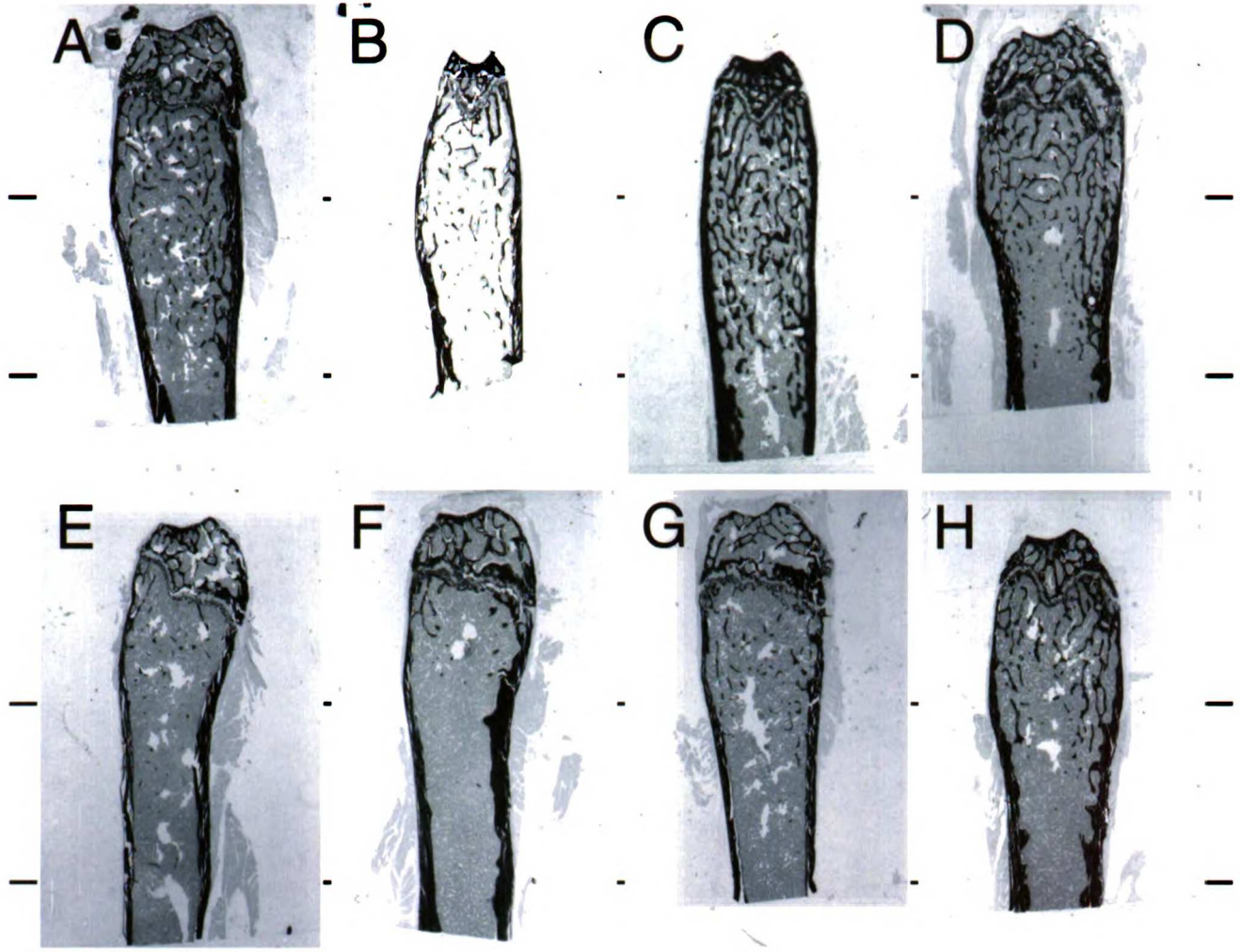
A
B
C
D
E
F
G
H

In accord with our X-ray analysis, phenotypic (high density) bones from TGF-$\beta 1^{+/-}$ mice (Fig. 4c and d) showed both a dramatic extension of cancellous bone down the length of the diaphysis and a dramatic increase in density of cancellous bone near the growth plate, as compared to both low density TGF-$\beta 1^{+/+}$ mice (Fig. 4e and f) and low density TGF-$\beta 1^{+/-}$ mice (Fig. 4g and i). This is shown quantitatively in Table 2, comparing the cancellous bone volume in an imaginary longitudinal core sample of the bone marrow cavity with 1 mm^2 cross-sectional area. Over the entire 7 mm closest to the growth plate, the two phenotypic high density TGF-$\beta 1^{+/-}$ mice showed a marked 5-fold increase in cancellous bone volume compared to the two wild-type low density mice.

In a rodent long bone, the density of cancellous bone in the metaphysis decreases as a function of distance from the growth plate, which reflects the continuous loss of bone after its initial formation at the growth plate, combined with the longitudinal growth of the bone. To estimate this rate of bone loss, we compared the volume of cancellous bone in the 1 mm of marrow space closest to the growth plate to the volume of bone at a 2.4-3.4 mm distance from the growth plate. This latter area of marrow space represents the last millimeter of longitudinal growth before one month of age, and so the bone it contains is at least five months old. As shown in Table 2, the percentage of bone lost over this five-month period, assuming that it was initially made respectively at the density currently closest to the growth plate, was much less in the two phenotypic TGF-$\beta 1^{+/-}$ than in two wild-type mice. Since bone remodeling is a surface phenomenon, changes in bone volume occur as fractions of the volume already present; thus, the percentage of bone lost is a more physiological index than the absolute volume of lost

Table 2. Cancellous bone volumes in the distal femoral metaphysis. Cancellous bone volumes (mm^3) were measured stereologically in the areas indicated as described in the Materials and Methods. Values shown are for the individual mice shown in panels e, f, c, and d of Figure 4 respectively. The percentage bone volume lost over a five month period was calculated from the 0.0-1.0 mm 2.4-3.4 mm areas.

TGF-β1 genotype	bone density	mm from growth plate 0-7	0.0-1.0	2.4-3.4	% lost
+/+	low	0.81	0.35	0.08	77.1
+/+	low	1.08	0.68	0.02	96.8
+/-	high	4.17	1.18	0.66	44.0
+/-	high	5.97	1.56	0.90	42.2

bone. If we assume that bone at the growth plate in all mice is initially made at the density seen in the phenotypic TGF-$\beta1^{+/-}$ mice, then the percentage of bone lost in the two wild-type mice is even more pronounced.

We also analyzed rates of bone formation and resorption by dynamic histomorphometry. As shown in Figure 5a, the percentage of eroded bone surface per total cancellous bone surface (ES/BS), which is a major histomorphometric index of bone resorption, was markedly decreased in the cancellous bone near the growth plate in all TGF-$\beta1^{+/-}$ mice regardless of phenotype (n=4), as compared to all TGF-$\beta1^{+/+}$ mice analyzed (n=5), again regardless of phenotype. Interestingly, wild-type mice showed a systematic decrease in eroded surface as a function of distance from the growth plate. In parallel, the mineralizing surface per total cancellous bone surface, which reflects the percentage of bone surface undergoing formation, also showed a similar trend, but there was no difference in this parameter in any the TGF-$\beta1^{+/-}$ mice analyzed compared to wild-type. Lastly, the mineral apposition rate, which reflects the rate of bone deposition on forming surfaces and thus the rate of bone production by individual osteoblasts, was also unchanged in TGF-$\beta1^{+/-}$ mice (1.12+/-0.11 μm/day [n=3]) compared to wild-type (1.06+/-0.08 μm/day [n=3]), and this parameter showed no spatial variations over the metaphysis. Since the percentage of mineralizing surface and the mineral apposition rate are both unchanged in TGF-$\beta1^{+/-}$ mice, multiplying these two parameters to give the final bone formation rate at the tissue level also reveals no difference between the mice. Therefore, our histomorphometric analysis only reveals changes in the rate of bone resorption as potentially underlying the TGF-$\beta1^{+/-}$ phenotype.

Figure 5. Histomorphometric analysis of TGF-$\beta 1^{+/-}$ and TGF-$\beta 1^{+/+}$ mice. Values are for bone marrow areas at different distances from the growth plate. The last two column are for all cancellous bone in the entire bone marrow cavity. (a) Percent eroded surface per total cancellous bone surface. * $P<0.002$; ** $P<0.005$ compared to wild-type. (b) Percent mineralizing surface per total bone surface.

A

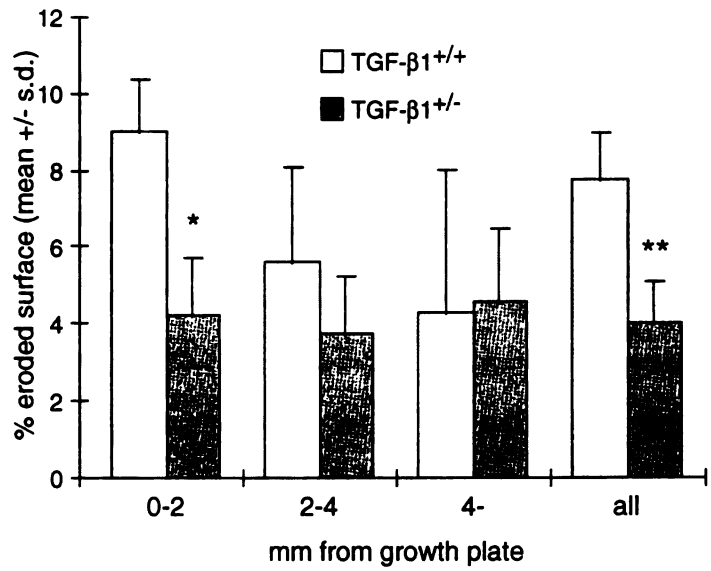
12
10
8
6
4
2
0
% eroded surface (mean +/- s.d.)
TGF-β1+/+
TGF-β1+/-
*
**
0-2
2-4
4-
all
mm from growth plate

B

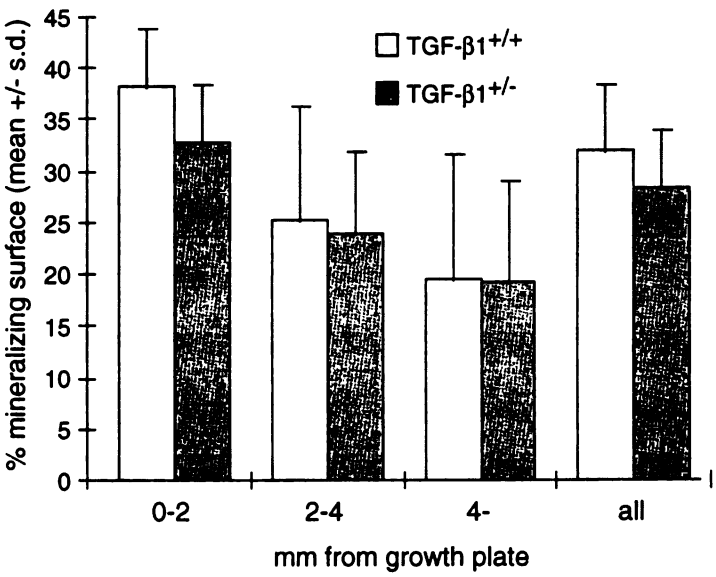
45
40
35
30
25
20
15
10
5
0
% mineralizing surface (mean +/- s.d.)
TGF-β1+/+
TGF-β1+/-
0-2
2-4
4-
all
mm from growth plate

DISCUSSION

In the present study, we have used mice heterozygous for an inactivated allele of TGF-β1 to study the skeletal consequences of TGF-β1 deficiency. All TGF-$\beta1^{+/-}$ mice analyzed had half the skeletal content of TGF-β1 and no upregulation of TGF-β2. These mice showed no evidence of osteopenia; rather, almost half the TGF-$\beta1^{+/-}$ mice showed a dramatic increase in cancellous bone mass. This is a surprising result given the prior positive association between skeletal TGF-β1 content and the amount of cancellous bone. However, the result is in accord with other transgenic experiments where we have perturbed TGF-β physiology specifically in bone. We have previously shown that the osteoblastic overexpression of TGF-β2 leads to severe osteopenia (Erlebacher and Derynck, 1996); reciprocally, dominant-negative interference with TGF-β signaling in osteoblasts leads to increased cancellous bone mass (Filvaroff et al., in preparation). The decrease in TGF-β1 expression in the skeletons of TGF-$\beta1^{+/-}$ mice and the consistency of the TGF-$\beta1^{+/-}$ phenotype with these other mouse models suggests that the TGF-β1 deficiency is locally affecting the behavior of bone cells, although we cannot rule out systemic effects.

The increase in cancellous bone volume in phenotypic TGF-$\beta1^{+/-}$ mice correlates with a decrease in bone resorption rather than an increase in bone formation, since we observe a decreased eroded surface in all TGF-$\beta1^{+/-}$ mice analyzed regardless of phenotype, yet no difference in bone formation compared to wild-type. Consistent with this finding, the rate of bone loss, as estimated by the percentage of cancellous bone lost over a five-month period, was much lower in phenotypic TGF-β1 mice than in wild-type mice. Thus,

the relative increase in bone volume appears to result from a relatively less negative overall bone balance during bone remodeling, especially near the growth plate where the relative difference in formation and resorption is greatest, rather than from an abnormally high volume of bone initially generated by the growth plate. A much more extensive histomorphometric analysis of TGF-β1$^{+/-}$ mice with predictable phenotypes at different ages will be required to confirm this point.

The phenotype of decreased bone resorption without changes in bone formation in TGF-β1$^{+/-}$ mice is also consistent with our other transgenic experiments. Thus, mice overexpressing TGF-β2 in osteoblasts show increased resorption as a primary defect, but increased formation only as a secondary compensatory response (Erlebacher and Derynck, 1996; Erlebacher *et al.*, submitted). Reciprocally, dominant-negative interference with TGF-β signaling causes increased cancellous bone mass, but no apparent increase in bone formation (Filvaroff et al., in preparation). It is interesting that TGF-β1 deficiency causes an decrease in the eroded surface, which closely reflects osteoclast density in rodents (see Beaudreuil et al., 1995 for example), but TGF-β2 overexpression does not cause a reciprocal increase in osteoclast density (Erlebacher and Derynck, 1996; Erlebacher et al., submitted). This suggests that TGF-β may control two distinct aspects of osteoclast physiology: it may first permissively regulate osteoclast differentiation, and then later instructively stimulate osteoclast activity. Alternatively, the apparent discrepancy may reflect differences in the respective biochemistries of TGF-β1 and TGF-β2. TGF-β2 has much less potent effects on hematopoetic cells than TGF-β1 (Ohta et al., 1987; Ottmann and Pelus, 1988) because these cells do not express betaglycan, the type III TGF-β receptor required for TGF-β2 binding

to the signaling type II and type I receptors (Derynck and Feng, 1997). Thus, TGF-β2 may not be able to regulate osteoclast differentiation as directly as TGF-β1. Indeed, we have recently shown that the effects of TGF-β2 on bone resorption are primarily mediated through effects on osteoblasts (Erlebacher et al., submitted).

It is very interesting that the increased bone phenotype in TGF-β1$^{+/-}$ mice was incompletely penetrant, especially since all TGF-β1$^{+/-}$ mice had half the skeletal content of TGF-β1. We could not correlate this variability with any environmental factor, suggesting the presence of specific genetic modifiers that modulate the effect of TGF-β on bone metabolism. Such modifiers have recently been shown to control the penetrance of the embryonic lethal phenotypes of TGF-β1-null mice (Bonyadi et al., 1997). Since all the mice analyzed here were the offspring of a single male TGF-β1$^{+/-}$ mouse on a mixed 129/SvJ X CF1 background mated to (129/SvJ X C57BL/6J) F1 females, the nearly 50% phenotypic penetrance raises the possibility that a single modifying locus may be responsible. Although extensive outcrossing of TGF-β1$^{+/-}$ mice will be required to isolate the modifier(s), we have preliminarily found that backcrossing phenotypic F1 TGF-β1$^{+/-}$ males, identified by radiography, with 129/SvJ females tends to give phenotypic TGF-β1$^{+/-}$ offspring (data not shown). Since all TGF-β1$^{+/-}$ mice not only had half the skeletal content of TGF-β1, but those analyzed also all had a reduction in erosion surface regardless of phenotype and no change in the rate of bone formation, we speculate that any modifying effects would act to increase the rate of bone resorption downstream from the regulation of osteoclast differentiation, so as to homeostatically achieve a wild-type level of cancellous bone density.

In conclusion, we find that inactivation of one TGF-β1 allele causes a 50% decrease in skeletal TGF-β1 content, but no evidence of osteopenia. Thus, skeletal TGF-β1 deficiency in itself does not lead to bone loss. These results suggest that the previously described association between TGF-β1 deficiency and ovariectomy-induced osteopenia (Finkelman, et al., 1992) is not a causal relationship, but rather reflects some other aspect of TGF-β physiology. One possibility is that the decrease in skeletal TGF-β1 content following ovariectomy results from a real decrease in TGF-β1 production by osteoblasts, but as part of a homeostatic mechanism to attenuate the bone loss caused by other local mechanisms induced by estrogen deficiency. This possibility is supported by our finding that skeletal TGF-β1 content is decreased in transgenic mice overexpressing TGF-β2 (Erlebacher and Derynck, 1996). Alternatively, decreased skeletal TGF-β may result from its sequestration in an extracellular compartment other than bone matrix, or its enhanced activation and cellular consumption. Since TGF-β2 overexpression in transgenic mice causes bone loss, this latter possibility is consistent with the idea that increased TGF-β activity may be directly involved in the pathogenesis of estrogen deficiency-induced osteopenia.

Chapter 7:
Conclusions

When I first started my thesis project, the role of TGF-β in bone development was something of a black box. Indeed, judging from the complex effects of TGF-β on bone cells in vitro, overexpression of TGF-β2 in vivo might have perturbed virtually any aspect of skeletal metabolism. Thus, as a starting point for discussion, it is worth emphasizing the many aspects of skeletal development and turnover that were not affected by the osteoblastic overexpression of TGF-β in transgenic mice. With the exception of the embryonic cleidocranial dysplasia phenotype (which could turn out to be the result of insertional mutagenesis), bone shape, size and growth were completely normal in D4 mice. Furthermore, as argued in Chapters 4 and 6, TGF-β does not directly control the rate of bone formation, contrary to the expectations of several in vitro and in vivo studies. Even the direct effects of TGF-β on osteoblastic differentiation are restricted to a kinetic control of differentiation rates, rather than to the steady-state modulation of relative differentiation stage-specific cell numbers within the osteoblastic lineage. Lastly, TGF-β does not directly affect osteoclast differentiation or activity, although differential effects of TGF-β1 versus TGF-β2 cannot be ruled out as argued in Chapter 6.

Thus, the role of TGF-β in the skeleton is surprisingly restricted to the regulation of bone remodeling, and this role is primarily, if not exclusively mediated through the actions of TGF-β on osteoblasts. A purely epistatic schematic representation of the effects of osteoblastic TGF-β2 overexpression on bone remodeling are shown in Figure 1. TGF-β directly controls the rate of osteoblastic differentiation, which leads to an increase in the density of terminally-differentiated osteocytes, and directly modulates some ill-defined aspects of bone matrix composition. Lastly, TGF-β stimulates the production

Figure 1. An overall epistatic representation of the skeletal effects of TGF-β2 overexpression in osteoblasts.

See text for discussion.

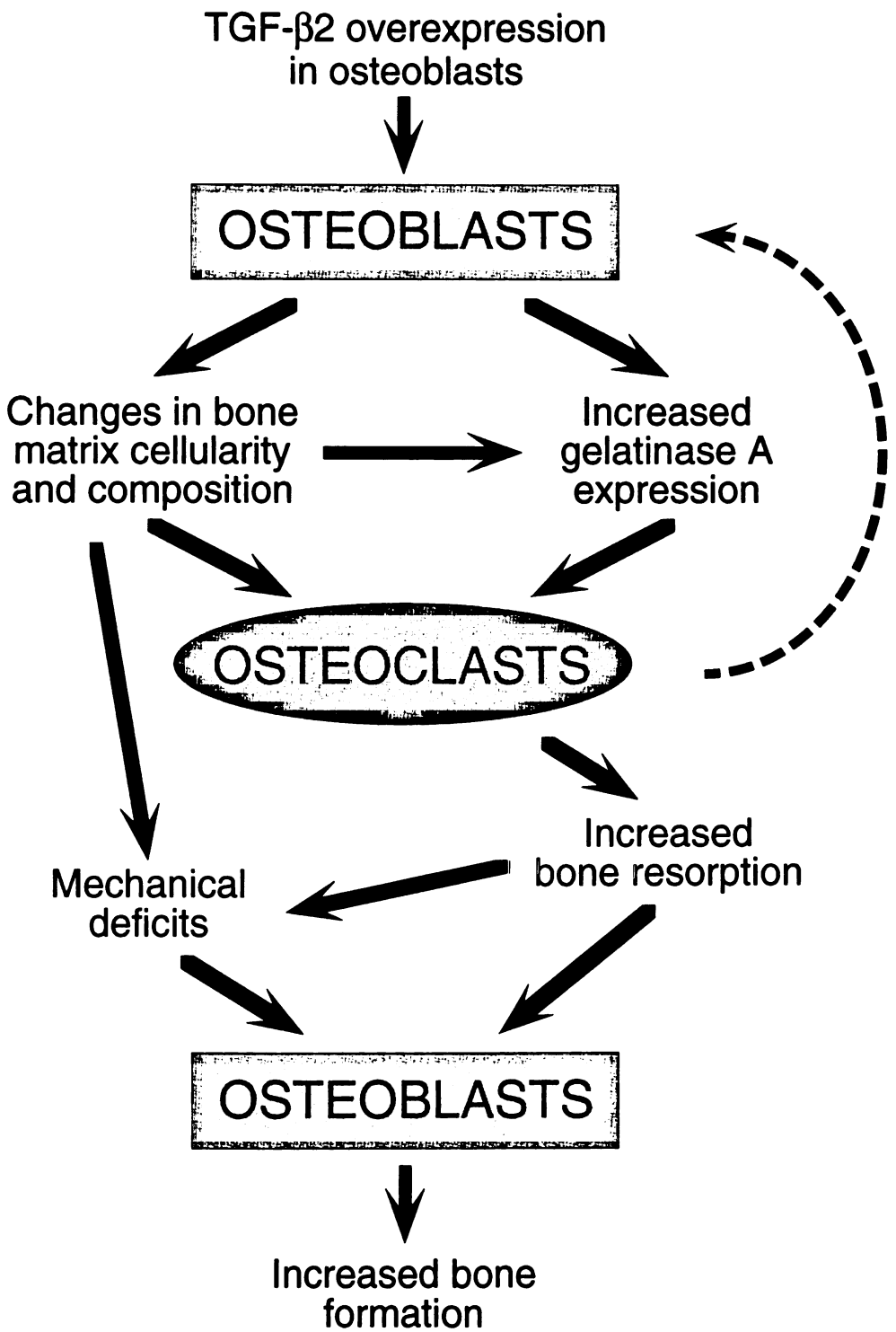
TGF-β2 overexpression
in osteoblasts
OSTEOBLASTS
Changes in bone
matrix cellularity
and composition
Increased
gelatinase A
expression
OSTEOCLASTS
Increased
bone resorption
Mechanical
deficits
OSTEOBLASTS
Increased bone
formation

of gelatinase A presumably by osteoblasts, although I cannot rule out the possibility that gelatinase A upregulation is a secondary consequence to the increase in bone resorption itself.

Through its direct effects on osteoblasts, TGF-β2 overexpression leads to increased bone resorption by osteoclasts, as argued in Chapter 5. This increase may be mediated through changes in bone matrix composition or cellularity, or through the upregulation of gelatinase A. The actual mechanism of increased bone resorption in D4 mice, however, remains unclear. Only secondary to its effects on bone resorption or bone matrix quality does TGF-β regulate the rate of bone formation. Lastly, osteoclasts increase the level that osteoblasts are stimulated by TGF-β, potentially creating a positive feedback loop.

A histological view of the skeletal physiology of TGF-β is shown in Figure 2. TGF-β produced by osteoblasts is mainly embedded in its latent form within bone matrix. I have shown in Chapter 4 that overexpressed TGF-β2 can be released from bone matrix during bone resorption, although the relevance of this process toward endogenous TGF-β physiology can only be inferred at this point. TGF-β2 overexpressed by osteoblasts can also bypass the latent bone matrix-embedded phase and have direct autocrine effects on osteoblasts, although again it is unclear whether such a direct autocrine loop applies to endogenous TGF-β. Certainly one or the other pathway occurs in vivo, since the increased cancellous bone mass in transgenic mice overexpressing a truncated TGF-β receptor clearly shows that osteoblastic exposure to TGF-β is relevant to skeletal physiology.

The effects of TGF-β during bone remodeling are mainly mediated through effects on osteoblasts, as described above. Thus, TGF-β directly

A model for TGF-β action in bone

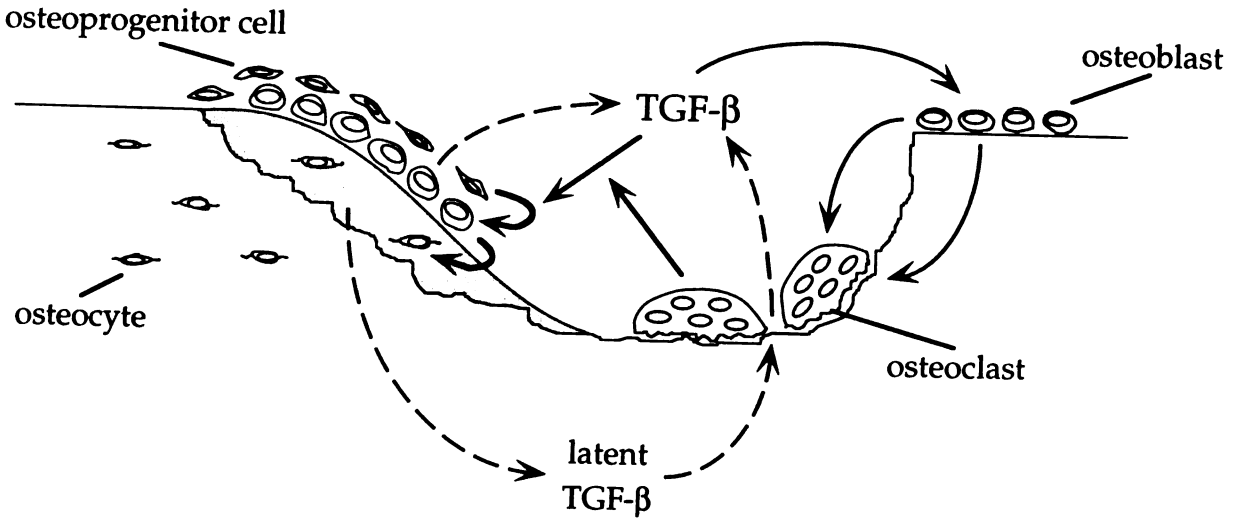

increases the rate of osteoblastic differentiation and causes an indirect stimulation of bone resorption. However, osteoclastic activity itself increases the level that osteoblasts are exposed to TGF-β. Thus, osteoblastic and osteoclastic function may be in part reciprocally coupled during bone remodeling through the single activity of TGF-β, which provides a simple mechanism to insure that osteoblastic differentiation proceeds spatially and temporally in sync with the continued stimulation of bone resorption by osteoclasts.

This last point, however exciting, rests on one unproven assumption: that the indirect stimulation of bone resorption is an immediate effect of TGF-β on osteoblasts. While the upregulation of gelatinase A may be consistent with this idea, an indirect effect mediated through changes in bone matrix composition or cellularity is certainly not. Given its potentially seminal importance to understanding the physiology of bone remodeling, I would suggest that this is the major question that follows from my thesis. One way to get at this question, of course, is to make osteoblast/bone matrix chimeras in vivo, but this is technically daunting. I tried to do the experiment by crossing the D4 mice with mice generated by David Corral in Gerard Karsenty's lab. These latter mice express the herpes virus thymidine kinase gene from the osteocalcin promoter, and so treatment with ganciclovir in vivo should kill all osteoblasts. Thus, in doubly transgenic mice, I intended to kill off osteoblasts while preserving their bone matrix for continued resorption by osteoclasts. Unfortunately, it didn't work. The problem was that I could not confirm that I was killing any osteoblasts, and even if I could it would be impossible to distinguish between permissive and instructive effects on bone resorption, given that osteoblasts are thought to be required for osteoclast

differentiation (although older osteocalcin-thymidine kinase mice treated for long periods with ganciclovir apparently still have normal levels of bone resorption in the absence of bone formation).

Another way to get at the question is if the upregulation of gelatinase A is fortuitously the actual means of communication between osteoblasts and osteoclasts. There is a lot of evidence that matrix metalloproteinases regulate the early stages of bone resorption, perhaps by allowing osteoclasts to have access to the mineralized bone surface. Since gelatinases have specifically been implicated in this process, and the gelatinase B knockout mice made by Thiennu Vu in Zena Werb's lab have no bone resorption defect, gelatinase A is implicated by default in this process. Thus, once gelatinase A knockout mice are made (and if they live), it will be very interesting if they have increased cancellous bone mass, and whether they can prevent the loss of bone caused by TGF-β2 overexpression.

My project of overexpressing TGF-β2 in osteoblasts has been one of the first specific investigations into the local regulation of bone remodeling using transgenic methodologies. As such, the mice I generated stand as somewhat isolated reagents in the bone field. More information can certainly be directly gleamed from these mice, especically in regard to the regulation of osteoblastic differentiation by TGF-β and the regulation of gelatinase A expression. However, I anticipate that their further usefulness will become much more apparent when other mice, disrupting other aspects of the remodeling process, are generated. Despite the difficulty of working on bone metabolism in vivo, the skeleton actually provides one of the few organ systems where tissue turnover can be observed directly. Thus, a systematic investigation into the regulation of bone remodeling using the kinds of

Bibliography

Aarden, E. M., Burger, E. H. and Nijweide, P. J. 1994. Function of osteocytes in bone. J Cell Biochem 55, 287-99.

Aimes, R. T. and Quigley, J. P. 1995. Matrix metalloproteinase-2 is an interstitial collagenase. Inhibitor- free enzyme catalyzes the cleavage of collagen fibrils and soluble native type I collagen generating the specific 3/4- and 1/4-length fragments. J Biol Chem 270, 5872-6.

Amizuka, N., Warshawsky, H., Henderson, J. E., Goltzman, D., and Karaplis, A. C. 1994. Parathyroid hormone-related peptide-depleted mice show abnormal epiphyseal cartilage development and altered endochondral bone formation. J. Cell. Biol. 126, 1611-1623.

Araki, N., Robinson, F. D., and Nishimoto, S. K. 1993. Rapid and sensitive method of quantitation of bone gla protein mRNA using competitive polymerase chain reaction. J. Bone Miner. Res. 8, 313-22.

Arnett, T. R., Boyde, A., Jones, S. J. and Taylor, M. L. 1994. Effects of medium acidification by alteration of carbon dioxide or bicarbonate concentrations on the resorptive activity of rat osteoclasts. J Bone Miner Res 9, 375-9.

Baker, A. R., Hollingshead, P. G., Pitts, M. S., Hansen, S., Taylor, R. and Stewart, T. A. 1992. Osteoblast-specific expression of growth hormone stimulates bone growth in transgenic mice. Mol. Cell. Biol. 12, 5541-7.

Baker, J., Liu, J. P., Robertson, E. J., and Efstratiadis, A. 1993. Role of insulin-like growth factors in embryonic and postnatal growth. Cell 75, 73-82.

Battegay, E. J., Raines, E. W., Seifert, R. A., Bowen-Pope, D. F. and Ross, R. 1990. TGF-β induces bimodal proliferation of connective tissue cells via complex control of an autocrine PDGF loop. Cell 63, 515-24.

Beaudreuil, J., Mbalaviele, G., Cohen-Solal, M., Morieux, C., De Vernejoul, M. C. and Orcel, P. 1995. Short-term local injections of transforming growth

factor-β 1 decrease ovariectomy-stimulated osteoclastic resorption in vivo in rats. J Bone Miner Res 10, 971-7.

Blavier, L. and Delaisse, J. M. 1995. Matrix metalloproteinases are obligatory for the migration of preosteoclasts to the developing marrow cavity of primitive long bones. J Cell Sci 108, 3649-59.

Boak, A. M., Roy, R., Berk, J., Taylor, L., Polgar, P., Goldstein, R. H. and Kagan, H. M. 1994. Regulation of lysyl oxidase expression in lung fibroblasts by transforming growth factor-β 1 and prostaglandin E2. Am J Respir Cell Mol Biol 11, 751-5.

Bonadio, J., Jepsen, K. J., Mansoura, M. K., Jaenisch, R., Kuhn, J. L. and Goldstein, S. A. 1993. A murine skeletal adaptation that significantly increases cortical bone mechanical properties. Implications for human skeletal fragility. J. Clin. Invest. 92, 1697-705.

Bonewald, L. F. and Dallas, S. L. 1994. Role of active and latent transforming growth factor β in bone formation. J. Cell. Biochem. 55, 350-7.

Bonyadi, M., Rusholme, S. A., Cousins, F. M., Su, H. C., Biron, C. A., Farrall, M. and Akhurst, R. J. 1997. Mapping of a major genetic modifier of embryonic lethality in TGF β 1 knockout mice. Nat Genet 15, 207-11.

Border, W. A. and Noble, N. A. 1994. Transforming growth factor β in tissue fibrosis. N Engl J Med 331, 1286-92.

Bottinger, E. P., Jakubczak, J. L., Roberts, I. S., Mumy, M., Hemmati, P., Bagnall, K., Merlino, G. and Wakefield, L. M. 1997. Expression of a dominant-negative mutant TGF-β type II receptor in transgenic mice reveals essential roles for TGF-β in regulation of growth and differentiation in the exocrine pancreas. Embo J 16, 2621-33.

Boyce, B. F., Wright, K., Reddy, S. V., Koop, B. A., Story, B., Devlin, R., Leach, R. J., Roodman, G. D. and Windle, J. J. 1995. Targeting simian virus 40 T antigen to the osteoclast in transgenic mice causes osteoclast tumors and transformation and apoptosis of osteoclasts. Endocrinology 136, 5751-9.

Boyde, A. 1972. Scanning electron microscope studies of bone. *In* Biochemistry and Physiology of Bone. G. H. Bourne, editor. Academic Press, New York and London. Vol. 1:259-310.

Bronckers, A. L., Gay, S., Dimuzio, M. T. and Butler, W. T. 1985. Immunolocalization of gamma-carboxyglutamic acid containing proteins in developing rat bones. Coll. Relat. Res. 5, 273-81.

Brunner, A. M., Marquardt, H., Malacko, A. R., Lioubin, M. N., and Purchio, A. F. 1989. Site-directed mutagenesis of cysteine residues in the pro region of the transforming growth factor β 1 precursor. Expression and characterization of mutant proteins. J. Biol. Chem. 264, 13660-4.

Byers, P. H., and Steiner, R. D. 1992. Osteogenesis Imperfecta. Annu. Rev. Med. 43, 269-282.

Canalis, E., McCarthy, T. L., and Centrella, M. 1991. Growth factors and cytokines in bone cell metabolism. Annu. Rev. Med. 42, 17-24.

Cané, V., Marotti, G., Volpi, G., Zaffe, D., Palazzini, S., Remaggi, F. and Muglia, M. A. 1982. Size and density of osteocyte lacunae in different regions of long bones. Calcif Tissue Int 34, 558-63.

Centrella, M., Horowitz, M. C., Wozney, J. M. and McCarthy, T. L. 1994. Transforming growth factor-β gene family members and bone. Endocr. Rev. 15, 27-39.

Centrella, M., McCarthy, T. L., and Canalis, E. 1988. Parathyroid hormone modulates transforming growth factor β activity and binding in osteoblast-

enriched cell cultures from fetal rat parietal bone. Proc. Natl. Acad. Sci. USA 85, 5889-93.

Chambers, T. J., Thomson, B. M. and Fuller, K. 1984. Effect of substrate composition on bone resorption by rabbit osteoclasts. J Cell Sci 70, 61-71.

Chen, R. H., Ebner, R. and Derynck, R. 1993. Inactivation of the type II receptor reveals two receptor pathways for the diverse TGF-β activities. Science 260, 1335-8.

Chenu, C., Pfeilschifter, J., Mundy, G. R., and Roodman, G. D. 1988. Transforming growth factor β inhibits formation of osteoclast-like cells in long-term human marrow cultures. Proc. Natl. Acad. Sci. USA 85, 5683-7.

Cui, W., Fowlis, D. J., Bryson, S., Duffie, E., Ireland, H., Balmain, A. and Akhurst, R. J. 1996. TGFβ1 inhibits the formation of benign skin tumors, but enhances progression to invasive spindle carcinomas in transgenic mice. Cell 86, 531-42.

Cui, W., Fowlis, D. J., Cousins, F. M., Duffie, E., Bryson, S., Balmain, A. and Akhurst, R. J. 1995. Concerted action of TGF-β 1 and its type II receptor in control of epidermal homeostasis in transgenic mice. Genes Dev 9, 945-55.

Dallas, S. L., Miyazono, K., Skerry, T. M., Mundy, G. R. and Bonewald, L. F. 1995. Dual role for the latent transforming growth factor-β binding protein in storage of latent TGF-β in the extracellular matrix and as a structural matrix protein. J Cell Biol 131, 539-49.

de Martin, R., Haendler, B., Hofer-Warbinek, R., Gaugitsch, H., Wrann, M., Schlusener, H., Seifert, J. M., Bodmer, S., Fontana, A., and Hofer, E. 1987. Complementary DNA for human glioblastoma-derived T cell suppressor factor, a novel member of the transforming growth factor-β gene family. EMBO J. 6, 3673-7.

Derynck, R. 1994. Transforming Growth Factor-β. *In* The Cytokine Handbook. A. W. Thomson, editor. Academic Press, London. 319-342.

Derynck, R. and Feng, X.-H. 1997. TGF-β receptor signaling. Published online Aug. 1. BBA Reviews in Cancer 1333, F105-F150.

Dickson, M. C., Martin, J. S., Cousins, F. M., Kulkarni, A. B., Karlsson, S. and Akhurst, R. J. 1995. Defective haematopoiesis and vasculogenesis in transforming growth factor-β 1 knock out mice. Development 121, 1845-54.

Diebold, R. J., Eis, M. J., Yin, M., Ormsby, I., Boivin, G. P., Darrow, B. J., Saffitz, J. E. and Doetschman, T. 1995. Early-onset multifocal inflammation in the transforming growth factor β 1-null mouse is lymphocyte mediated. Proc Natl Acad Sci U S A 92, 12215-9.

Dieudonné, S. C., Foo, P., van, Z. E., and Burger, E. H. 1991. Inhibiting and stimulating effects of TGF-β 1 on osteoclastic bone resorption in fetal mouse bone organ cultures. J. Bone Miner. Res. 6, 479-87.

Dollé, P., Dierich, A., LeMeur, M., Schimmang, T., Schuhbaur, B., Chambon, P. and Duboule, D. 1993. Disruption of the Hoxd-13 gene induces localized heterochrony leading to mice with neotenic limbs. Cell 75, 431-441.

Ducy, P., Zhang, R., Geoffry, V., Ridall, A. L. and Karsenty, G. 1997. Osf2/Cbfa1: a transcriptional activator of osteoblast differentiation. Cell 89, 747-754.

Ek-Rylander, B., Barkhem, T., Ljusberg, J., Ohman, L., Andersson, K. K. and Andersson, G. 1997. Comparative studies of rat recombinant purple acid phosphatase and bone tartrate-resistant acid phosphatase. Biochem J 321, 305-11.

Engler, B. G., Meier, M., Frank, J., and Muller, G. A. 1993. Reduction of background problems in nonradioactive northern and Southern blot analyses enables higher sensitivity than 32P-based hybridizations. Anal. Biochem. 210, 235-44.

Eriksen, E. F., Hodgson, S. F., Eastell, R., Cedel, S. L., O'Fallon, W. M. and Riggs, B. L. 1990. Cancellous bone remodeling in type I (postmenopausal) osteoporosis: quantitative assessment of rates of formation, resorption, and bone loss at tissue and cellular levels. J Bone Miner Res 5, 311-9.

Erlebacher, A. and Derynck, R. 1996. Increased expression of TGF-β2 in osteoblasts results in an osteopororsis-like phenotype. J. Cell Biol. 132, 195-210.

Erlebacher, A., Filvaroff, E. H., Gitelman, S. E., and Derynck, R. 1995. Toward a molecular understanding of skeletal morphogenesis. Cell 80, 371-378.

Fassler, R., Schnegelsberg, P. N. J., Dausman, J., Shinya, T., Muragaki, Y., McCarthy, M.T., Olsen, B.R., and Jaenisch, R. 1994. Mice lacking α1(IX) collagen develop noninflammatory degenerative joint disease. Proc. Natl. Acad. Sci. 91, 5070-5074.

Federman, D. D. 1994. Life without estrogen. New Engl. J. Med. 331, 1088-1089.

Feres-Filho, E. J., Choi, Y. J., Han, X., Takala, T. E. and Trackman, P. C. 1995. Pre- and post-translational regulation of lysyl oxidase by transforming growth factor-β 1 in osteoblastic MC3T3-E1 cells. J Biol Chem 270, 30797-803.

Finkelman, R. D., Bell, N. H., Strong, D. D., Demers, L. M. and Baylink, D. J. 1992. Ovariectomy selectively reduces the concentration of transforming

growth factor β in rat bone: implications for estrogen deficiency-associated bone loss. Proc. Natl. Acad. Sci USA 89, 12190-3.

Finkelman, R. D., Linkhart, T. A., Mohan, S., Lau, K. H., Baylink, D. J. and Bell, N. H. 1991. Vitamin D deficiency causes a selective reduction in deposition of transforming growth factor β in rat bone: possible mechanism for impaired osteoinduction. Proc. Natl. Acad. Sci. USA 88, 3657-60.

Foster, J. W., Dominguez-Steglich, M. A., Guioli, S., Kwok, C., Weller, P. A., Stevanovic, M., Weissenbach, J., Mansour, S., Young, I.D., Goodfellow, P.N., Brook, J.D., and Schafer, A.J. 1994. Campomelic dysplasia and autosomal sex reversal caused by mutations in an SRY-related gene. Nature 372, 525-530.

Freisinger, P., Ala-Kokko, L., LeGuellec, D., Franc, S., Bouvier, R., Ritvaniemi, P., Prockop, D.J., and Bonaventure, J. 1994. Mutation in the COL2A1 gene in a patient with hypochondrogenesis. J. Biol. Chem. 269, 13663-13669.

Frost, H. M. 1985. The skeletal intermediary organization: a synthesis. In Bone and Mineral Research, vol. 3, W. A. Peck, ed. (New York: Elsevier), pp. 49-107.

Gacheru, S. N., Thomas, K. M., Murray, S. A., Csiszar, K., Smith-Mungo, L. I. and Kagan, H. M. 1997. Transcriptional and post-transcriptional control of lysyl oxidase expression in vascular smooth muscle cells: effects of TGF-β 1 and serum deprivation. J Cell Biochem 65, 395-407.

Gelb, B. D., Shi, G. P., Chapman, H. A. and Desnick, R. J. 1996. Pycnodysostosis, a lysosomal disease caused by cathepsin K deficiency. Science 273, 1236-8.

Gendron-Maguire, M., Mallo, M., Zhang, M., and Gridley, T. 1993. Hoxa-2 mutant mice exhibit homeotic transformation of skeletal elements derived from cranial neural crest. Cell 75, 1317-1331.

Givol, D., and Yayon, A. 1992. Complexity of FGF receptors: genetic basis for structural diveristy and functional specificity. FASEB J. 6, 3362-3369.

Glick, A. B., Kulkarni, A. B., Tennenbaum, T., Hennings, H., Flanders, K. C., O'Reilly, M., Sporn, M. B., Karlsson, S. and Yuspa, S. H. 1993. Loss of expression of transforming growth factor β in skin and skin tumors is associated with hyperproliferation and a high risk for malignant conversion. Proc Natl Acad Sci U S A 90, 6076-80.

Glick, A. B., Lee, M. M., Darwiche, N., Kulkarni, A. B., Karlsson, S. and Yuspa, S. H. 1994. Targeted deletion of the TGF-β 1 gene causes rapid progression to squamous cell carcinoma. Genes Dev 8, 2429-40.

Grigoriadis, A. E., Wang, Z. Q., Cecchini, M. G., Hofstetter, W., Felix, R., Fleisch, H. A. and Wagner, E. F. 1994. c-Fos: a key regulator of osteoclast-macrophage lineage determination and bone remodeling. Science 266, 443-8.

Groot, C. G., Danes, J. K., Blok, J., Hoogendijk, A., and Hauschka, P. V. 1986. Light and electron microscopic demonstration of osteocalcin antigenicity in embryonic and adult rat bone. Bone 7, 379-85.

Hahn, S. A., Schutte, M., Hoque, A. T., Moskaluk, C. A., da Costa, L. T., Rozenblum, E., Weinstein, C. L., Fischer, A., Yeo, C. J., Hruban, R. H. and Kern, S. E. 1996. DPC4, a candidate tumor suppressor gene at human chromosome 18q21.1. Science 271, 350-3.

Hall, B. K. 1986. The role of movement and tissue interactions in the development and growth of bone and secondary cartilage in the clavicle of the embryonic chick. J. Embryol. Exp. Morphol. 93, 133-52.

Hastbacka, J., de la Chapelle, A., Mahtani, M. M., Clines, G., Reeve-Daly, M. P., Daly, M., Hamilton, B. A., Kusumi, K., Trivedi, B., Weaver, A., Coloma, A., Lovett, M., Buckler, A., Kaitila, I., and Lander, E.S. 1994. The diastrophic dysplasia gene encodes a novel sulfate transporter - positional cloning by fine-structure linkage disequilibrium mapping. Cell 78, 1073-1087.

Hattersley, G., and Chambers, T. J. 1991. Effects of transforming growth factor β 1 on the regulation of osteoclastic development and function. J. Bone Miner. Res. 6, 165-72.

Hayman, A. R., Jones, S. J., Boyde, A., Foster, D., Colledge, W. H., Carlton, M. B., Evans, M. J. and Cox, T. M. 1996. Mice lacking tartrate-resistant acid phosphatase (Acp 5) have disrupted endochondral ossification and mild osteopetrosis. Development 122, 3151-62.

Hill, P. A., Docherty, A. J., Bottomley, K. M., O'Connell, J. P., Morphy, J. R., Reynolds, J. J. and Meikle, M. C. 1995. Inhibition of bone resorption in vitro by selective inhibitors of gelatinase and collagenase. Biochem J 308, 167-75.

Hock, J. M. and Canalis, E. 1994. Platelet-derived growth factor enhances bone cell replication, but not differentiated function of osteoblasts. Endocrinology 134, 1423-8.

Hock, J. M. and Gera, I. 1992. Effects of continuous and intermittent administration and inhibition of resorption on the anabolic response of bone to parathyroid hormone. J. Bone Miner. Res. 7, 65-72.

Hodgkinson, C. A., Moore, K. J., Nakayama, A., Steingrimsson, E., Copeland, N. G., Jenkins, N. A., and Arnheiter, H. 1993. Mutations at the mouse microphthalmia locus are associated with defects in a gene encoding a novel basic-helix-loop-helix-zipper protein. Cell 74, 395-404.

Hogan, B., Constantini, F., and Lacy, E. 1986. Manipulating the mouse embryo. A laboratory manual. (Cold Spring Harbor: Cold Spring Harbor Laboratory).

Huang, S. S., O'Grady, P., and Huang, J. S. 1988. Human transforming growth factor β.alpha 2-macroglobulin complex is a latent form of transforming growth factor β. J. Biol. Chem. 263, 1535-41.

Hughes, D. E., Dai, A., Tiffee, J. C., Li, H. H., Mundy, G. R. and Boyce, B. F. 1996. Estrogen promotes apoptosis of murine osteoclasts mediated by TGF-β. Nat Med 2, 1132-6.

Jabs, E. W., Li, X., Scott, A. F., Meyers, G., Chen, W., Eccles, M., Mao, J., Charnas, L. R., Jackson, C. E., and Jaye, M. 1994. Jackson-Weiss and Crouzon syndromes are allelic with mutations in fibroblast growth factor receptor 2. Nature Genet. 8, 275-279.

Jabs, E. W., Muller, U., Li, X., Ma, L., Luo, W., Haworth, I.S., Klisak, I., Sparkes, R., Warman, M. L., Mulliken, J. B., Snead, M. L., and Maxson, R. 1993. A mutation in the homeodomain of the human MSX2 gene in a family affected with autosomal dominant craniosynostosis. Cell 75, 443-450.

Jacenko, O., Olsen, B. R. and Warman, M. L. 1994. Of mice and men: heritable skeletal disorders. Am. J. Hum. Genet. 54, 163-168.

Jhappan, C., Geiser, A. G., Kordon, E. C., Bagheri, D., Hennighausen, L., Roberts, A. B., Smith, G. H. and Merlino, G. 1993. Targeting expression of a

transforming growth factor β 1 transgene to the pregnant mammary gland inhibits alveolar development and lactation. Embo J 12, 1835-45.

Johnson, R. S., Spiegelman, B. M. and Papaioannou, V. 1992. Pleiotropic effects of a null mutation in the c-fos proto-oncogene. Cell 71, 577-86.

Jones, K. L., ed. 1988. Smith's recognizable patterns of human malformation. (Philadelphia: W.B. Saunders Co.).

Joyce, M. E., Roberts, A. B., Sporn, M. B., and Bolander, M. E. 1990. Transforming growth factor-β and the initiation of chondrogenesis and osteogenesis in rat femur. J. Cell Biol. 110, 2195-2207.

Kaartinen, V., Voncken, J. W., Shuler, C., Warburton, D., Bu, D., Heisterkamp, N. and Groffen, J. 1995. Abnormal lung development and cleft palate in mice lacking TGF-β 3 indicates defects of epithelial-mesenchymal interaction. Nat Genet 11, 415-21.

Kalu, D. N. 1991. The ovariectomized rat model of postmenopausal bone loss. Bone Miner 15, 175-91.

Karaplis, A. C., Luz, A., Glowacki, J., Bronson, R. T., Tybulewicz, V. L., Kronenberg, H. M. and Mulligan, R. C. 1994. Lethal skeletal dysplasia from targeted disruption of the parathyroid hormone-related peptide gene. Genes Dev. 8, 277-289.

Katagiri, T., Yamaguchi, A., Komaki, M., Abe, E., Takahashi, N., Ikeda, T., Rosen, V., Wozney, J. M., Fujisawa-Sehara, A., and Suda, T. 1994. Bone morphogenetic protein-2 converts the differentiation pathway of C2C12 myoblasts into the osteoblast lineage. J. Cell Biol. 127, 1755-1766.

Kaufman, M. H. 1992. The atlas of mouse development. (London: Academic press).

Kawaguchi, N., DeLuca, H. F. and Noda, M. 1992. Id gene expression and its suppression by 1,25-dihydroxyvitamin D3 in rat osteoblastic osteosarcoma cells. Proc. Natl. Acad. Sci. USA 89, 4569-4572.

Kingsley, D. M. 1994. The TGF-β superfamily: new members, new receptors, and new genetic tests of function in different organisms. Genes Dev 8, 133-46.

Kingsley, D. M. 1994. What do BMPs do in mammals? Clues from the mouse short-ear mutation. Trends Genet. 10, 16-21.

Kingsley, D. M., Bland, A. E., Grubber, J. M., Marker, P. C., Russell, L. B., Copeland, N. G., and Jenkins, N. A. 1992. The mouse short ear skeletal morphogenesis locus is associated with defects in a bone morphogenetic member of the TGF β superfamily. Cell 71, 399-410.

Kinoh, H., Sato, H., Tsunezuka, Y., Takino, T., Kawashima, A., Okada, Y. and Seiki, M. 1996. MT-MMP, the cell surface activator of proMMP-2 (pro-gelatinase A), is expressed with its substrate in mouse tissue during embryogenesis. J Cell Sci 109, 953-9.

Komori, T., Yagi, H., Nomura, S., Yamaguchi, A., Sasaki, K., Deguchi, K., Shimizu, Y., Bronson, R. T., Gao, Y.-H., Inada, M., Sato, M., Okamoto, R., Kitamura, Y., Yoshiki, S. and Kishimoto, T. 1997. Targeted disruption of Cbfa1 results in a complete lack of bone formation owing to maturational arrest of osteoblasts. Cell 89, 755-764.

Kopp, J. B., Factor, V. M., Mozes, M., Nagy, P., Sanderson, N., Bottinger, E. P., Klotman, P. E. and Thorgeirsson, S. S. 1996. Transgenic mice with increased plasma levels of TGF-β 1 develop progressive renal disease. Lab Invest 74, 991-1003.

Kordon, E. C., McKnight, R. A., Jhappan, C., Hennighausen, L., Merlino, G. and Smith, G. H. 1995. Ectopic TGF β 1 expression in the secretory mammary epithelium induces early senescence of the epithelial stem cell population. Dev Biol 168, 47-61.

Kronenberg, H. M. 1993. Parathyroid hormone: mechanism of action. In Primer on the metabolic bone diseases and disorders of mineral metabolism, M. J. Favus, ed. (New York: Raven Press), pp. 58-60.

Krumlauf, R. 1994. Hox genes in vertebrate development. Cell 78, 191-201.

Kuivaniemi, H., Tromp, G., and Prockop, D. J. 1991. Mutations in collagen genes: causes of rare and common diseases in humans. FASEB J. 5, 2052-2060.

Kulkarni, A. B., Huh, C. G., Becker, D., Geiser, A., Lyght, M., Flanders, K. C., Roberts, A. B., Sporn, M. B., Ward, J. M. and Karlsson, S. 1993. Transforming growth factor β 1 null mutation in mice causes excessive inflammatory response and early death. Proc Natl Acad Sci U S A 90, 770-4.

Laird, P. W., Zijderveld, A., Linders, K., Rudnicki, M. A., Jaenisch, R., and Berns, A. 1991. Simplified mammalian DNA isolation procedure. Nucleic Acids Res. 19,

Laufer, E., Nelson, C. E., Johnson, R. L., Morgan, B. A., and Tabin, C. 1994. Sonic hedgehog and FGF-4 act through a signaling cascade and feedback loop to integrate growth and patterning of the developing limb bud. Cell 79, 1-20

Lawrence, D. A., Pircher, R., and Jullien, P. 1985. Conversion of a high molecular weight latent β-TGF from chicken embryo fibroblasts into a low

molecular weight active β-TGF under acidic conditions. Biochem. Biophys. Res. Commun. 133, 1026-1034.

Lee, M. S., Gu, D., Feng, L., Curriden, S., Arnush, M., Krahl, T., Gurushanthaiah, D., Wilson, C., Loskutoff, D. L., Fox, H. and et al. 1995. Accumulation of extracellular matrix and developmental dysregulation in the pancreas by transgenic production of transforming growth factor-β 1. Am J Pathol 147, 42-52.

Lerner, U. H. 1987. Modifications of the mouse calvarial technique improve the responsiveness to stimulators of bone resorption. J Bone Miner Res 2, 375-83.

Lewis, D. B., Liggitt, H. D., Effmann, E. L., Motley, S. T., Teitelbaum, S. L., Jepsen, K. J., Goldstein, S. A., Bonadio, J., Carpenter, J., and Perlmutter, R. M. 1993. Osteoporosis induced in mice by overproduction of interleukin 4. Proc. Natl. Acad. Sci. USA 90, 11618-22.

Li, Y., Lacerda, D. A., Warman, M. L., Beier, D. R., Yoshioka, H., Ninomiya, Y., Oxford, J. T., Morris, N. P., Andrikopoulos, K., Ramirez, F., Wardell, B. B., Lifferth, G. D., Teuscher, C., Woodward, S. R., Taylor, B. A., Seegmiller, R. E., and Olsen, B. R. 1995. A fibrillar collagen gene, *Col11a1*, is essential for skeletal morphogenesis. Cell, 80.

Ljunggren, O., Ransjo, M. and Lerner, U. H. 1991. In vitro studies on bone resorption in neonatal mouse calvariae using a modified dissection technique giving four samples of bone from each calvaria. J Bone Miner Res 6, 543-50.

Lorenzo, J. A., Pilbeam, C. C., Kalinowski, J. F. and Hibbs, M. S. 1992. Production of both 92- and 72-kDa gelatinases by bone cells. Matrix 12, 282-90.

Lowe, C., Yoneda, T., Boyce, B. F., Chen, H., Mundy, G. R. and Soriano, P. 1993. Osteopetrosis in Src-deficient mice is due to an autonomous defect of osteoclasts. Proc. Natl. Acad. Sci. USA 90, 4485-4489.

Lyons, K. M., Pelton, R. W., and Hogan, B. L. M. 1989. Patterns of expression of murine Vgr-1 and BMP-2a suggest that transforming growth factor-β-like genes coordinately regulate aspects of embryonic development. Genes Dev. 1, 1657-1668.

Malluche, H. H. and Faugere, M. 1990. Bone biopsies: histology and histomorphometry of bone. *In* Metabolic bone disease and clinically related disorders. L. V. Avioli and S. M. Krane, editor. W. B. Saunders Co., Philadelphia. 283-328.

Manolagas, S. C., and Jilka, R. L. 1995. Bone marrow, cytokines, and bone remodeling: emerging insights into the pathophysiology of osteoporosis. New Engl. J. Med. 332, 305-311.

Mansell, J. P., Tarlton, J. F. and Bailey, A. J. 1997. Expression of gelatinases within the trabecular bone compartment of ovariectomized and parathyroidectomized adult female rats. Bone 20, 533-8.

Marie, P., and Sainton, P. 1897. Observation d'hydrocephalie héréditaire (pere et fils) par vice de développement du crane et du cerveau. Bull Mem. Soc. Med. Hop. (Paris). 14, 706.

Markowitz, S. D. and Roberts, A. B. 1996. Tumor suppressor activity of the TGF-β pathway in human cancers. Cytokine Growth Factor Rev 7, 93-102.

Massagué, J., Cheifetz, S., Endo, T., and Nadal-Ginard, B. 1986. Type β transforming growth factor is an inhibitor of myogenic differentiation. Proc. Natl. Acad. Sci. USA 83, 8206-8210.

McAllister, K. A., Grogg, K. M., Johnson, D. W., Gallione, C. J., Baldwin, M. A., Jackson, C. E., Helmbold, E. A., Markel, D. S., McKinnon, W. C., Murrell, J. and et al. 1994. Endoglin, a TGF-β binding protein of endothelial cells, is the gene for hereditary haemorrhagic telangiectasia type 1. Nat Genet 8, 345-51.

McSheehy, P. M., and Chambers, T. J. 1986. Osteoblastic cells mediate osteoclastic responsiveness to parathyroid hormone. Endocrinology 118, 824-8.

Meikle, M. C., Bord, S., Hembry, R. M., Compston, J., Croucher, P. I. and Reynolds, J. J. 1992. Human osteoblasts in culture synthesize collagenase and other matrix metalloproteinases in response to osteotropic hormones and cytokines. J Cell Sci 103, 1093-9.

Merwin, J. R., Newman, W., Beall, L. D., Tucker, A. and Madri, J. 1991. Vascular cells respond differentially to transforming growth factors β 1 and β 2 in vitro. Am J Pathol 138, 37-51.

Meunier, P. J., Sellami, S., Briançon, D. and Edouard, C. 1980. Histological heterogeneity of apparently idiopathic osteoporosis. *In* Osteoporosis: recent advances in pathogenesis and treatment. H. F. DeLuca, H. M. Frost, W. S. S. Jee, C. C. J. Johnston and A. M. Parfitt, editor. University Park Press, Baltimore. 293-301.

Meyer, R. A., Jr., Tenenhouse, H. S., Meyer, M. H. and Klugerman, A. H. 1989. The renal phosphate transport defect in normal mice parabiosed to X-linked hypophosphatemic mice persists after parathyroidectomy. J. Bone Miner. Res. 4, 523-32.

Miller, D. A., Lee, A., Pelton, R. W., Chen, E. Y., Moses, H. L., and Derynck, R. 1989. Murine transforming growth factor-β2 cDNA sequence and

expression in adult tissues and embryos. Mol. Endocrinology 89, 1108-1114.

Morgan, B. A., and Tabin, C. J. 1993. The role of homeobox genes in limb development. Curr. Opin. Genet. Dev. 3, 668-674.

Morrison, N. A., Qi, J. C., Tokita, A., Kelly, P. J., Crofts, L., Nguyen, T. V., Sambrook, P. N., and Eisman, J. A. 1994. Prediction of bone density from vitamin D receptor alleles. Nature 367, 284-287.

Muenke, M., Schell, U., Hehr, A., Robin, N. H., Wolfgang Losken, H., Schinzel, A., Pulleyn, L. J., Rutland, P., Reardon, W., Malcolm, S., and Winter, R. M. 1994. A common mutation in the fibroblast growth factor receptor 1 gene in Pfeiffer syndrome. Nature Genet. 8, 269-274.

Mullender, M. G., van der Meer, D. D., Huiskes, R. and Lips, P. 1996. Osteocyte density changes in aging and osteoporosis. Bone 18, 109-13.

Mundy, G. R. 1993. Cytokines in bone. In Physiology and Pharmacology of Bone. Handbook of Experimental Pharmacology, G. R. Mundyand T. J. Martin, ed. (New York: Springer), pp. 185-214.

Murray, S. S., Glackin, C. A., Winters, K. A., Gazit, D., Kahn, A. J., and Murray, E. J. 1992. Expression of helix-loop-helix regulatory genes during differentiation of mouse osteoblastic cells. J. Bone Miner. Res. 7, 1131-1138.

Nakase, T., Nomura, S., Yoshikawa, H., Hashimoto, J., Hirota, S., Kitamura, Y., Oikawa, S., Ono, K., and Takaota, K. 1994. Transient and localized expression of bone morphogenetic protein 4 messenger RNA during fracture healing. J. Bone Miner. Res. 9, 651-659.

Nakata, K., Ono, K., Miyazaki, J., Olsen, B. R., Muragaki, Y., Adachi, E., Yamamura, K., and Kimura, T. 1993. Osteoarthritis associated with mild

chondrodysplasia in transgenic mice expressing α1(IX) collagen chains with a central deletion. Proc. Natl. Acad. Sci. 90, 2870-2874.

Nicolas, V., Prewett, A., Bettica, P., Mohan, S., Finkelman, R. D., Baylink, D. J. and Farley, J. R. 1994. Age-related decreases in insulin-like growth factor-I and transforming growth factor-β in femoral cortical bone from both men and women: implications for bone loss with aging. J Clin Endocrinol Metab 78, 1011-6.

Noda, M., and Camilliere, J. J. 1989. In vivo stimulation of bone formation by transforming growth factor-β. Endocrinology 124, 2991-4.

O'Connor, M. M., and Wakefield, L. M. 1987. Latent transforming growth factor-β in serum. A specific complex with alpha 2-macroglobulin. J. Biol. Chem. 262, 14090-9.

O'Hare, K., Benoist, C., and Breathnach, R. 1981. Transformation of mouse fibroblasts to methotrexate resistance by a recombinant plasmid expressing a prokaryotic dihydrofolate reductase. Proc. Natl. Acad. Sci. USA 78, 1527-31.

Ogata, T., and Noda, M. 1991. Expression of Id, a negative regulator of helix-loop-helix DNA binding proteins, is down-regulated at confluence and enhanced by dexamethasone in a mouse osteoblastic cell line, MC3T3E1. Biochem. Biophys. Res. Commun. 180, 1194-1199.

Ohta, M., Greenberger, J. S., Anklesaria, P., Bassols, A. and Massague, J. 1987. Two forms of transforming growth factor-β distinguished by multipotential haematopoietic progenitor cells. Nature 329, 539-41.

Olson, E. N., and Klein, W.H. 1994. bHLH factors in muscle development: dead lines and commitments, what to leave in and what to leave out. Genes Dev. 8, 1-8.

Olson, E. N., Sternberg, E., Hu, J. S., Spizz, G., and Wilcox, C. 1986. Regulation of myogenic differentiation by type β transforming growth factor. J. Cell Biol. 103, 1799-1805.

Oreffo, R. O., Mundy, G. R., Seyedin, S. M. and Bonewald, L. F. 1989. Activation of the bone-derived latent TGF β complex by isolated osteoclasts. Biochem. Biophys. Res. Commun. 158, 817-23.

Oshima, M., Oshima, H. and Taketo, M. M. 1996. TGF-β receptor type II deficiency results in defects of yolk sac hematopoiesis and vasculogenesis. Dev Biol 179, 297-302.

Ottmann, O. G. and Pelus, L. M. 1988. Differential proliferative effects of transforming growth factor-β on human hematopoietic progenitor cells. J Immunol 140, 2661-5.

Otto, F., Thornell, A. P., Crompton, T., Denzel, A., Gilmour, K. C., Rosewell, I. R., Stamp, G. W. H., Beddington, R. S. P., Mundlos, S., Olsen, B. R., Selby, P. B. and Owen, M. J. 1997. Cbfa1, a candidate gene for cleidocranial dysplasia syndrome, is essential for osteoblast differentiation and bone development. Cell 1997, 765-771.

Oursler, M. J. 1994. Osteoclast synthesis and secretion and activation of latent transforming growth factor β. J. Bone Miner. Res. 9, 443-52.

Oursler, M. J., Cortese, C., Keeting, P., Anderson, M. A., Bonde, S. K., Riggs, B. L. and Spelsberg, T. C. 1991. Modulation of transforming growth factor-β production in normal human osteoblast-like cells by 17 β-estradiol and parathyroid hormone. Endocrinology 129, 3313-20.

Pai, A. C. 1965. Developmental genetics of a lethal mutation, muscular dysgenesis (mdg) in the mouse. I. Genetic analysis and gross morphology. Dev. Biol. 11, 82-92.

Parfitt, A. M. 1983. The physiological and clinical significance of bone histomorphometric data. In Bone histomorphometry: techniques and interpretation, R. R. Recker, ed. (Boca Raton: CRC Press, pp. 143-223.

Parfitt, A. M. 1994. Osteonal and hemi-osteonal remodeling: the spatial and temporal framework for signal traffic in adult human bone. J. Cell. Biochem. 55, 273-86.

Parfitt, A. M., Drezner, M. K., Glorieux, F. H., Kanis, J. A., Malluche, H., Meunier, P. J., Ott, S. M. and Recker, R. R. 1987. Bone histomorphometry: standardization of nomenclature, symbols, and units. Report of the ASBMR Histomorphometry Nomenclature Committee. J. Bone Miner. Res. 2, 595-610.

Parfitt, A. M., Mathews, C., Rao, D., Frame, B., Kleerekoper, M. and Villanueva, A. R. 1980. Impaired osteoblast function in metabolic bone disease. *In* Osteoporosis: recent advances in pathogenesis and treatment. H. F. DeLuca, H. M. Frost, W. S. S. Jee, C. C. J. Johnston and A. M. Parfitt, editor. University Park Press, Baltimore. 321-330.

Pelton, R. W., Saxena, B., Jones, M., Moses, H. L., and Gold, L. I. 1991. Immunohistochemical localization of TGF β 1, TGF β 2, and TGF β 3 in the mouse embryo: expression patterns suggest multiple roles during embryonic development. J. Cell. Biol. 115, 1091-105.

Pereira, R. F., Hume, E. L., Halford, K. W. and Prockop, D. J. 1995. Bone fragility in transgenic mice expressing a mutated gene for type I procollagen (COL1A1) parallels the age-dependent phenotype of human osteogenesis imperfecta. J. Bone Miner. Res. 10, 1837-43.

Peters, K., Ornitz, D., Werner, S., and Williams, L. T. 1993. Unique expression pattern of the FGF receptor 3 gene during mouse organogenesis. Devel. Biol. 155, 423-430.

Pfeilschifter, J. and Mundy, G. R. 1987. Modulation of type β transforming growth factor activity in bone cultures by osteotropic hormones. Proc. Natl. Acad. Sci. USA 84, 2024-8.

Pfeilschifter, J., Laukhuf, F., Muller-Beckmann, B., Blum, W. F., Pfister, T. and Ziegler, R. 1995. Parathyroid hormone increases the concentration of insulin-like growth factor-I and transforming growth factor β 1 in rat bone. J Clin Invest 96, 767-74.

Pfeilschifter, J., Seyedin, S. M., and Mundy, G. R. 1988. Transforming growth factor β inhibits bone resorption in fetal rat long bone cultures. J. Clin. Invest. 82, 680-5.

Pierce, D. F., Jr., Gorska, A. E., Chytil, A., Meise, K. S., Page, D. L., Coffey, R. J., Jr. and Moses, H. L. 1995. Mammary tumor suppression by transforming growth factor β 1 transgene expression. Proc Natl Acad Sci U S A 92, 4254-8.

Pierce, D. F., Jr., Johnson, M. D., Matsui, Y., Robinson, S. D., Gold, L. I., Purchio, A. F., Daniel, C. W., Hogan, B. L. and Moses, H. L. 1993. Inhibition of mammary duct development but not alveolar outgrowth during pregnancy in transgenic mice expressing active TGF-β 1. Genes Dev 7, 2308-17.

Poli, V., Balena, R., Fattori, E., Markatos, A., Yamamoto, M., Tanaka, H., Ciliberto, G., Rodan, G. A., and Costantini, F. 1994. Interleukin-6 deficient mice are protected from bone loss caused by estrogen depletion. EMBO J. 13, 1189-96.

Proetzel, G., Pawlowski, S. A., Wiles, M. V., Yin, M., Boivin, G. P., Howles, P. N., Ding, J., Ferguson, M. W. and Doetschman, T. 1995. Transforming growth factor-β 3 is required for secondary palate fusion. Nat Genet 11, 409-14.

Qian, S. W., Burmester, J. K., Merwin, J. R., Madri, J. A., Sporn, M. B. and Roberts, A. B. 1992. Identification of a structural domain that distinguishes the actions of the type 1 and 2 isoforms of transforming growth factor β on endothelial cells. Proc Natl Acad Sci U S A 89, 6290-4.

Reardon, W., Winter, R. M., Rutland, P., Pulleyn, L. J., Jones, B. M., and Malcolm, S. 1994. Mutations in the fibroblast growth factor receptor 2 gene cause Crouzon syndrome. Nature Genet. 8, 98-103.

Reponen, P., Sahlberg, C., Munaut, C., Thesleff, I. and Tryggvason, K. 1994. High expression of 92-kD type IV collagenase (gelatinase B) in the osteoclast lineage during mouse development. J Cell Biol 124, 1091-1102.

Rhodes, R. K. and Miller, E. J. 1978. Physicochemical characterization and molecular organization of the collagen A and B chains. Biochemistry 17, 3442-8.

Riddle, R. D., Johnson, R. L., Laufer, E., and Tabin, C. 1993. Sonic hedgehog mediates the polarizing activity of the ZPA. Cell 75, 1401-1416.

Rifas, L., Halstead, L. R., Peck, W. A., Avioli, L. V. and Welgus, H. G. 1989. Human osteoblasts in vitro secrete tissue inhibitor of metalloproteinases and gelatinase but not interstitial collagenase as major cellular products. J Clin Invest 84, 686-94.

Rijli, F. M., Mark, M., Lakkaraju, S., Dierich, A., Dolle, P., and Chambon, P. 1993. A homeotic transformation is generated in the rostral branchial

region of the head by disruption of Hoxa-2, which acts as a selector gene. Cell 75, 1333-1349.

Rimoin, D. L. and Lachman, R. S. 1993. Genetic disorders of the osseous skeleton. *In* McKusick's Heritable Disorders of Connective Tissue. P. Beighton, editor. Mosby, St. Louis. 650-652.

Roberts, A. B. and Sporn, M. B. 1990. *In* Peptide Growth Factors and their Receptors. M. B. Sporn and A. B. Roberts, editor. Springer-Verlag, Heidelberg. 421-472.

Roberts, A. B., Sporn, M. B., Assoian, R. K., Smith, J. M., Roche, N. S., Wakefield, L. M., Heine, U. I., Liotta, L. A., Falanga, V., Kehrl, J. H. and et al. 1986. Transforming growth factor type β: rapid induction of fibrosis and angiogenesis in vivo and stimulation of collagen formation in vitro. Proc Natl Acad Sci U S A 83, 4167-71.

Robey, P. G., Young, M. F., Flanders, K. C., Roche, N. S., Kondaiah, P., Reddi, A. H., Termine, J. D., Sporn, M. B. and Roberts, A. B. 1987. Osteoblasts synthesize and respond to transforming growth factor-type β (TGF-β) in vitro. J. Cell. Biol. 105, 457-63.

Rodan, G. A. and Fleisch, H. A. 1996. Bisphosphonates: mechanisms of action. J. Clin. Invest. 97, 2692-6.

Rodan, G. A., and Martin, T. J. 1981. Role of osteoblasts in hormonal control of bone resorption - a hypothesis. Calcif. Tissue Int. 33, 349-351.

Rodan, G. A., and Noda, M. 1991). Gene expression in osteoblastic cells. Crit. Rev. Euk. Gene Expr. 1, 85-98.

Rosen, D., Miller, S. C., DeLeon, E., Thompson, A. Y., Bentz, H., Mathews, M., and Adams, S. 1994. Systemic administration of recombinant transforming

growth factor β 2 (rTGF-β 2) stimulates parameters of cancellous bone formation in juvenile and adult rats. Bone 15, 355-9.

Rousseau, F., Bonaventure, J., Legeai-Mallet, L., Pelet, A., Rozet, J. M., Maroteaux, P., Le Merrer, M., and Munnich, A. 1994. Mutations in the gene encoding fibroblast growth factor receptor-3 in achondroplasia. Nature 371, 252-254.

Rudnicki, M. A., Schnegelsberg, P. N., Stead, R. H., Braun, T., Arnold, H. H., and Jaenisch, R. 1993. MyoD or Myf-5 is required for the formation of skeletal muscle. Cell 75, 1351-1359.

Sandberg, M., Vuorio, T., Hirvonen, H., Alitalo, K. and Vuorio, E. 1988. Enhanced expression of TGF-β and c-fos mRNAs in the growth plates of developing human long bones. Development 102, 461-70.

Sanderson, N., Factor, V., Nagy, P., Kopp, J., Kondaiah, P., Wakefield, L., Roberts, A. B., Sporn, M. B. and Thorgeirsson, S. S. 1995. Hepatic expression of mature transforming growth factor β 1 in transgenic mice results in multiple tissue lesions. Proc Natl Acad Sci U S A 92, 2572-6.

Sanford, L. P., Ormsby, I., Gittenberger-de Groot, A. C., Sariola, H., Friedman, R., Boivin, G. P., Cardell, E. L. and Doetschman, T. 1997. TGFβ2 knockout mice have multiple developmental defects that are non-overlapping with other TGFβ knockout phenotypes. Development 124, 2659-70.

Satokata, I., and Maas, R. 1994. Msx1 deficient mice exhibit cleft palate and abnormalities of craniofacial and tooth development. Nature Genet. 6, 348-356.

Schneider, H. G., Michelangeli, V. P., Frampton, R. J., Grogan, J. L., Ikeda, K., Martin, T. J., and Findlay, D. M. 1992. Transforming growth factor-β modulates receptor binding of calciotropic hormones and G protein-

mediated adenylate cyclase responses in osteoblast-like cells. Endocrinology 131, 1383-9.

Seitz, P. K., Zhu, B. T., and Cooper, C. W. 1992. Effect of transforming growth factor β on parathyroid hormone receptor binding and cAMP formation in rat osteosarcoma cell. J. Bone Miner. Res. 7, 541-6.

Sellheyer, K., Bickenbach, J. R., Rothnagel, J. A., Bundman, D., Longley, M. A., Krieg, T., Roche, N. S., Roberts, A. B. and Roop, D. R. 1993. Inhibition of skin development by overexpression of transforming growth factor β 1 in the epidermis of transgenic mice. Proc Natl Acad Sci U S A 90, 5237-41.

Seyedin, S. M., Thomas, T. C., Thompson, A. Y., Rosen, D. M. and Piez, K. A. 1985. Purification and characterization of two cartilage-inducing factors from bovine demineralized bone. Proc. Natl. Acad. Sci. USA 82, 2267-71.

Sheehan, D. C., and Hrapchak, B. B., ed. 1980. Theory and practice of histotechnology, 2nd ed. (Columbus: Batelle Press).

Shiang, R., Thompson, L. M., Zhu, Y. Z., Church, D. M., Fielder, T. J., Bocian, M., Winokur, S. T., and Wasmuth, J. J. 1994. Mutations in the transmembrane domain of FGFR3 cause the most common genetic form of dwarfism, achondroplasia. Cell 78, 335-342.

Shull, M. M., Ormsby, I., Kier, A. B., Pawlowski, S., Diebold, R. J., Yin, M., Allen, R., Sidman, C., Proetzel, G., Calvin, D. and et al. 1992. Targeted disruption of the mouse transforming growth factor-β 1 gene results in multifocal inflammatory disease. Nature 359, 693-9.

Siddhanti, S. R., and Quarles, L. D. 1994. Molecular to pharmacologic control of osteoblast proliferation and differentiation. J. Cell. Biochem. 55, 310-320.

Sillence, D. O., Ritchie, H. E., and Selby, P. B. 1987. Animal model: skeletal abnormalities in mice with cleidocranial dysplasia. Am. J. Med. Genet. 27, 75-85.

Sissons, H. A. and O'Connor, P. 1977. Quantitative histology of osteocyte lacunae in normal human cortical bone. Calcif. Tissue Res. 22, 530-533.

Smith, E. P., Boyd, J., Frank, G. R., Takahashi, H., Cohen, R. M., Specker, B., Williams, T. C., Lubahn, D. B., and Korach, K. S. 1994. Estrogen resistance caused by a mutation in the estrogen-receptor gene in a man. N. Engl. J. Med. 331, 1056-1061.

Soriano, P., Montgomery, C., Geske, R., and Bradley. A. 1991. Targeted disruption of the c-src proto-oncogene leads to osteopetrosis in mice. Cell 64, 693-702.

Storm, E. E., Huynh, T. V., Copeland, N. G., Jenkins, N. A., Kingsley, D. M., and Lee, S. J. 1994). Limb alterations in brachypodism mice due to mutations in a new member of the TGF β-superfamily. Nature 368, 639-643.

Strewler, G. J., and Nissenson, R. A. 1993. Parathyroid hormone-related protein. In Primer on the metabolic bone diseases and disorders of mineral metabolism, M. J. Favus, ed. (New York: Raven Press), pp. 61-63.

Tashjian, A. J., Voelkel, E. F., Lazzaro, M., Singer, F. R., Roberts, A. B., Derynck, R., Winkler, M. E., and Levine, L. 1985. Alpha and β human transforming growth factors stimulate prostaglandin production and bone resorption in cultured mouse calvaria. Proc. Natl. Acad. Sci. USA 82, 4535-8.

Tezuka, K., Tezuka, Y., Maejima, A., Sato, T., Nemoto, K., Kamioka, H., Hakeda, Y. and Kumegawa, M. 1994. Molecular cloning of a possible

cysteine proteinase predominantly expressed in osteoclasts. J Biol Chem 269, 1106-9.

Tilstra, D. J., and Byers, P. H. 1994. Molecular basis of hereditary disorders of connective tissue. Annu. Rev. Med. 45, 149-163.

Tournier, J. M., Polette, M., Hinnrasky, J., Beck, J., Werb, Z. and Basbaum, C. 1994. Expression of gelatinase A, a mediator of extracellular matrix remodeling, by tracheal gland serous cells in culture and in vivo. J Biol Chem 269, 25454-64.

Tran, S., and Hall, B. K. 1989. Growth of the clavicle and development of clavicular secondary cartilage in the embryonic mouse. Acta Anat. (Basel) 135, 200-7.

Uzawa, T., Hori, M., Ejiri, S. and Ozawa, H. 1995. Comparison of the effects of intermittent and continuous administration of human parathyroid hormone(1-34) on rat bone. Bone 16, 477-84.

Vainio, S., Karavanova, I., Jowett, A., and Thesleff, I. 1993. Identification of BMP-4 as a signal mediating secondary induction between epithelial and mesenchymal tissues during early tooth development. Cell 75, 45-58.

van der Rest, M., and Garrone, R. 1991. Collagen family of proteins. FASEB J. 5, 2814-2823.

Vermeulen, A. H., Vermeer, C., and Bosman, F. T. 1989. Histochemical detection of osteocalcin in normal and pathological human bone. J. Histochem. Cytochem. 37, 1503-8.

Vikkula, M., Mariman, E. C. M., Lui, C. H., Zhidkova, N., Tiller, G. E., Goldring, M. B., van Beersum, S. E. C., Malefijt, M., van den Hoogen, F. H. J., Ropers, H.-H., Mayne, R., Cheah, K., Olsen, B. R., Warman, M. L., and Brunner, H. G. 1995. Autosomal dominant and recessive

osteochondrodysplasias associated with the *Col11A2* locus. Cell 80, 431-437.

Vikkula, M., Metasaranta, M., and Ala-Kokko, L. 1994. Type II collagen mutations in rare and common cartilage diseases. Annals of Medicine 26, 107-114.

Wang, X. J., Greenhalgh, D. A., Bickenbach, J. R., Jiang, A., Bundman, D. S., Krieg, T., Derynck, R. and Roop, D. R. 1997. Expression of a dominant-negative type II transforming growth factor β (TGF-β) receptor in the epidermis of transgenic mice blocks TGF-β-mediated growth inhibition. Proc Natl Acad Sci U S A 94, 2386-91.

Wang, Z. Q., Ovitt, C., Grigoriadis, A. E., Mohle-Steinlein, U., Ruther, U. and Wagner, E. F. 1992. Bone and haematopoietic defects in mice lacking c-fos. Nature 360, 741-5.

Weibel, E. R. 1969. Stereological principles for morphometry in electron microscopic cytology. Int. Rev. Cytol. 26, 235-302.

Whyte, M. P. 1996. Osteogenesis Imperfecta. *In* Primer on the Metabolic Bone Diseases and Disorders of Mineral Metabolism. M. J. Favus, editor. Lippincott-Raven, Philadelphia. 382-384.

Whyte, M. P., Bergfeld, M. A., Murphy, W. A., Avioli, L. V. and Teitelbaum, S. L. 1982. Postmenopausal osteoporosis, a heterogeneous disorder as assessed by histomorphometric analysis of iliac crest bone from untreated patients. Am. J. Med. 72, 193-202.

Wiktor-Jedrzejczak, W., Bartocci, A., Ferrante, A. W. J., Ahmed-Ansari, A., Sell, K. W., Pollard, J. W., and Stanley, E. R. 1990. Total absence of colony-stimulating factor 1 in the macrophage-deficient osteopetrotic (op/op) mouse. Proc. Natl. Acad. Sci. USA 87, 4828-4832.

Willing, M. C., Pruchno, C. J., and Byers, P. H. 1993. Molecular heterogeneity in osteogenesis Imperfecta type I. Am. J. Med. Genet. 45, 223-227.

Woessner, J. F. 1961. The determination of hydroxyproline in tissue and protein samples containing small proportions of this imino acid. Arch Biochem Biophys 93, 440-447.

Wozney, J. M., Rosen, V., Celeste, A., Mitsock, L. M., Whitters, M. J., Kriz, R. W., Hewick, R. M., and Wang, E. A. 1988. Novel regulators of bone formation: molecular clones and activities. Science 242, 1528-1534.

Wozney, J.M. 1992. The bone morphogenetic protein family and osteogenesis. Molec. Reprod. Devel. 32, 160-167.

Wronski, T. J., Lowry, P. L., Walsh, C. C., and Ignaszewski, L. A. 1985. Skeletal alterations in ovariectomized rats. Calcif. Tissue Int. 37, 324-328.

Wronski, T. J., Walsh, C. C., and Ignaszewski, L. A. 1986. Histologic evidence for osteopenia and increased bone turnover in ovariectomized rats. Bone 7, 119-123.

Wyss-Coray, T., Feng, L., Masliah, E., Ruppe, M. D., Lee, H. S., Toggas, S. M., Rockenstein, E. M. and Mucke, L. 1995. Increased central nervous system production of extracellular matrix components and development of hydrocephalus in transgenic mice overexpressing transforming growth factor-β 1. Am J Pathol 147, 53-67.

Yamaguchi, A., Katagiri, T., Ikeda, T., Wozney, J. M., Rosen, V., Wang, E. A., Kahn, A. J., Suda, T., and Yoshiki, S. 1991. Recombinant human bone morphogenetic protein-2 stimulates osteoblastic maturation and inhibits myogenic differentiation in vitro. J. Cell Biol. 113, 681-687.

Yayon, A., Klagsbrun, M., Esko, J. D., Leder, P., and Ornitz, D. M. 1991. Cell surface, heparin-like molecules are required for binding of basic fibroblast growth factor to its high affinity receptor. Cell 64, 841-848.

Yoshida, H., Hayashi, S., Kunisada, T., Ogawa, M., Nishikawa, S., Okamura, H., Sudo, T., Shultz, L. D., and Nishikawa, S. 1990. The murine mutation osteopetrosis is in the coding region of the macrophage colony stimulating factor gene. Nature 345, 442-444.

Young, R. W. 1962. Cell proliferation and specialization during endochondral osteogenesis in young rats. J. Cell Biol. 14, 357-370.

Zhou, L., Dey, C. R., Wert, S. E. and Whitsett, J. A. 1996. Arrested lung morphogenesis in transgenic mice bearing an SP-C-TGF-β 1 chimeric gene. Dev Biol 175, 227-38.